Commande et observation des exosquelettes pour la rééducation fonctionnelle du membre supérieur

Akram Riani

université PARIS-SACLAY

NNT : 2018SACLV026

UNIVERSITÉ DE VERSAILLES ST-QUENTIN-EN-YVELINES

université PARIS-SACLAY

Control and observation of exoskeletons for upper limb functional rehabilitation

Thèse de doctorat de l'Université Paris-Saclay
préparée à l'Université de Versailles Saint Quentin en Yvelines

École doctorale n°580 Sciences et technologies de l'information et de la communication
Spécialité de doctorat: Robotique

Thèse présentée et soutenue à Vélizy, le 25 Septembre 2018, par

Akram Riani

Composition du Jury :

M. Olivier Bruneau Professeur, Paris-Sud (– ENS Cachan)	Président
M. Rochdi Merzouki Professeur, Université de Lille 1 (– LAGIS.CNRS)	Rapporteur
M. Boubaker Daachi Professeur, Université de Paris 8 (– LIASD)	Rapporteur
M. Nathanael Jarrassé Chargé de recherche, UPMC (– ISIR)	Examinateur
Mme. Nelly Nadjar-Gauthier Maître de conférences, UVSQ (– LISV)	Examinateur
M. Lotfi Benziane Chargé de recherche, CRD Reghaia, Algérie	Examinateur
M. Abdelaziz Benallegue Professeur, UVSQ (– LISV)	Directeur de thèse
M. Tarek Madani Maître de conférences, UPEC (– LISSI)	Co-Directeur de thèse

Thèse de doctorat

université PARIS-SACLAY | ÉCOLE DOCTORALE Sciences et technologies de l'information et de la communication (STIC)

Titre : Commande et observation des exosquelettes pour la rééducation fonctionnelle du membre supérieur

Mots clés : Exosquelette, Rééducation fonctionnelle, Commande robuste, Observation

Résumé : Cette thèse s'adresse à la problématique de contrôle/commande et d'observation des exosquelettes du membre supérieur pour l'assistance à la mobilité des personnes qui souffrent d'un déficit moteur, caractérisé par une perte totale ou partielle des capacités motrices. Le robot utilisé pour les validations est conçu par RB3D dans le but des travaux de recherches sur les lois de commandes pour la rééducation du membre supérieur au sien du Laboratoire LISSI (Laboratoire Images, Signaux et Systèmes Intelligents) de l'UPEC, appelé ULEL (Upper Limb Exoskeleton of LISSI).
Deux approches de commande d'exosquelettes pour la rééducation fonctionnelle du membre supérieur ont été proposées. La première commande est conçue sur la base d'un estimateur en-ligne des paramètres dynamiques. Cette méthode d'adaptation permet d'améliorer les performances de contrôle de ce système, et de compenser les erreurs paramétriques dues au couplage de l'exosquelette avec le membre humain.
La deuxième contribution consiste en une stratégie de commande robuste basée sur les modes glissants. Cette stratégie non-linéaire, garantie la convergence des erreurs de poursuite vers zéro en temps fini lorsque le régime de glissement est atteint. Ce type de commande est connu par sa robustesse vis-à-vis les variations paramétriques et les perturbations externes. L'efficacité de la méthode proposée est démontrée expérimentalement pour le mode de rééducation passif.
Dans la dernière partie de la thèse, un observateur en mode glissant d'ordre supérieur est proposé pour estimer les couples d'interactions homme-exosquelette. L'observateur proposé est capable d'estimer les efforts au niveau de l'interface d'interaction entre l'exosquelette et le membre humain, en utilisant les mesures de position et l'entrée de commande. Les résultats obtenus montrent l'efficacité des solutions proposées sur l'exosquelette ULEL.

Title : Control and observation of exoskeletons for upper limb functional rehabilitation

Keywords : Exoskeleton, Functional rehabilitation, Robust control, Observation

Abstract: This thesis addresses the problem of control of an upper limb exoskeleton for mobility assistance of people who suffer from a motor deficit, characterized by a total or partial loss of motor skills. The robot used is designed by RB3D for the purpose of research work on the control laws for the rehabilitation of the upper limb at LISSI Laboratory (Laboratory Images, Signals and Intelligent Systems) of the UPEC university; this exoskeleton is called ULEL (Upper Limb Exoskeleton of LISSI).
Two approaches to control exoskeletons for functional rehabilitation of the upper limb have been proposed. The first control is based on an online estimator of dynamic parameters. This adaptation method makes it possible to improve the control performance of this system, and to compensate for parametric errors due to coupling the exoskeleton with the human limb.
The second contribution consists of a robust control strategy based on sliding modes. This nonlinear strategy guarantees the convergence of tracking errors to zero in finite time when the sliding mode is reached. This type of control is known by its robustness with respect to parametric variations and external disturbances. The effectiveness of the proposed method is experimentally demonstrated for the passive rehabilitation mode.
Finally, in the last part of this thesis, a higher order sliding mode observer is proposed to estimate interactions torques of the human-exoskeleton system. The proposed observer is able to estimate the forces at the interaction interface between the exoskeleton and the human limb, using the position measurements and the control input. The obtained results show the effectiveness of the proposed solutions using the exoskeleton ULEL.

Université Paris-Saclay
Espace Technologique / Immeuble Discovery
Route de l'Orme aux Merisiers RD 128 / 91190 Saint-Aubin, France

Abstract

Robots have been identified as a possible way to improve and automate patient's access to rehabilitation therapy, and also to provide new tools for therapists. Several researchers have already proposed the use of robots for the delivery of this type of physiotherapy. The first large-scale study on the acceptance of robotics in occupational therapy for both patients and therapists was conducted using a simple therapy robot. This study indicates a wide acceptance of the two groups, with many valuable suggestions for improvement. The benefits of robot-assisted therapy include the availability of the robot to successively repeat movements without complaint, as well as the ability to record these movements.

Recently, research in robotics rehabilitation has focused on exoskeletons. These devices have a structure that resembles the human limb, having joint axes that correspond to those of the limb. Exoskeletons are designed to work side-by-side with the limb, and thus can be attached to the limb in multiple locations, allowing the exoskeleton to fully determine the limb posture and the torques applied to each joint separately. In addition, it allows to expand the workspace, allowing a greater variety of movements in rehabilitation exercises.

My PhD work addresses the problem of control of an upper limb exoskeleton for mobility assistance of people who suffer from motor deficit, characterized by a total or partial loss of motor skills. The robot used is designed by RB3D for the purpose of research work on the control laws for the rehabilitation of the upper limb at LISSI Laboratory (Laboratory Images, Signals and Intelligent Systems) of the UPEC university, this exoskeleton is called ULEL (Upper Limb Exoskeleton of LISSI).

The first proposed control law is based on an online estimator of dynamic parameters. This adaptation method makes it possible to improve the control performance, and to compensate for parametric errors due to coupling the exoskeleton with the human limb.

The second contribution is a robust control strategy based on sliding mode technique. It guarantees the convergence of the tracking errors to zero in finite time when the sliding mode is reached. This type of control is known by its robustness with respect to parametric uncertainties and external disturbances. The effectiveness of the proposed method is experimentally demonstrated for the passive rehabilitation mode.

Finally, in the last part of my thesis, a higher order sliding mode observer is proposed to estimate interaction torques of the human-exoskeleton system. The proposed observer is able to estimate the forces at the interaction interface between the exoskeleton and the human limb, using the position measurements and the control input. The simulation results obtained show the effectiveness of the proposed solutions using the exoskeleton ULEL.

Résumé

Les robots ont été identifiés comme un moyen possible pour améliorer et automatiser l'accès des patients à la thérapie de rééducation, et fournir de nouveaux outils pour les thérapeutes. Plusieurs études ont déjà proposé l'utilisation des robots pour la prestation de ce type de physiothérapie. La première étude de grande envergure sur l'acceptation de la robotique en ergothérapie, aussi bien pour les patients que pour les thérapeutes, a été réalisée à l'aide d'un simple robot manipulateur. Cette étude signale une large acceptation des deux groupes, avec un grand nombre de précieuses suggestions d'amélioration. Les avantages de la thérapie assistée par les robots comprennent la disponibilité du robot pour répéter successivement les mouvements sans plainte, ainsi que la possibilité de les enregistrer.

Depuis, la recherche en robotique de rééducation s'est orientée vers les exosquelettes. Ces dispositifs ont une structure qui ressemble au membre humain, ayant des axes d'articulations qui correspondent à ceux du membre. Les exosquelettes sont conçus pour fonctionner côte à côte avec le membre, et donc peuvent être attachés à ce dernier en plusieurs endroits, pour permettre à l'exosquelette de déterminer pleinement la posture du membre et les couples appliqués à chaque articulation séparément. Leur utilisation d'élargir l'espace de travail, ce qui permet une plus grande variété de mouvements dans les exercices de rééducation.

Mes travaux de thèse s'adressent à la problématique de contrôle/commande et d'observation d'un exosquelette du membre supérieur pour l'assistance à la mobilité des personnes qui souffrent d'un déficit moteur, caractérisé par une perte totale ou partielle des capacités motrices. Le robot utilisé est conçu et réalisé par RB3D pour les applications de rééducation du membre supérieur au sien du Laboratoire LISSI (Laboratoire Images, Signaux et Systèmes Intelligents) de l'UPEC, appelé ULEL (Upper Limb Exoskeleton of LISSI).

L'une des contribution de ma thèse est la conception d'une loi de commande d'exosquelettes pour la rééducation fonctionnelle des membres supérieurs, basée sur un estimateur en-ligne des paramètres dynamiques. Cette méthode d'adaptation per-

met d'améliorer les performances de contrôle du système, et de compenser les erreurs paramétriques dues au couplage de l'exosquelette avec le membre humain.

Une stratégie de commande robuste basée sur les modes glissants est également proposée, elle garantie la convergence des erreurs de poursuite vers zéro en temps fini lorsque le régime de glissement est atteint. Ce type de commande est connu par sa robustesse vis-à-vis des variations paramétriques et des perturbations externes. L'efficacité de la méthode proposée est démontrée expérimentalement pour le mode de rééducation passif.

Finalement, dans la dernière partie de ma thèse, un observateur par mode glissant d'ordre supérieur est proposé pour estimer les couples d'interactions homme-exosquelette. Cet observateur est capable d'estimer les efforts au niveau de l'interface d'interaction entre l'exosquelette et le membre humain, en utilisant les mesures de position et les entrées de commande. La validation de la méthode est réalisé en simulation et les résultats obtenus montrent l'efficacité des solutions proposées sur l'exosquelette ULEL.

Contents

List of Figures

List of Tables

Acknowledgements

First and foremost, I would like to pay my gratitude to almighty ALLAH, who gives me the strength, courage and patience for completing this thesis work at last. I dedicate this modest work and my deep gratitude to the memory of my father, the one that taught me the meaning of life.

My heartiest thanks to Mr Abdelaziz Benallegue, Professor at UVSQ, who received me for the doctoral program at Versailles Engineering Systems Laboratory and gave me the opportunity to carry out my research work under his kind supervision. He is not only scientifically my mentor, but also my teacher and philosopher. I appreciate the lively discussions we had in which he supplied me with academic arguments that have aided the understanding of my research. I value very highly the fact that he was always available to answer my questions. His strengths lie in his intelligence and consistency, straight-forwardness and compassion. These traits make him both a great advisor and, most importantly, a wonderful person.

The following of my thanks will go naturally to my co-supervisor Mr Tarek Madani, Associate Professor at UPEC (LISSI), for his support and his full involvement in this work. Without our many discussions and confrontations of ideas, the evolution of this work would not have been as presented in this manuscript. Thank you for teaching me the pragmatic side of things and making me benefit from your experience and expertise. Thank you for everything Tarek.

I would like to express my deep gratitude to Mr Olivier Bruneau, Professor at Paris-Sud (ENS Cachan), for having done me the great honor of accepting to chair my thesis jury. I also warmly thank Mr Rochdi Merzouki and Boubaker Daachi, respectively Professor at Université de Lille 1 (LAGIS.CNRS) and Professor at Université de Paris 8 (LIASD) for having accepted to report this thesis; your remarks and your very constructive comments allowed me to take the necessary step back to the preparation of my defense. I would also like to thank Mrs Nelly Nadjar-Gauthier, Associate Professor at Versailles Engineering Systems Laboratory for taking part in my thesis jury and having thoroughly examined this work. I would also like to thank Mr Nathanael Jarrassé, Re-

searcher at UPMC (ISIR) for having accepted to be part of this jury and for his remarks questions as a specialist in the field testifying the interest of this work. I would like to express my gratitude to Mr. Lotfi Benziane, researcher at CRD Reghaia, Algeria, who did me the honor to be part of my jury and to have made the trip from Algeria to attend my defense, thank you for your support and valuable advices that helped me a lot to develop personally and professionally.

My thanks to Mr Luc Chassagne, director of the LISV, who welcomed me into the laboratory to do my thesis. I also take the opportunity to thank the administration staff who helped me in my tedious administrative procedures.

I wish to thank all the staff of LISV especially Hafid Elhadri for his great availability and his valuable help. A special dedication to Olivier, for his good humor, his kindness and his indispensable help for the realization of the experimental tests.

I am grateful to many friends and colleagues in the LISV with whom I shared pleasant moments in recent years. I would like to thank Ali, Elhadj, Sido, Adel, Madjid, Nahla, Ibrahim, Tayba, Fouz, Elaswad, Khaled et Khaled, Saad, Tahoune, and others. I spent memorable moments in your company.

A special thought for my friends and faithful comrades. I'm happy to take this opportunity to thank infinitely Ayoub, Adel, Farhat, Sofiane, Abdelali, Amine, Saleh, Ahmed, Houssine, Moustafa, Farid, Abdellah, Fouad, Karim, and others, for all the support and creating a great atmosphere which allowed me to release the stress.

These last lines are for my family and friends in Algeria and France who have always supported me during theses years of study in France. I thank infinitely my mother who have always support me, for her gratitude, her love and especially for her prayers. I warmly thank my brother and sister for encouraging me. I would like to emphasize that my success is first and foremost their success. I thank my cousin Nadia and her small family for making the trip to attend the defense of my PhD, it touches me deeply. I do not know how to express my gratitude to Hafida and her little family Ali, Ines et Charles; I owe her a lot, she always considered me a member of her family and she were there for me when I needed, and I hope to be able to do the same for her. I hope I have realized your ambitions and that I was up to it.

Finally, I extend my sincere thanks to everyone who has contributed, from near or far, to the accomplishment of my thesis.

Introduction

Robots are mechatronic devices designed to automatically perform tasks that imitate or reproduce human actions in a specific area, that's why they have been strongly associated with human beings. Indeed, The first robots have been distended for industrial purposes in the early 1970s. Despite their high cost they are meant to replace or help human operator in repetitive, challenging or dangerous tasks. Today, the evolution of electronics and computing allows to develop robots more precise, faster and with a better autonomy, enabling greater data exchange as in the example of teleoperation robotics. Furthermore, the arrival of wearable robots leads to investigate aspects of physical interaction.

In general one can distinguish two types of wearable robots, prostheses and exoskeletons. Unlike prostheses which aim to replace the lost member, exoskeletons are designed to operate side by side with the human limb. They have joint axes corresponding to those of the wearer's limb, imitating its structure. Exoskeletons have several application fields including the increase of power for military and rescue applications, diagnostic and technical assistance for the disabled or elderly people, and physical therapy which allows motor rehabilitation, in which fits the work of this thesis, and more precisely with upper limb exoskeletons.

The main treatment of disabilities after stroke is rehabilitation therapy which allows the patient to recover his voluntary movements and relearn performing activities of daily living [1]. Stroke is the leading cause of serious and long-term disability [2]. Depending on the location of the lesion and its importance, stroke can result in partial or total paralysis [3]. As the number of disabled patients is growing, providing appropriate treatment can become increasingly difficult and very costly.

The use of exoskeletons makes it possible to meet this growing demand and can improve the well-being of this kind of patients. Having a similar kinematics to the human limb, exoskeletons can provide a permanent and intensive rehabilitation for long time periods [4], with reduced costs. Furthermore, exoskeletons can provide some data and measurements that could be used to evaluate the patient's recovery. In recent

years many upper limb exoskeletons for rehabilitation have been developed. The list of examples of existing devices is long but we can cite: the Armeo products (Hocoma, Switzerland), including the 7 DoF ArmeoPower active exoskeleton, which is based on the ARMin III exoskeleton [5], the 4 axes exoskeleton ABLE (CEA-LIST Interactive Robotics Unit) [6], the 7 DoF exoskeleton CADEN-7 (University of Washington, Seattle) [7], the lightweight 5 DoF pneumatic exoskeleton RUPERT (Arizona State University) [8], and the 7 DoF exoskeleton ETS-MARSE [9], etc.

In this context, the work presented in this dissertation consists of several parts: modeling and parametric identification of the exoskeleton, control of the exoskeleton in the case of passive rehabilitation (without efforts applied by the patient) and then an estimation of the interaction between the robot and the patient in order to prepare the ground for a force control or an impedance control. The proposed solutions for the parts mentioned above are detailed in the rest of this manuscript, which is organized into five chapters (in addition to an introduction and a conclusion).

The first chapter gives an overview of robotic systems for the rehabilitation of patients with upper limb motor impairment. First, some elements of the upper limb anatomy and its kinematics are introduced. Then, methods of upper limb rehabilitation as well as existing rehabilitation robots are presented. Finally, an overview of the existing control strategies for upper limb rehabilitation is given.

The second chapter presents the geometric, kinematic and dynamic modeling of the exoskeleton ULEL which is the experimental platform used in this thesis. In addition, a multi-body dynamic model based on a complete CAD model is developed using the SimMechanics library of MatLab software. Dynamic parameter identification is carried out to identify the dynamic parameters of ULEL. This step is mandatory in order to obtain an accurate dynamic model, which will be used in simulations and control system design.

The third chapter presents an adaptive control strategy based on an online dynamic parameter estimator. Its goal is to improve the control performance of this system which plays a vital role in assisting patients with shoulder, elbow and wrist movements. In general, the dynamic parameters of the human limb are unknown and differ from one person to another, which degrades the performance of the exoskeleton-human control system. For this reason, the proposed control scheme contains an additional loop based on an effective online dynamic parameters estimator. The latter acts on the adaptation of the controller parameters to ensure the performance of the system in the presence of parametric uncertainties and disturbances. The physical model of the exoskeleton ULEL, interacting with a 7 degrees of freedom upper limb model is used to illustrate

the effectiveness of the proposed approach, and an example of passive rehabilitation movements (which aims to maneuver the exoskeleton that drives the passive upper limb to follow the predefined desired trajectories) is performed using multi-body dynamic simulation.

Chapter 4 provides an original adaptive sliding mode control approach for upper limb rehabilitation using exoskeletons. In this case, a non-linear sliding surface is proposed to ensure the convergence of tracking errors to zero in finite time when the sliding mode is reached. This type of control is known to be robust against parametric variations and external disturbances. Experimental results show the effectiveness of the proposed method for the passive rehabilitation mode.

The last chapter presents a third-order like sliding mode observer to estimate human-exoskeleton interaction torques. The proposed observer is able to estimate torques caused by the interaction of the exoskeleton with the human limb, using only joint position measurements and the control input. The proposed approach has been tested in simulation using the exoskeleton ULEL muti-body model, and has shown its effectiveness. The great interest of the interaction torques estimation is its application for the phase of active rehabilitation mode, which is a very important step to develop an exoskeleton able to perform upper limb rehabilitation effectively.

The manuscript is closed with a general conclusion and perspectives for future work.

Chapter 1

Exoskeletons for upper limb rehabilitation

Contents

1.1 Introduction

Cerebral Vascular Accident (CVA) or stroke is the most common cause of disability, it is characterized by the sudden interruption of blood supply to the brain, resulting in oxygen deprivation. Depending on the location of the lesion and its importance, stroke can result in partial or total paralysis [3]. It is the third cause of death and the leading cause of disability in France [10]. Over 138 600 hospitalizations were registered with disabling stroke in 2009 [11]. The main treatment of these disabilities is rehabilitation, which allows the patient to recovery his voluntary movements and relearn performing activities of daily living [1].

Rehabilitation aims primarily to optimize the recovery of motor function deficits, in order to reduce the impact of brain damage on this function and to develop compensation strategies to ensure the replacement of injured functions. It aims to enable the patient to regain physical and social activities and a more independent lifestyle. Motor rehabilitation can be prescribed for:

- Prevention or treatment of pathologies related to stroke;
- Reduction of motor deficits and the normalization of muscle tone (spasticity);
- Correction of standing and balance pathologies, involving the head, trunk and lower limbs;
- Correction of walk that involves the whole body;
- Recovering upper limb mobility and grasping function;
- Regaining independence in the functions of everyday life.

Rehabilitation can continue in most cases the whole life of stroke patients, and can become very costly. In France, the total health care of stroke patients was about €5.3 billion in 2007 [12], including costs associated with lost productivity and disability. In addition, nursing care costs were estimated at €2.4 billion [12]. The use of robotic technologies can improve the care strategies, and reduces significantly the disabling stroke costs.

Robots have been identified as a possible way to improve and automate patient access to rehabilitation therapy, and also to provide new tools for therapists. Several researchers have already proposed the use of robots for this type of physiotherapy [13]. The first large-scale study on the acceptance of robotics in occupational therapy for

both patients and therapists was carried out by Dijkers and his colleagues, using a simple therapy robot [14]. This study indicates a wide acceptance of both groups, with many valuable suggestions for improvements. The benefits of robotic therapy include the availability of the robot to successively repeat the movements without complaint and the ability to record these movements.

This chapter aims to provide an overview of rehabilitation robotic systems of patients with motor impairment, and is particularly focused on robots for upper limb rehabilitation. First, some elements of the upper limb anatomy and its kinematics are introduced. Then methods of upper limb rehabilitation as well as existing rehabilitation robots are presented. Finely, an overview of the existing control strategies for upper limb rehabilitation is given.

1.2 Elements of the upper limb anatomy

The upper limb (or arm in the common language) is the member connected to the trunk through the shoulder. The upper limb consists of three segments: the arm, the forearm and the hand. The arm is connected to the forearm with the elbow, and the wrist connects the forearm to the hand (see Fig.1.1).

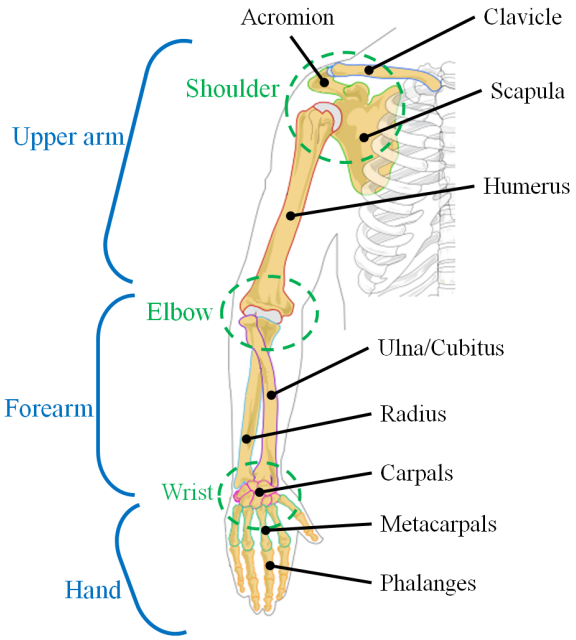

Figure 1.1: Anatomy of the upper limb

1.2.1 The shoulder

The shoulder is the most mobile of all the joints of the human body. This articulation is composed of three bones: the Clavicle, the Scapula (Omoplate), and the Humerus (Fig.1.1). The shoulder is not a simple articulation but a set of two functional groups which permits three Degrees of Freedom (DoF), allowing flexion / extension, adduction / abduction, and axial rotations of the upper limb [15].

1.2.2 The elbow

The elbow is the intermediate articulation of the upper limb constituting the mechanical connection between the arm and the forearm. Three bones participate in this articulation: the Humerus, the Radius, and the ulna (Fig.1.1). This joint complex Has two distinct functions: flexion / extension and pronation / supination. Therefore, we can consider that the elbow allows two DoF, one pivot joint for flexion / extension of the forearm and another one for the pronation / supination [15].

1.2.3 The wrist

The wrist is the distal articulation of the upper limb, allowing the hand, which is the effector segment, to perform the optimal position for grasping. The wrist complex has essentially two DoF allowing ulnar / radial deviation, and flexion / extension movements of the hand [15] (Fig.1.1).

1.3 Kinematics of the upper limb

The upper limb has a total of nine DoF without counting the fingers joints [16]. The shoulder can be considered as a ball joint allowing three rotations, these movements are commonly known as flexion / extension (Fig. 1.2a), abduction / adduction (Fig. 1.2b), and Internal rotation / external rotation (Fig. 1.2c). Furthermore, the sternoclavicular joint has two DoF allowing movements of elevation / depression, and retraction/ protraction which moves the center of rotation of the shoulder ball joint (Fig. 1.2d). Thus, the shoulder has a total of five DoF [17]. The elbow has two DoF, the flexion / extension (Fig. 1.2e), and the pronation / supination (Fig. 1.2f). Finally, the wrist joint has two DoF, flexion / extension (Fig. 1.2g) and ulnar deviation / radial deviation (Fig. 1.2h) [18].

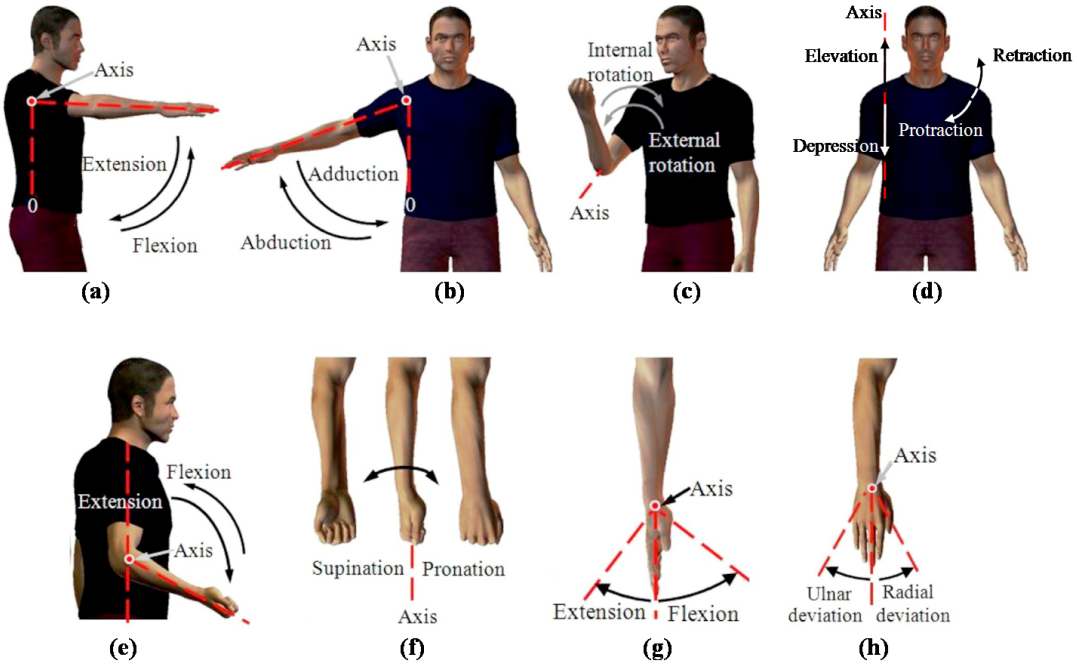

Figure 1.2: The upper limb movements, adapted from [19]

1.4 Upper limb disabilities and Conventional rehabilitation techniques

Motor deficit of the right or left upper limb is characterized by a total or partial loss of the voluntary movements capacities. It is most often due to a CVA, affecting one or both of the hemispheres of the brain. Stroke is the first factor of acquired physical handicaps in developed countries [12]. About half of stroke patients, remained with motor deficit of the upper limb after the accident. This deficiency is of very variable importance: from slight motor troubles to almost complete paralysis. In addition, spontaneous recovery, which occurs in the acute phase (up to one month after the accident) is also variable from one patient to another, some recover their full capacity after a few days, when others will have almost no spontaneous recovery.

Most of the non-spontaneous recovery of patients is now due to physical therapy. In particular, it consists of physiotherapy sessions aiming to mobilize the affected member to allow the recovery of voluntary movements inducing the reconstruction of the sensory-motor loop. In the early stages of rehabilitation therapists will promote passive mobilizations of the limb because the subject has little or no voluntary control ability. In a second phase, they tend to favor movements, at least partially active. At this stage the subject is able to produce a movement, either incorrect or incomplete (or

even both), and the therapist will seek to improve the performance of the patient by assisting and correcting his movements. Also, external stimulations like encouragement, visual feedback and games are introduced. Finally, from this period, exercises called Activities of Daily Living (ADL) are also proposed, which participate in the motivation and involvement of the patient in the process of rehabilitation.

Rehabilitation aiming to restore motor impairment is a major public health issue. Thus, several rehabilitation methods have been proposed. The main ones are [20]:

- The Motor Learning Approach suggested by Carr and Shepherd [21], consists of learning the same tasks as those normally performed by healthy people, the therapist analyzes for each movement the difficulties of execution and assists the subject to perform the task.
- The Bobath method [22] is the most widely used in the Western world, initially based on the inhibition of spasticity and the facilitation of motor activities, to improve the quality of performing tasks and especially the coordination between the different joints during movements.
- The Perfetti method [23], is based on the stimulation of proprioception which can facilitate motor recovery, in order to obtain selective motor skills by exercises based on specific tasks.
- Cotton and Kinsman [24] present the Conductive Education technique developed by Pete at the Motor Disabled and Conductor's College in Budapest, Hungary. This method focuses on treatment of the affected side to facilitate normal voluntary movement, breaking up abnormal motor patterns, and reducing spasticity. It also pays attention to sensory feedback and the importance of perception in the initiation and control of movement.
- The approach of Rood [25][26], is focused on the interaction of somatic, automatic and psychic factors and their participation in the motor behavior.
- The Proprioceptive Neuromuscular Facilitation (PNF) method proposed by Kabat [27][28] is generally used in the athletic and clinical environments to enhance active and passive range of motion in order to optimize motor performance and rehabilitation [29].

In addition to rehabilitation techniques mentioned above, advances in the field of neuroscience are helping to better understand the mechanisms of brain plasticity that offer the possibility of recovery, several innovative and promising approaches have been developed, such as:

- *Mirror therapy:* observing the reflection of a movement performed by the healthy limb can improve the recovery of the affected limb behind the mirror [30] (Fig.1.3). This method consists in observing and moving the reflection of the hand of the healthy limb which gives the illusion of displacement of the injured hand located behind the mirror.

Figure 1.3: Mirror therapy [31]

- *Functional Electrical Stimulation (FES):* It consists of the continuous application of an electrical current to the skin, at a precise point facing a nerve or a muscle, to obtain contractions (Fig.1.4), which led to improvements in muscle strength, cardiovascular function and walking, which persists even after stopping the FES therapy [32].

Figure 1.4: Functional Electrical Stimulation [33]

1.5 Effectiveness of rehabilitation techniques

Even if the current state of knowledge does not allow concluding on the interest of the different approaches of therapies, nor that one treatment is more effective than any

other [34][35][36][37], there are a number of factors that contribute significantly to the improvement and acceleration of motor recovery. First of all it is recommended to start rehabilitation as soon as possible [3]. In addition, intense, active, and repetitive therapy promotes faster and better recovery [38][39][40][41]. Also the involvement of the patient and the respect of his intentions during exercises are paramount [35]. As the number of disabled patients is growing, providing appropriate treatment can become increasingly difficult given its long term and intensive nature.

Robotic systems have the capacity to meet this increasing demand. They can provide a permanent and intensive rehabilitation for a long time periods [4]. With the use of such robotic systems, patients may receive treatment at home and without the therapist assistance, allowing highly repetitive movement training and considerably reduced costs. Besides, they can precisely provide measurements and quantitative data to evaluate the patient's recovery. In addition, the use of specially designed virtual games can provide more entertaining therapy and encourage patients to put more effort into the exercises. These systems are classically distinguished into two categories: end-effector robots (Fig. 1.5a) that interact with the user at a single point (usually the hand), and exoskeletons (Fig. 1.5b) that exploit several contact points distributed along the limb. The next section reviews the existing upper limb rehabilitation robots.

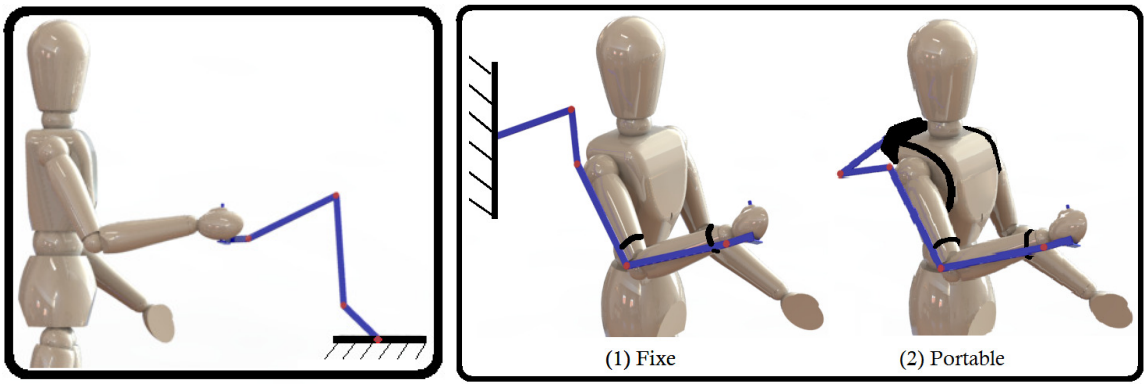

(a) (b)

Figure 1.5: Upper limb rehabilitation robots: (a) End-effector robots, (b) Exoskeletons

1.6 End-effector robots for upper limb rehabilitation

Early research on upper limb rehabilitation robots was based on manipulator robots (also known as end-effector robots). In general, only one physical contact point is used between the extremity of the patient's limb and the end-effector of the robot. The articulations of these robots do not Match with those of the human limb. Examples of

existing end-effector robots intended for rehabilitation of the upper limb are presented below:

- *InMotion:* this robot (subsequently known as MIT-Manus) was developed by Krebs and Hogan [42] at the Massachusetts Institute of Technology (MIT) in the early 1990s. It has 2 DoF, allowing hand displacement in a horizontal plane that causes movements of shoulder and elbow joints (Fig.1.6). It is the most clinically tested rehabilitation robot [43]. Several clinical studies have been carried out with this robot on a large number of patients [44, 45, 46], these tests show that the improvement in motor abilities is greater for patients receiving robotic therapy than for those in the control group. But as these patients receive robotic therapy in addition to conventional therapy, this does not necessarily demonstrate the superiority of the robotic therapy over the conventional one, but at least the robotic solution offers the possibility of more intensive and efficient therapy.

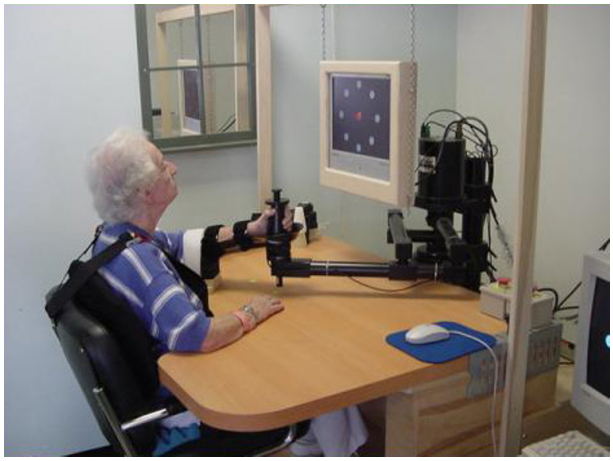

Figure 1.6: InMotion (or MIT-Manus) [46]

- *Assisted Rehabilitation and Measurement-guide:* the ARM-guide robot developed by the Chicago Institutes of Rehabilitation and the university of California. It consists of a handle mounted on an actuated linear slide which is itself attached to a system allowing two passive rotations and equipped with electromagnetic brakes. This mechanism allows the orientation of the actuated slide in the three space axes (Fig.1.7). This system is able to assist the patient in an active or constrained way, and it is possible to measure the displacements and the efforts generated by the patient [47, 48].

Figure 1.7: Assisted Rehabilitation and Measurement-guide (ARM-guide) [47]

- *Mirror-image movement enabler (Mime):* this robot was developed at Stanford University, from the industrial robot Puma562. The particularity of this robot is the ability to study Methods of mirror therapies. The Mime's end-effector is fixed to a splint in which the patient places his forearm [49, 50], allowing it to perform large amplitude movements in a 3D space. In addition to the conventional modes, the Mime robot allows a "Mirror" rehabilitation mode, using a second passive device to measure the position and orientation of the healthy limb while the robot assisted the affected limb by guiding the latter along a trajectory symmetrical to that achieved by the healthy limb (Fig.1.8).

Figure 1.8: Mirror image movement enabler (Mime) [51]

- The GENTLE/s is based on neuro-physical rehabilitation approach aiming to develop haptics and Virtual Reality (VR) technologies to provide challenging and motivating therapies to upper limb impaired stroke patients. This system, aims

to increase the sensory input, relearning stimulation in the brain, and improve independence and coordination during movements [52, 53, 54, 55]. Fig. 1.9 show the GENTLE/s system.

Figure 1.9: The GENTLE/s system [55]

This type of robots is simple, easier to manufacture, and can be easily adjusted to fit different arm lengths of patients. However, determining the posture of the arm is relatively difficult with only one contact point, especially if the contact interface is on the patient's hand. Also, the control of all joint torques of the limb is impossible. As a result, the generation of an isolated movement of a single joint of the limb is difficult since movement of the effector causes a combination of movements at the wrist, elbow and shoulder joints. Moreover, the range of motion of these robots tends to be limited, therefore only a limited set of rehabilitation exercises can be produced. In the following section, exoskeletons for upper limb rehabilitation are presented and examples of existing systems are thus described.

1.7 Exoskeletons for upper limb rehabilitation

Recently, research in rehabilitation robotics has been oriented towards exoskeletons. These robotic devices have a structure which resembles the human limb, with a joint axes matching the articulations of the limb. Exoskeletons are designed to function side by side with the limb, thus, they can be attached to the limb in more then one location. Several contact points allows the exoskeleton to fully determine the posture of the limb and apply torques to each joint separately, but this may make adaptation to different arm lengths and morphologies more difficult. Furthermore, exoskeletons have the ability to target specific muscles during exercises by generating a calculated combination

of efforts at certain joints. In addition, a greater amplitude of movements can be realized compared to end-effector robots, which allows a greater variety of movements in rehabilitation exercises.

In the 1960s, Ralph Mosher, an American engineer working for General Electric, developed an exoskeleton called Hardiman (Fig.1.10). This was the first serious attempt to manufacture a motorized exoskeleton. The mechanical combination is composed of arms and legs. Despite the great hopes that General Electric had for Hardiman, the machine weighed in three-quarters of a ton, and any attempts to make it work properly ended in failure. Only one of its arms was finally used in the 1970s [56].

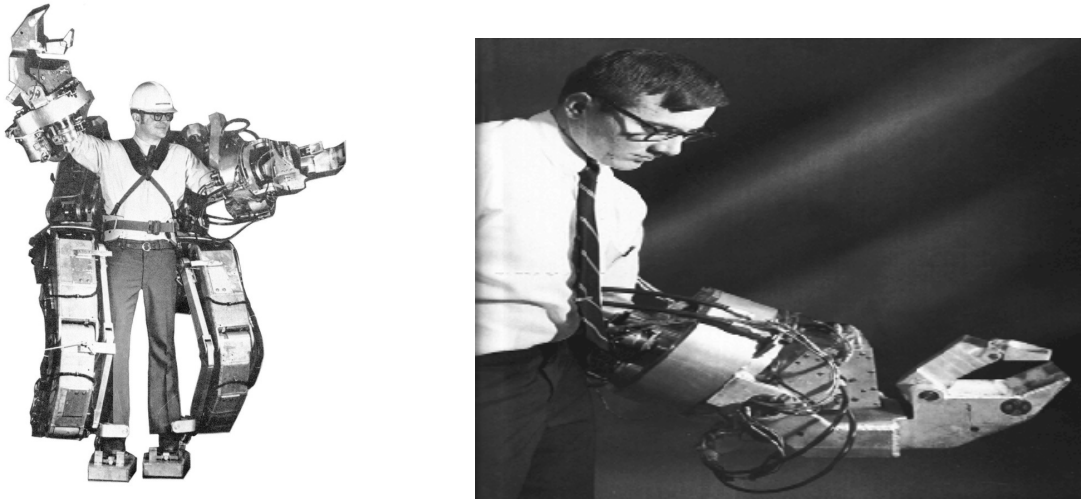

Figure 1.10: The Hardiman exoskeleton prototype of General Electric [57]

Numerous exoskeletons intended for rehabilitation have been developed in recent years, many of which are described in the rest of this section.

- *ARMin:* the first version of this robot (ARMin I) was presented in 2005 [58]. The ARMinIII version as shown in Fig.1.11, has 6 active DoF, three for the shoulder, one for the elbow, and two for the wrist, which provides an important workspace. In addition it has a passive 3 DoF adjustment system to match the robot's ball joint with the subject's shoulder. Also the lengths of the robot segments are adjustable to fit with the different user's morphologies [59][5]. The system is equipped with an haptic feedback interface and an audiovisual interface to illustrate tasks and movements to the patient. This can increase motivation and involvement of the patient during exercises, and therefore the progress of therapy [60].

Figure 1.11: The Armeo power system, commercial version of ARMinIII [61]

- *Cable Actuated Dexterous Exoskeleton for Neurorehabilitation (CADEN-7):* developed at the University of Washington. The device has 7 active DoF [62], which 4 of them are positioned on the fixed base (Fig.1.12). In addition to EMG signals, the exoskeleton is equipped with several force sensors to enable the use of force control [7].

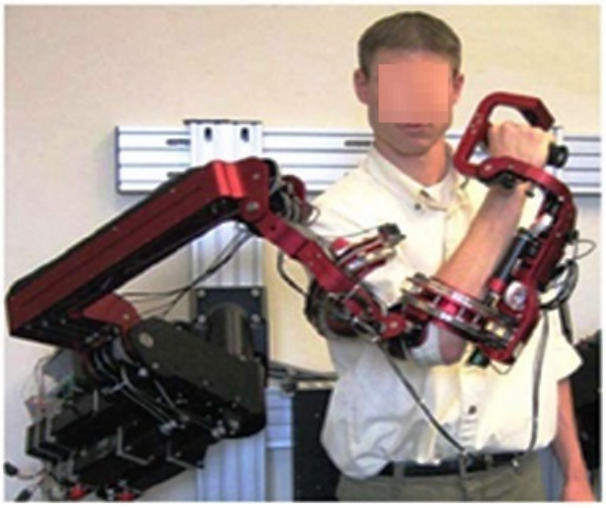

Figure 1.12: The CADEN-7 exoskeleton of the University of Washington [7]

- *Maryland Georgetown Army (MGA):* collaboration between Georgetown University and the University of Maryland has resulted in the development of a 5 DoF, exoskeleton for upper limb rehabilitation, that takes into consideration the complex movements of shoulder scapula [63]. This exoskeleton (Fig.1.13) is electrically powered, allowing a light and powerful design. Each joint of MGA is actuated by a brushless DC motor, while encoders and force sensors are mounted on the shoulder, elbow and wrist joints. The transmission train is able to exert a torque up to 92 Nm on the shoulder [64, 65].

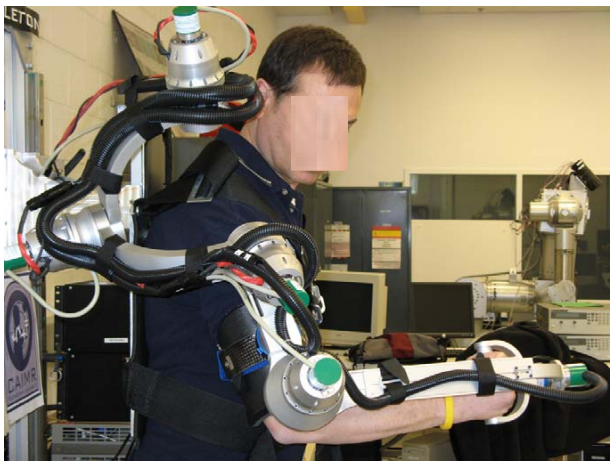

Figure 1.13: The MGA exoskeleton [65]

- *Light Exoskeleton (L-Exos):* is a force feedback exoskeleton for the right arm (Fig.1.14). It can provide either active orientation or active arm weight compensation during the exercise [66]. L-Exos has 5 DoF, which 4 of them are active and used to actuate the abduction / adduction, flexion / extension, and inner / outer shoulder movements, as well as the elbow flexion / extension joint, and one passive joint corresponding to the pronation / supination of the wrist [4].

Figure 1.14: The L-Exos force feedback exoskeleton [4]

- *Robot assisted UPper Extremity Repetitive Therapy (RUPERT):* (shown in Fig. 1.15) is a 5-DOF upper limb pneumatic exoskeleton. The device is equipped with artificial pneumatic Muscles Actuators (pMA) at the shoulder, elbow and wrist

joints. Aiming to get more effective functional recovery, RUPERT is designed to assist repetitive therapy tasks of daily living activities. Because of its low-cost, lightweight, and ease to wear this device is very portable [8].

Figure 1.15: RUPERT IV [8]

- *Pneumatic Upper Body Rehabilitation Exoskeleton:* (shown in Fig. 1.16) is a 7-DOF upper body rehabilitation exoskeleton developed by Tsagarakis and Caldwell [67], using pneumatic muscle actuators. The use of pneumatic muscles allows an excellent power to weight ratio, therefore this exoskeleton weighs less than 2Kg. In addition, this type of actuator provides excellent power to weight ratio, Inherent safety, natural compliance, ease of fabrication and low cost. This type of actuator has a displacement limit which provides safety to the user. The 7-DOF allows the exoskeleton to fit with the human arm joints from the shoulder to the wrist.

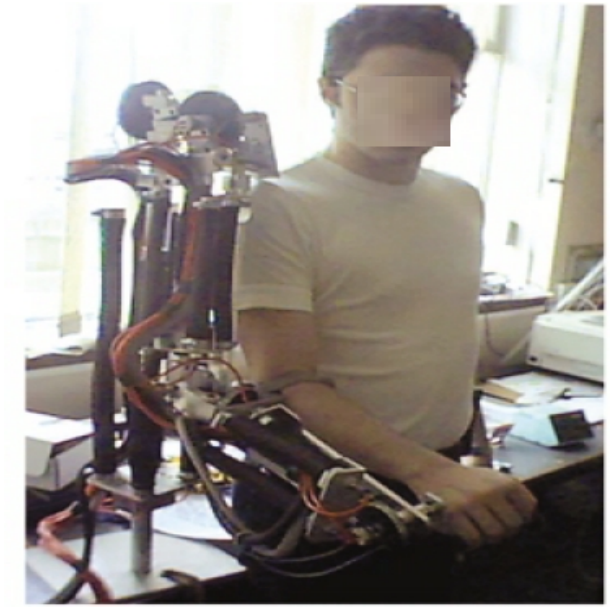

Figure 1.16: Pneumatic Upper Body Rehabilitation Exoskeleton [67]

- *ArmAssist:* (shown in Fig. 1.17) is a portable robotic device dedicated for tele-rehabilitation. The device can be used at home. It is composed of a mobile base connected to the user arm with a forearm orthesis allowing to record movements of the shoulder and elbow joints. Arm movements are animated in a video game to provide an interesting and entertaining rehabilitation experience, and helps to motivate patients. The quantitative data recorded from the games allows the therapist to evaluate and monitor the patient's performance on-line. The ArmAssist is equipped with two types of low-cost sensors, a 2-axis position and 1-axis force sensor. A tele-rehabilitation software is included with this device allowing communication between the patient and the therapist, which enables patient's training at home when the doctor can ensure that rehabilitation exercises are performed correctly. The ArmAssist is low cost, compact and weighs less than 4 kg which make it highly portable and affordable [68].

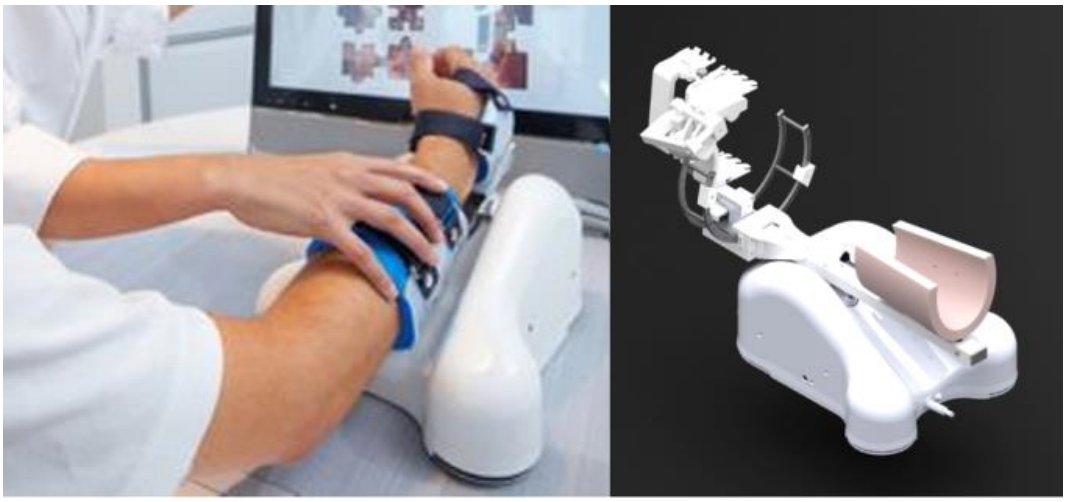

Figure 1.17: ArmAssist Exoskeleton [69]

- *MyoPro Orthosis:* (shown in Fig. 1.18) is a commercially available exoskeleton for elbow, wrist and hand active assistance. The device is driven by the user's electromyographic (EMG) signal, through patented software on-board. The device has EMG sensors placed on the limb's skin enabling detection of even a very faint muscle signal. The filtered EMG signal activates the correspondent motor to assist in completing the desired movement. MyoPro Orthosis has a range of motion from 3 to 130 degrees and weighs approximately 1.8 g and can deliver a torque of 7 Nm at the elbow and 1 to 2.7 Nm for the fingers [70].

Figure 1.18: MyoPro Orthosis [70]

- *BONES:* (shown in Fig. 1.19) is an upper limb exoskeleton that uses a parallel mechanism with mechanically grounded actuators to achieve 3 DOF shoulder movement [71]. The elbow is actuated by two pneumatic cylinders driving two rods that can also slide passively. The Range Of Motion (ROM) is close to the human one, except for the elbow joint, which have a limited flexion to prevent collusion with the subject's torso. The segments of the exoskeleton have adjustable lengths in order to accommodate a wide range of subjects. BONES targets patients with severe to moderate arm impairment. The total weight of the robot, including the mechanically grounded actuators is 18.5kg [72].

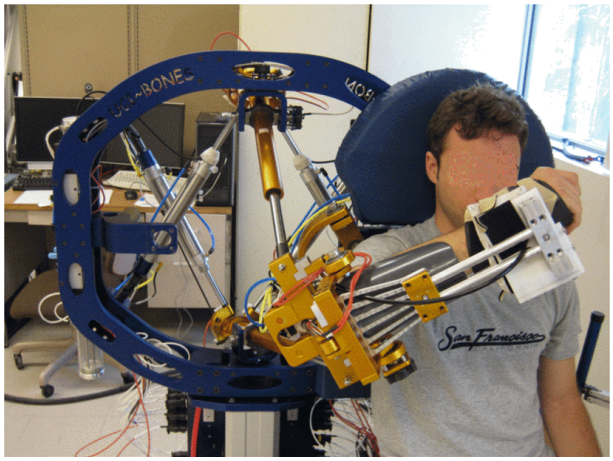

Figure 1.19: BONES Exoskeleton [72]

- *Motion Assistive Robotic-exoskeleton for Superior Extremity (MARSE-7):* (shown on Fig. 1.20) is a 7DOF robotic exoskeleton designed to provide movement assistance for daily upper-limb motion. MARSE-7 is developed to mimic the human upper limb biomechanics. The entire device is made of aluminum allowing a structure with relatively light weight with reasonable strength characteristics. This exoskeleton is intended to be worn on the lateral side of the upper limb in

order to provide shoulder, elbow and wrist joint movements. Sliding mode control strategy combined with exponential reaching law was proposed and implimented for the trajectory tracking [73].

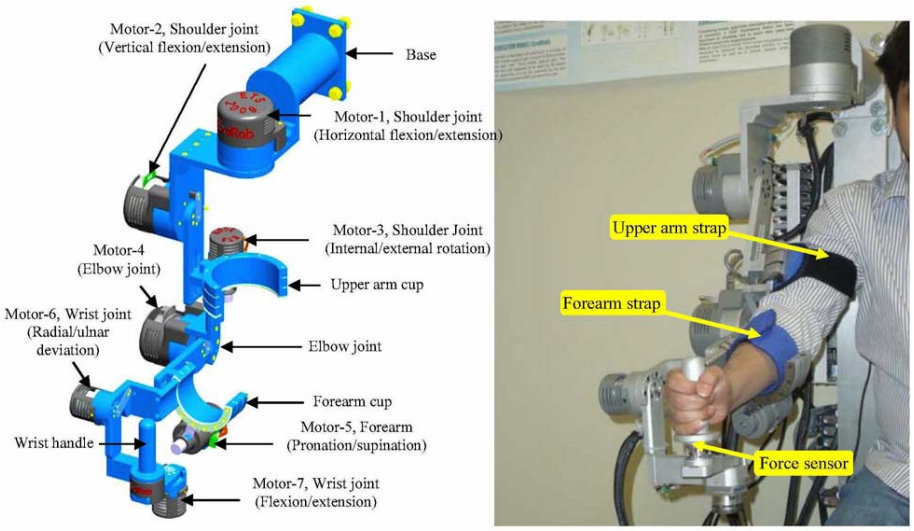

Figure 1.20: MARSE-7 upper limb exoskeleton [73]

- *Therapy Wilmington Robotic Exoskeleton:* (shown on left of Fig. 1.21) more commonly known as T- WREX, is a passive 5 DOF upper limb exoskeleton designed to provide assistance against gravity to individuals with significant arm weakness in their rehabilitation training. It provides a large 3D workspace, enabling large range of motion. This exoskeleton can achieve gravity compensation by mains of elastic bands. Joints are equipped with position sensors, and a custom grip sensor was designed to detect patient's hand grasp allowing the use of computer games during exercises. These games included activities of daily living, such as cooking, shopping, bathing, and cleaning [74]. The rehabilitative robot arm T-WREX has an active pneumatic version called Pneu-WREX shown on the right of Fig. 1.21.

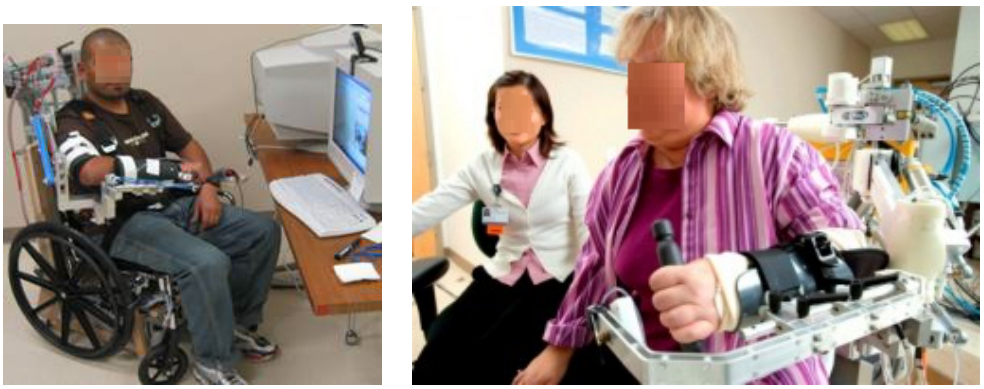

Figure 1.21: T-WREX (left) and Pneu-WREX (right) [75]

1.8 State of the art of existing control laws for rehabilitation upper limb exoskeletons

Effective upper limb rehabilitation using robotic exoskeletons needs development of control strategies able to handle the interaction with the human limb. Several control methods include position and impedance control are proposed [76, 77, 78, 65, 79]. Furthermore, it can be seen that a greater number of control strategies has been developed for end-effector robots than for exoskeletons, and therefore operating in the operational space of the arm. Somme of these commands were adapted to exoskeleton systems, but capabilities of such multi-contact systems to interact and control the interaction at the joint level are not fully exploited, because theses strategies still work in the operational space [43]. Indeed, the existing rehabilitation therapies can be classified into three different modes: *assistive*, *corrective* and *resistive*, that underlie the development of the various control strategies of exoskeletons intended to upper limb rehabilitation.

- Assistive rehabilitation: seek to help the patient to perform movements that he is unable to do alone. We can distinguish the following subcategories of this mode:
  - Passive: in this mode, the subject remains completely passive during movement while the robot drive the patient's limb during rehabilitation exercises. The system generally operates in simple position control. This mode of operation is interesting in the first phase of the rehabilitation process.
  - Assistance-as-needed: in this case, the patient is the one who initiates the movement, and the robot is there only to assist, guide, and complete this movement. This mode of therapy is adapted in rehabilitation phases where the patient has partially recovered his ability to move.
  - Active: this mode of control is not really intended for the rehabilitation but is very often used to carry out diagnostic and evaluation of movements performed by healthy or injured subjects. Generally speaking, there will be a tendency to favor control strategies that only provide the minimum assistance necessary for the subject.
- Corrective rehabilitation: in this mode, the subject realizes the movement, and the robot aims to correct it or force it to perform the gesture with a particular articular configuration, or only using certain joints or muscle groups. This mode, can come in a second phase of rehabilitation, in order to improve the way the patient performs a task.

- Resistive rehabilitation: aims to make the task more difficult to accomplish. In this case, the robot applies forces which are opposite to the desired movement, in order to encourage the patient to exercise more effort during movements.

1.8.1 Assistive control strategies

A control strategy in which robot provides the physical assistance to help the patient in accomplishing a desired movement. This strategy makes it safer and easier to accomplish tasks, allowing possibility of more intensive and repetitive therapy. In general, at early stages of the rehabilitation therapy, passive techniques are prescribed to patients, because they can not perform the exercises themselves. Passive technique is the simplest way to control an exoskeleton, the device aims to track a desired trajectory using position feedback with high tunning gains. However, high gains can compromise patient safety, so they need to be tuned carefully, to allow an acceptable level of compliance, which can provide a way to minimize undesired interaction torques [80]. This compliance can also be achieved by using pneumatic Muscle Actuators (pMA) as in [67], or by means of elastic straps which also, can dynamically compensate for some misalignment between human limb axis and those of exoskeleton.

In [8], an adaptive controller combining a PID-based feedback controller and an Iterative learning Controller (ILC-based controller) is proposed for the 5 DOF exoskeleton RUPERT. Experiments with two healthy subjects were carried on to show the ability of the proposed controller to adapt to different subject and different tasks. PID control strategy is used in [81], for a 7 DOF upper limb exoskeleton. This method allows the calculation of the PID parameters directly without exact model of the plant, when semi-global asymptotic stability is achieved. The robotic systems driven by linear controllers like PD or PID techniques are limited, unless gravity and friction compensations are applied, which requires an accurate model of the system's dynamic [4]. Many researchers have introduced gravity and friction compensation controllers [5, 65, 76, 82, 83]. To improve performances of rehabilitation robots, researchers tend to implement more and more advanced controllers. Rahman et al. in [84], proposed trajectory tracking using nonlinear computed torque control, and also a nonlinear sliding mode control implemented on MARES-7 exoskeleton in [73].

Passive control mode dose not involve the patient intentions, which remains inactive during movements without delivering any efforts. Therefore, effectiveness of passive rehabilitation remains limited to the acute stages of the rehabilitation therapy, when the patient is completely unable to move his limb. As soon as the patient starts to recover his motor capacity, the exoskeleton must let the user participate in completing

the movement [85]. Recently, assistive forces impact on motor learning rehabilitation has been the object of several recherches [47, 86]. Robot assistance during rehabilitation movements, makes patients incorporate these forces in their motor scheme, then they tend to minimize efforts in performing the desired task, which can degrade the recovery [87]. To avoid this problem it is recommended that robotic assistance remains as much as possible at a minimal amount [88], which is also known as: *assistance-as-needed [89]*. This assistance mode was adopted in several control strategies [89, 90, 91, 92].

In [90], a controller uses a standard model-based, adaptive control approach in order to learn the patient's abilities and assist in completing movements while remaining compliant is proposed. Assistance-as-needed is achieved by using force reducing term in the adaptive control law, allowing to minimize the force applied by the robot when errors in are small. Experiments were carried out using the Pneu-WREX exoskeleton to evaluate the performance of the proposed controller with stroke patients. Experiments show that including assist-as-needed technique to the controller increases participation from the motor system.

Another approach presented in [91], proposes an assist-as-needed protocol, consisting in a minimum robot assistance which is continuously adjusted during movement. To stimulate proprioceptive functions, trials were alternated with and without vision. Nine chronic stroke patients participated in the study, which consisted of a total of ten 1-hour exercise sessions. Testes show that, subjects exhibited an increased amount of voluntary control. Moreover, training without vision appeared to be beneficial for patients with abnormal proprioception. Alternating trials between vision and no-vision blocks can improve the proprioception ability as well as its integration it with vision.

In [92], haptic robot Braccio di Ferro is used with a tracking task. The proposed controller is based on three modules:

- Force field generator which combines a non linear attractive field and a viscous field;
- Performance evaluation module;
- Adaptive controller.

The force field's gain is progressively decreased and the controller remembers the minimum gain achieved in a session and propagates it to the next one. Initialization of the assistance gains is chosen according to a minimal assistance strategy. Ten chronic hemiplegic patients participated in the trials. Preliminary results show robustness of the

proposed controller, which provides a significant improvement in performance indicators as well as a recalibration of the visual and proprioceptive abilities.

There is also a particular control mode implemented on bi-manual systems. The idea is to drive movements of the injured limb connected to a slave robot, with the movements of the healthy limb acting on a master system. The most accomplished systems using this technique to date are the MIME [49] and Bi-manu Track [93].

1.8.2 Corrective control strategies

Corrective control can be performed by applying forces along the orthogonal direction of the desired movement, which aims to correct the way the task is accomplished. This correction can be achieved by Tunneling, which consists in adding virtual channels for the exoskeleton position (which can be applied in the operational space or in the articular space), in which the subject moves. when he starts to move away from the channels, the controller apply a corrective force field to get him back into the channel.

In [94], control strategies to enhance transparency and to constrain movement with virtual tunnels are presented. ARMin and Lokomat rehabilitation exoskeletons for upper and lower extremities, respectively are used. The proposed controller aims to improve transparency in free movements inside an allowed spatial region, and which impose movement constraints to confine the user to this allowed region. Experimental results show that, both transparent control with imposed motion constraints can be realized effectively.

Stroke patients often show pathologic muscle co-activation [95], and a loss of joint coordination [96]. Theses abnormal movement coordinations are known in clinical rehabilitation as pathological synergies. Another way to achieve corrective mode is to introduce correction on the joints pathological synergies. In [97], a controller aiming to reproduce the physical therapist corrections was developed. No desired trajectory is imposed on the patient's hand, only the coordination law is acting during movements. Principal Component Analysis (PCA) is used to describe joint velocities synergies, in order to characterize the patient's movements, with or without the assistance, and to program the exoskeleton during trials. Experimental results demonstrate that the programed joint coordinations was enforced, without significantly modifying the trajectory of the hand.

The Arm Coordination Training 3-D (ACT 3D) robotic system (shown on Fig. 1.22), based on modified HapticMASTER robot (developed by FCS Control Systems, The Netherlands), is used to provide additional insight into the dynamic expression of the

upper limb synergies. The device can measure joint torques during motion and provide levels of partial assistance to the arm. Protocol and clinical applications are discussed in [98].

Figure 1.22: Arm Coordination Training 3-D (ACT 3D) robotic system [99]

1.8.3 Resistive control strategies

The role of exoskeleton is not to replace the human limbs but only to assist them. Users are still required to keep physical activities like walking, shopping and doing other daily tasks. The misuse of robots to assist activities of daily living can cause muscle degeneration, especially for long term users. In order to handle this problem, the exoskeleton should provide a resistant mode exercises to improve muscles strength. Resistive force field was proposed by Shadmehr and Mussa-Ivaldi in [100], to study how the motor control system adapts to a change in the dynamics of a well-rehearsed task. A 2 DOF planar manipulator was used and arm movements were made by the subject while grasping the handle of the manipulator. The location of the handle as well as reaching movement targets were displayed on a monitor placed in front of the subject.

In [101], a 2 DOF end-effector robot is used to study the effects of a disturbance force orthogonal to the speed, applied to patient's hand. Error augmentation can also be virtual, by using a visual return depending on the performance of the subject when obscuring the direct visual return. Wei et al. in [102], developed a real-time controller for a 2 DOF robotic system using xPC Target. This system was used to investigate how different methods of performance error feedback, can lead to faster and more complete motor learning. Early results suggest that error augmentation can facilitate neurorehabilitation strategies in brain injuries such as stroke. The above mentioned control strategies were applied to end-effector robots, and to our knowledge, there are no resistive controllers developed for exoskeletons. However, this control techniques could be adapted to be used with exoskeletons.

1.9 Conclusion

Rehabilitation is the most important treatment for patients with motor impairment. It has undergone several developments, from the traditional rehabilitation through the use of end-effector systems to multi-contact exoskeletons. In the future, rehabilitation robots are expected to play an important role in physical therapy, as they provide consistent and maintainable therapy when reducing significantly the costs. In addition the use of virtual reality games increase motivation and implication of patients during rehabilitation exercises, which can improve significantly their recovery. As we see robotic technologies become more efficient, we should see more wearable technologies such as exoskeletons appearing.

Many robotic systems dedicated to upper limb rehabilitation have been developed to date. These robotic devices are of very varied design and conception, attempting to manage safety needs and ability of fine interaction with the user. The clinical tests carried out with end-effector robots allowed to show the effectiveness and advantages of robotic rehabilitation [103][49][104][105][50][106]. Despite of their simplicity and ease of use, end-effector rehabilitation systems show some limits in their interaction capabilities with the affected limb, due to the fact that they interact with the limb in one location (the hand in general), and also their limited work space. Therefore, recent recherches are tending to focuses on the development of exoskeletons, which have the ability to target specific articulations (or segments) of the limb separately during rehabilitation, as they interact with the subject member at several contact points, which seems very interesting in this type of therapy.

Indeed, we can distinguish two major complexities of upper limb exoskeletons, limiting their abilities. One is the important weight of theses devices, because if we cannot transfer the weight of the exoskeleton to the ground, then the weight must be borne by the wearer, which cannot be allowed for disabled people. The other one is the complexity of the upper limb which has 9 DOF, without counting the fingers joints. Therefore, design of actuators and control strategies is very challenging to replicate all the arm movements and rang of motion with a compact and light weight system. The rehabilitation devices presented in this chapter are only some of the available systems, to provide an overview of recent developments in the field. The interaction capabilities of exoskeletons mentioned above motivated our choice of using the exoskeleton ULEL in the framework of this thesis, which will be presented in the next chapter.

Chapter 2

Exoskeleton modelization and parameter identification

Contents

2.1 Introduction

The system considered in this study is the exoskeleton ULEL[1] (Fig.2.1), which is specially designed by RB3D[2] company for LISSI[3] Laboratory of University Paris-Est

[1]Upper Limb Exoskeleton of LISSI
[2]www.rb3d.com
[3]Laboratoire Images, Signaux et Systèmes Intelligents

Créteil in France. ULEL is designed with 3 active DoF, to be worn on the lateral side of the upper limb, allowing it to provide effective rehabilitation for the shoulder (flexion / extension), elbow (flexion / extension) and wrist (flexion / extension) movements. These characteristics are detailed in Section 2.2.

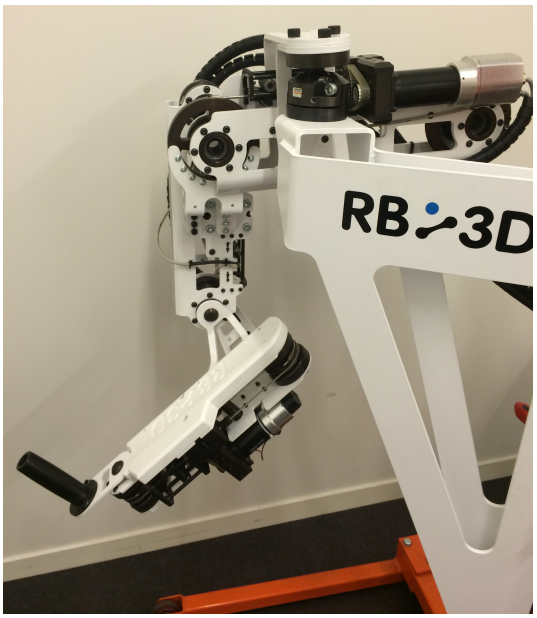

Figure 2.1: The exoskeleton ULEL

One of the first steps in our work was to set up conventional models, such as geometric, kinematic and dynamic models. In addition, a dynamic multi-body model based on a complete CAD model of ULEL is developed using the SimMechanics library of Simulink-MatLab software. The main elements of this work and the results are presented in section 2.3.

Whether for dynamic control that uses the inverse dynamic model or for the dynamic simulations that uses the direct dynamic model, it is necessary to have a good knowledge of the dynamic parameters numerical values. In this chapter, we show how to exploit the linearity of the dynamic model with respect to these parameters in order to identify them. The principle is then to seek the solution of an over-determined linear system in the sense of least squares. It is assumed that the geometric parameters are known.

2.2 Mechanical design of ULEL

ULEL has 3 active revolute joints allowing the movements of flexion/extension for the shoulder, elbow and wrist joints. Besides, it is connected to a frame base with a passive ball joint which can be blocked or released by means of an adjustable friction system. The mechanical architecture of ULEL is illustrated in Fig.2.2

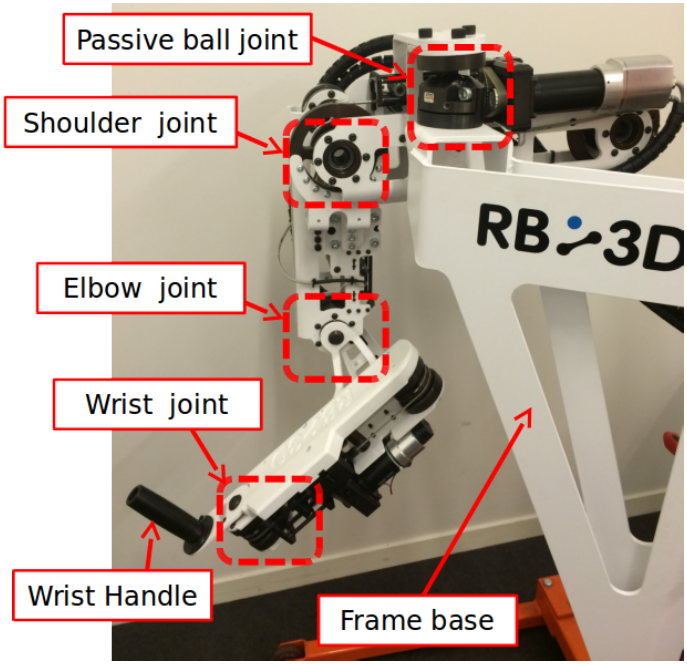

Figure 2.2: Mechanical architecture of ULEL

Indeed ULEL is made up of four modules. The frame module (base) has a height adjustable stand with a hydraulic system, thereby matching the shoulder axis of the exoskeleton with that of the subject. The carrier of the frame module is movable using wheels, which one of them has a brake. This system allows operating without the exoskeleton lifted by the subject. The shoulder module contains a revolute joint with an on-board actuator and it is connected with the frame by a passive adjustable ball joint. The arm module mounted on the shoulder embeds the actuator corresponding to the elbow joint. Finally, the wrist is powered by the on-board actuator on the forearm module. The actuation and transmission system of ULEL is based on an embedded Screw and Cable System [107]. Each joint is provided with a DC Brushes motor and an encoder to measure the angle of rotation. ULEL is supposed to be in direct interaction with the user, that's why safety is very important. Thus a power-off applied brake and limit switches are added to each active joint. Some specifications of the three ULEL active axis are summarized in Table.2.1.

The actuation and transmission system of ULEL is based on an embedded Screw and Cable System (SCS) [108]. The joint is driven by a standard push-pull cable while the cable is driven on one side by a ball-screw locked in rotation, which translate directly in its nut without any linear guiding as shown in Fig.2.3. This system enables high operational torques thanks to high reduction ratios. Besides, it allows high reversibility and backdrivability. The alignment of the motor shaft with the cable provides a compact size of the structure which means low inertia.

Table 2.1: Mechanical characteristics of ULEL

Joint	Shoulder	Elbow	Wrist
Movements	Flexion/Extension		
Motors	DC Brushes	DC Brushes	
Transmission	Screw and Cable System (SCS)		
Amplitude (deg)	90	120	80
Transmission Ratios	251.3	167.6	47.1
Nominal speed (rpm)	18.39	41.93	149
Joint nominal torque (Nm)	85.08	23.9	6.72
Motors power (W)	200	150	150

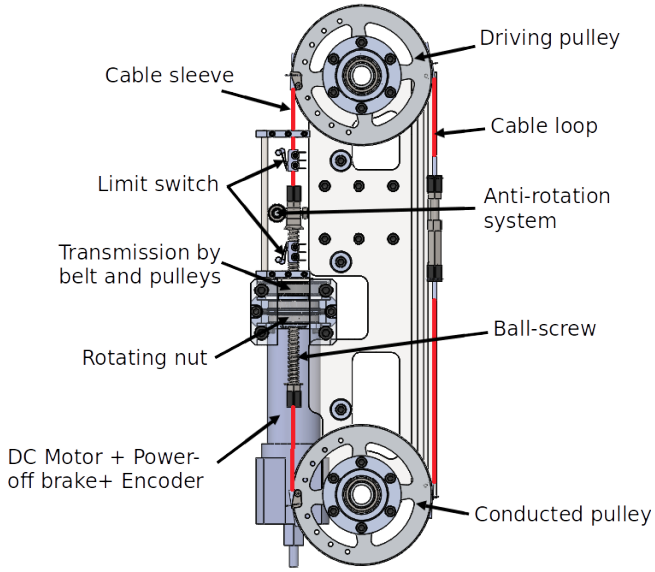

Figure 2.3: Embedded shoulder actuator

2.3 Modeling

Modeling has an important role in the characterization of the used device and in the design process of eventual controllers. Models are used to carry out simulations in order to test the behavior of the system and to study and validate control schemes safely. Also, they are used to identify the kinematic and dynamic parameters that are required for control and simulations.

The exoskeleton ULEL is modeled using a modified Denavit-Hartenberg (DH) notation [109]. The orientation of the axes is defined by considering the measured joint position zero, for which the arm and forearm hang vertically downwards and the wrist axis is perpendicular to the frontal plane (Fig.2.4).

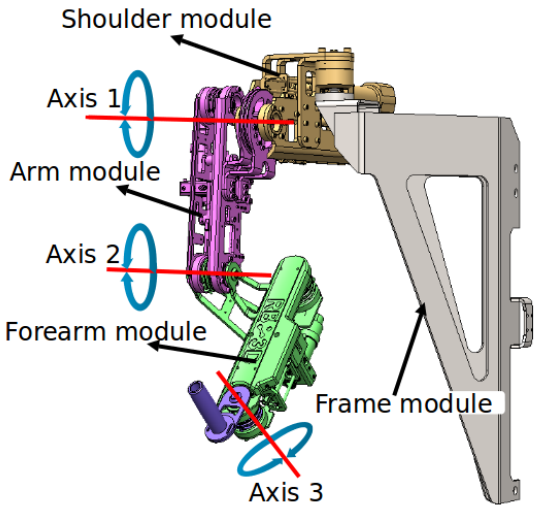

Figure 2.4: CAD model of the exoskeleton ULEL (with the permission of RB3D)

The kinematic diagram of the exoskeleton ULEL is shown Fig.2.5, where $R_i(O_i, x_i, y_i, z_i)$ is the frame attached to the link i and q_i is the joint angle such that: $q = \begin{bmatrix} q_1 & q_2 & q_3 \end{bmatrix}^T$.

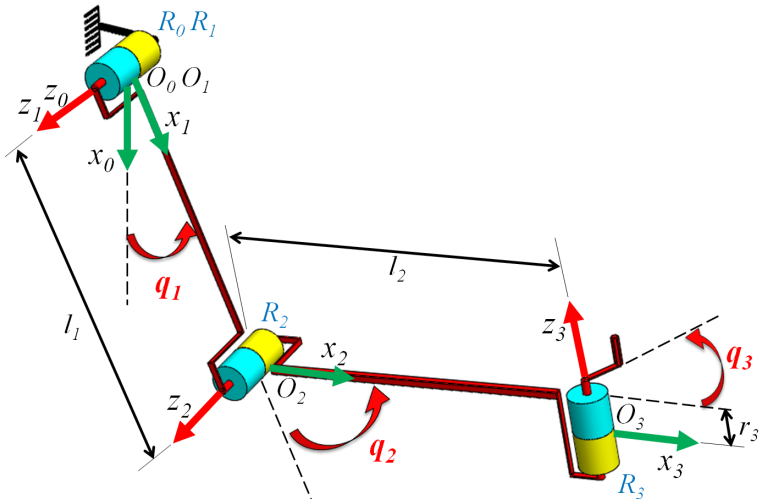

Figure 2.5: Kinematic diagram of ULEL

The possible range of motion of ULEL joints, with the limit switches, is listed in Table. 2.2

Joint	Corresponding articulation	Range of motion (deg)
q_1	Flexion/extension of the shoulder	$0 \rightarrow 90$
q_2	Flexion/extension of the elbow	$10 \rightarrow 110$
q_3	Flexion/extension of the wrist	$-40 \rightarrow +40$

Table 2.2: Range of motion of ULEL

2.3.1 Geometric model

The Direct Geometric Model (DGM) allows to express position and orientation of the end-effector (the wrist handle in our case) as a function of the joint positions. In accordance with the DH notation [110], the general transformation matrix defining frame R_i relative to frame R_{i-1} is given as

$$
{}^{i-1}T_i = \begin{bmatrix} cos(\theta_i) & -sin(\theta_i) & 0 & d_i \\ cos(\alpha_i)\, sin(\theta_i) & cos(\alpha_i)\, cos(\theta_i) & -sin(\alpha_i) & -r_i\, sin(\alpha_i) \\ sin(\alpha_i)\, sin(\theta_i) & sin(\alpha_i)\, cos(\theta_i) & cos(\alpha_i) & r_i\, cos(\alpha_i) \\ 0 & 0 & 0 & 1 \end{bmatrix} \tag{2.1}
$$

where:

- α_i is the angle between z_{i-1} and z_i about x_{i-1};
- d_i is the distance between z_{i-1} and z_i along x_{i-1};
- θ_i is the angle between x_{i-1} and x_i about z_i;
- r_i is the distance between x_{i-1} and x_i along z_i.

The DH parameters (according to the plans provided by the RB3D) are given in Table.2.3.

Table 2.3: Modified Denavit-Hartenberg parameters.

i	α_i	d_i	θ_i	r_i
1	0	0	q_1	0
2	0	l_1	q_2	0
3	$-\frac{\pi}{2}$	l_2	q_3	r_3

We can use (2.1) to compute the successive transformation matrices ${}^0T_1$, ${}^1T_2$ and ${}^2T_3$:

$$ {}^0T_1 = \begin{bmatrix} C_1 & -S_1 & 0 & 0 \\ S_1 & C_1 & 0 & 0 \\ 0 & 0 & 1 & 0 \\ 0 & 0 & 0 & 1 \end{bmatrix} $$

$$ {}^1T_2 = \begin{bmatrix} C_2 & -S_i & 0 & l_1 \\ S_2 & C_2 & 0 & 0 \\ 0 & 0 & 1 & 0 \\ 0 & 0 & 0 & 1 \end{bmatrix} $$

$$ {}^2T_3 = \begin{bmatrix} C_3 & -S_3 & 0 & l_2 \\ 0 & 0 & 1 & r_3 \\ -S_3 & -C_3 & 0 & 0 \\ 0 & 0 & 0 & 1 \end{bmatrix} $$

where $C_i = cos\,(q_i)$ and $S_i = sin\,(q_i)$.

The multiplication of these matrices and after simplification gives the above transformation matrix

$$ {}^0T_3 = \begin{bmatrix} C_{12}C_3 & -C_{12}S_3 & -S_{12} & l_1C_1 + l_2C_{12} - r_3S_{12} \\ S_{12}C_3 & -S_{12}S_3 & C_{12} & l_1S_1 + l_2S_{12} + r_3C_{12} \\ -S_3 & -C_3 & 0 & 0 \\ 0 & 0 & 0 & 1 \end{bmatrix} \tag{2.2} $$

where $C_{ij} = cos\,(q_i + q_j)$ and $S_{ij} = sin\,(q_i + q_j)$.

It is well known in robotics [109] that for any arbitrary point P located at the Cartesian coordinates $({}^iP_x, {}^iP_y, {}^iP_z)$ with respect to the frame R_i, the computation of the Cartesian coordinates $({}^jP_x, {}^jP_y, {}^jP_z)$ of P with respect to an other frame R_j can be obtained by

$$ {}^jP = {}^jT_i\,{}^iP \tag{2.3} $$

where

$$ {}^iP = \begin{bmatrix} {}^iP_x \\ {}^iP_y \\ {}^iP_z \\ 1 \end{bmatrix}, \; {}^jP = \begin{bmatrix} {}^jP_x \\ {}^jP_y \\ {}^jP_z \\ 1 \end{bmatrix} \tag{2.4} $$

are the homogeneous coordinates of P with respect to R_i and R_j respectively.

Let $({}^3P_x, {}^3P_y, {}^3P_z)$ be the Cartesian coordinates of one terminal fixed point in the frame R_3 of ULEL. The absolute Cartesian coordinates of this position in the frame R_0 can be given by

$$\begin{bmatrix} {}^0P_x \\ {}^0P_y \\ {}^0P_z \\ 1 \end{bmatrix} = {}^0T_3 \begin{bmatrix} {}^3P_x \\ {}^3P_y \\ {}^3P_z \\ 1 \end{bmatrix} \tag{2.5}$$

Using (2.2) and (2.5) it yields

$$\begin{cases} {}^0P_x = {}^3P_x C_{12}C_3 - {}^3P_y C_{12}S_3 - {}^3P_z S_{12} + l_1 C_1 + l_2 C_{12} - r_3 S_{12} \\ {}^0P_y = {}^3P_x S_{12}C_3 - {}^3P_y S_{12}S_3 + {}^3P_z C_{12} + l_1 S_1 + l_2 S_{12} + r_3 C_{12} \\ {}^0P_z = -{}^3P_x S_3 - {}^3P_y C_3 \end{cases} \tag{2.6}$$

Having calculated the DGM of ULEL, in the next section we perform the computing the kinematic model.

2.3.2 Kinematic model

By considering the point $({}^3P_x, {}^3P_y, {}^3P_z)$ as the terminal point of ULEL, the DGM is:

$$X = \begin{bmatrix} {}^0P_x \\ {}^0P_y \\ {}^0P_z \end{bmatrix}$$

where ${}^0P_x$, ${}^0P_y$ and ${}^0P_z$ are given in (2.6).

The Direct Kinematic Model of ULEL gives the velocity of the end-effector $\dot{X}$ in terms of the joint velocities $\dot{q}$ and it can be written as: $\dot{X} = J(q)\dot{q}$, where $J(q) \in \mathbb{R}^{3\times3}$ denotes the Jacobian matrix. The Jacobian matrix is obtained by differentiating the DGM expressions with respect to the joint positions such that:

$$J_{i,j} = \frac{\partial X_i}{\partial q_j} \tag{2.7}$$

where $J_{i,j}$ is the element (i, j) of the Jacobian matrix J, then we get

$$\begin{cases} J_{1,1} &= -l_3C3S12 - l_4C12 - l_2S12 - l_1S1 - r_3C12 \\ J_{1,2} &= -l_3C3S12 - l_4C12 - l_2S12 - r_3C12 \\ J_{1,3} &= -l_3S3C12 \\ J_{2,1} &= l_3C3C12 - l_4S12 + l_2C12 + l_1C1 - r_3S12 \\ J_{2,2} &= l_3C3C12 - l_4S12 + l_2C12 - r_3S12 \\ J_{2,3} &= -l_3S3S12 \\ J_{3,1} &= 0 \\ J_{3,2} &= 0 \\ J_{3,3} &= -l_3C3 \end{cases} \tag{2.8}$$

Computing kinematic model of ULEL using the basic Jacobian matrix allows us to compute the linear and angular velocities of the end-effector in terms of the joint velocities. The necessary tool to obtain the dynamic behavior of our exoskeleton is the dynamic model, which is the topic of the next section.

2.3.3 Dynamic model

The two models used to represent the dynamics of serial robots are:

- The Direct Dynamic Model (DDM): describes the joint accelerations as function of the joint positions, velocities and torques. It can be represented as:

$$\ddot{q} = g(q, \dot{q}, \tau) \tag{2.9}$$

- The Inverse Dynamic Model (IDM): (often called the dynamic model) provides the joint torques and forces as function of the joint positions, velocities and accelerations. It can be written as:

$$\tau = f(q, \dot{q}, \ddot{q}) \tag{2.10}$$

  where, τ is the vector of joint torques; and q, $\dot{q}$, $\ddot{q}$ are the joint positions, velocities and accelerations respectively. In general, this model is the most used in the world of robotics. In this chapter we will only detail the calculation of the IDM because we will use it in the framework of this thesis.

Several methods have been proposed to compute the dynamic model [111][112]. We have chosen to use the Lagrange formulation because it is a simple and efficient approach,

besides, the equations used have a physical meaning. Also, this model is linear with respect to inertial parameters and thereafter it will be used for the identification of these parameters.

The Lagrange formulation describes the dynamics of the system as a function of kinetic and potential energy of the system. The Lagrange equations of the exoskeleton ULEL can be written in the form:

$$\tau_i = \frac{d}{dt}\frac{\partial L}{\partial \dot{q}_i} - \frac{\partial L}{\partial q_i} \;\; ; \;\; i = 1, \ldots, 3 \tag{2.11}$$

with

- τ_i is the generalized torque in the joint i
- $L = E - U$ is Lagrangian system with E is the kinetic energy and U is the potential energy.

The kinetic energy of the system can be written in the following form:

$$E = \frac{1}{2}\dot{q}^T M(q)\, \dot{q} \tag{2.12}$$

with $M(q) \in \mathbb{R}^{3\times 3}$ is the symmetric and positive definite inertia matrix of the system

By developing the equation of kinetic energy, we obtain

$$E = \frac{1}{2}\sum_{i=1}^{3}\left[{}^{i}\omega_i^T\, {}^{i}I_i\, {}^{i}\omega_i + m_i\, {}^{i}V_i^T\, {}^{i}V_i + 2\, {}^{i}MS_i^T\, ({}^{i}V_i \wedge {}^{i}\omega_i)\right] \tag{2.13}$$

where all the elements of (2.13) are expressed in the same frame R_i, and we note:

- ${}^{i}V_i \in \mathbb{R}^3$ and ${}^{i}\omega_i \in \mathbb{R}^3$ are the linear and angular velocity of O_i expressed in the frame R_i defined as

$${}^{i}V_i = {}^{i}M_{i-1}\left({}^{i-1}V_{i-1} + {}^{i-1}\omega_{i-1} \wedge {}^{i-1}P_i\right) \tag{2.14}$$

$${}^{i}\omega_i = {}^{i}M_{i-1}\, {}^{i-1}\omega_{i-1} + \dot{q}_i\, {}^{i}a_i = {}^{i}\omega_{i-1} + \dot{q}_i\, {}^{i}a_i \tag{2.15}$$

- ${}^{i}I_i \in \mathbb{R}^{3\times 3}$ is the inertia matrix of link i expressed in O_i with respect to frame R_i, with $I_i = \begin{bmatrix} XX_i & XY_i & XZ_i \\ XY_i & YY_i & YZ_i \\ XZ_i & YZ_i & ZZ_i \end{bmatrix}$

- ${}^{i}a_i \in \mathbb{R}^3$ is the unit vector along the z_i axis in the frame R_i
- ${}^{i-1}P_i \in \mathbb{R}^3$ is the position vector between O_{i-1} and O_i expressed in the frame R_{i-1}
- $m_i \in \mathbb{R}$ is the mass of link i
- G_i denotes the center of mass of link i
- $S_i \in \mathbb{R}^3$ is the center of mass coordinates of link i. It is equal to O_iG_i
- $MS_i \in \mathbb{R}^3$ is first moments of link i with respect to frame R_i, equal to $m_i\, S_i$. The components of ${}^{i}MS_i$ are denoted by $[MX_i\, MY_i\, MZ_i]^T$

Equation (2.11) can be written in the following form [109]

$$M(q)\ddot{q} + C(q,\dot{q})\dot{q} + G(q) = \tau \tag{2.16}$$

where $q \in \mathbb{R}^3$, $\dot{q} \in \mathbb{R}^3$ and $\ddot{q} \in \mathbb{R}^3$ are the joints positions, velocities and accelerations respectively, $M(q) \in \mathbb{R}^{3\times3}$ is the inertia matrix, $C(q,\dot{q}) \in \mathbb{R}^{3\times3}$ is the Coriolis/centrifugal matrix, $G(q) \in \mathbb{R}^3$ is the gravity vector and $\tau \in \mathbb{R}^3$ is the generalized torques vector.

To calculate the elements of the matrices M, C and G, we must first calculate the kinetic (E) and potential (U) energies of the system. Then, we proceed as follows:

Calculation of the elements of the matrix M

- M_{ii} is equal to the coefficient of $\frac{\dot{q}_i^2}{2}$ in the expression of the kinetic energy
- M_{ij}, for $i \neq j$, is equal to the coefficient of $\dot{q}_i\dot{q}_j$

To calculate the elements of the matrix M, we need to compute ${}^{i}\omega_i$ and ${}^{i}V_i$ using (2.14) and (2.15).

Since the base of the ULEL is fixed, the previous equations are initialized by ${}^{0}V_0 = 0$ and ${}^{0}\omega_0 = 0$

Calculation of the angular velocities

$${}^{0}\omega_0 = \begin{bmatrix} 0 \\ 0 \\ 0 \end{bmatrix}$$

$$
{}^{1}\omega_1 = \begin{bmatrix} 0 \\ 0 \\ \dot{q}_1 \end{bmatrix}
$$

$$
{}^{2}\omega_2 = \begin{bmatrix} 0 \\ 0 \\ \dot{q}_1 + \dot{q}_2 \end{bmatrix}
$$

$$
{}^{3}\omega_3 = \begin{bmatrix} -sin(q_3)(\dot{q}_1 + \dot{q}_2) \\ -cos(q_3)(\dot{q}_1 + \dot{q}_2) \\ \dot{q}_3 \end{bmatrix}
$$

Calculation of the linear velocities

$$
{}^{0}V_0 = \begin{bmatrix} 0 \\ 0 \\ 0 \end{bmatrix}
$$

$$
{}^{1}V_1 = \begin{bmatrix} 0 \\ 0 \\ 0 \end{bmatrix}
$$

$$
{}^{2}V_2 = \begin{bmatrix} sin(q_2)\dot{q}_1 l_1 \\ cos(q_2)\dot{q}_1 l_1 \\ 0 \end{bmatrix}
$$

$$
{}^{3}V_3 = \begin{bmatrix} cos(q_3)\left(sin(q_2)\dot{q}_1 l_1 - (\dot{q}_1 + \dot{q}_2)\, r_3\right) \\ -sin(q_3)\left(sin(q_2)\dot{q}_1 l_1 - (\dot{q}_1 + \dot{q}_2)\, r_3\right) \\ cos(q_2)\dot{q}_1 l_1 + (\dot{q}_1 + \dot{q}_2)\, l_2 \end{bmatrix}
$$

Calculation of the elements of the matrix C

The C_{ij} elements of C, are calculated using the Christoffell symbols c_{ijk}, such as [109]:

$$
\begin{cases} C_{ij} &= \sum_{k=1}^{3} c_{ijk}\, \dot{q}_k \\ c_{ijk} &= \frac{1}{2}\left[\frac{\partial M_{ij}}{\partial q_k} + \frac{\partial M_{ik}}{\partial q_j} - \frac{\partial M_{jk}}{\partial q_i}\right] \end{cases} \tag{2.17}
$$

Calculation of the potential energy and elements of the vector G

The potential energy can be obtained according to:

$$
U = \sum_{i=1}^{3} U_i \tag{2.18}
$$

with $U_i = -{}^0g^T \left(m_i {}^0P_i + {}^0M_i {}^iMS_i\right)$, where g is the gravitational acceleration vector.

Then the elements of G are computed in the following way:

$$G_i = \frac{\partial U}{\partial q_i} \tag{2.19}$$

Considering the friction in the dynamic model

Regarding friction, many models exist [113][114][115]. The friction torque $D(\dot{q}) \in \mathbb{R}^n$ is usually modeled at non zero velocity as [109]:

$$D(\dot{q}) = F_c sign(\dot{q}) + F_v \dot{q} \tag{2.20}$$

where $F_c = diag(F_{ci}, \ldots, F_{cn}) \in \mathbb{R}^{n \times n}$, and $F_v = diag(F_{vi}, \ldots, F_{vn}) \in \mathbb{R}^{n \times n}$, (for $i = 1, \ldots, 3$) are the diagonal matrices of the Coulomb and viscous friction coefficients respectively.

Then, the dynamic model in (2.16) can be written as

$$M(q)\ddot{q} + C(q, \dot{q})\dot{q} + G(q) + D(\dot{q}) = \tau \tag{2.21}$$

2.4 Dynamic multi-body modeling

Simulations were carried out using a multi-body dynamic model of ULEL interacting with an articulated arm model. The mass and inertial characteristics of a typical adult's upper limb are used in the arm model (given in [116, 117]). Dynamic multi-body modeling is a safe way to test control schemes for exoskeletons because it allows simulation of both, human limb and dynamics of the exoskeleton [118]. Therefore, it can provide real-time evaluation of the interaction efforts, then in case of dangerous torque levels applied on the arm model, no human would get harmed.

The dynamic physical model is constructed from a complete CAD model and exported to Simulink-Matlab environment using the SimMechanics library as shown in Fig. 2.6.

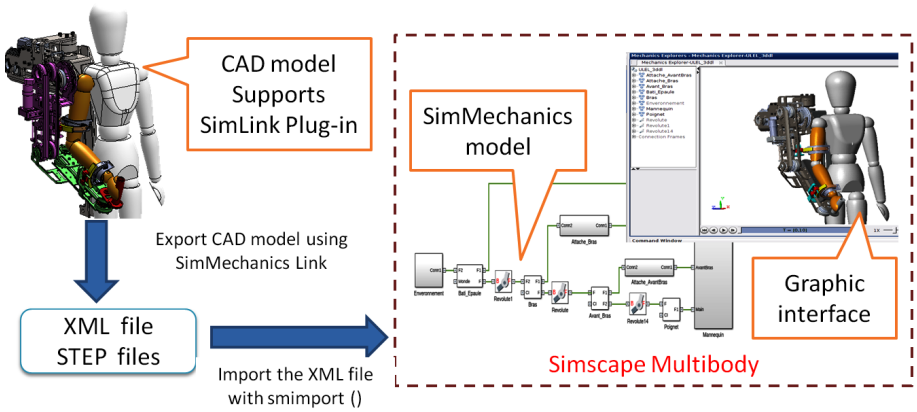

Figure 2.6: Creating the physical model using the SimMechanics library

Fig. 2.7 shows the arm model which has 7 DoF (three for the shoulder, two for the elbow and two for the wrist). This model is assembled to the exoskeleton model and used in simulations.

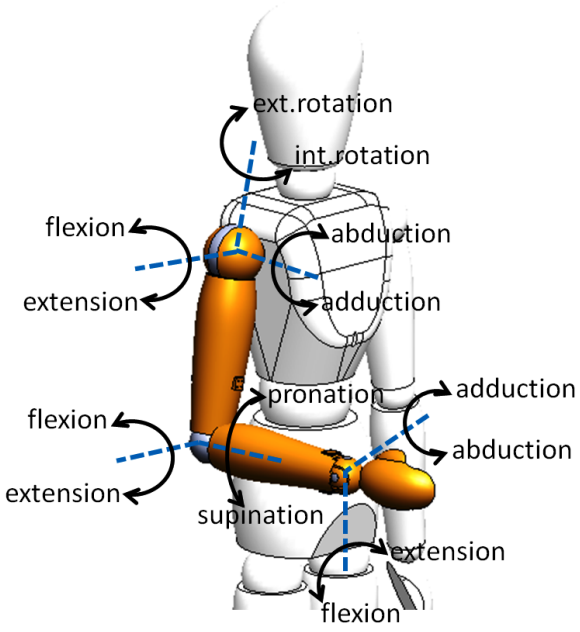

Figure 2.7: Multi-body model of the arm at the initial position

After having established the dynamic model equations, and build a multi-body dynamic model of our exoskeleton, it was necessary to determine the dynamic parameters of this model, which are typically unknown. Three main methods can be used to estimate the inertial parameters:

- Physical experiments : needs to disassemble the robot, then identify the deferent parameters (mass, coordinates of the center-of-mass, diagonal elements of the

inertia tensor, ...) by performing physical experiment on each single link. This method is very tedious and needs to be realized before assembling the robot.

- Using CAD models: in general, CAD softwares provide tools to calculate the inertia parameters from 3D models. This method gives a good approximation of the dynamic model, but it still prone to errors due to the complicated geometry of the links, and that certain parts such as bearings, bolts, and electrical parts are generally neglected.

- Identification: which is an approach based on the analysis of the "input/output" behavior of the robot under exiting trajectories, by minimizing the error between a function of the measured robot variables and its mathematical model. This method is the one used in this work, given its good precision of the identified values and ease of experimentation.

First, we need to calculate a linear form of the IDM with respect to these parameters, to be able to identify them. Calculation of the linear dynamic model is presented in the next section.

2.5 Calculation of the base dynamic parameters

The dynamic model can be written in a linear form in a set of standard dynamic parameters [119]. The base inertial parameters are the minimum set of parameters that are needed to compute the dynamic model. They are obtained from the standard inertial parameters, by eliminating the parameters that have no effect on the dynamic model, and grouping linearly some others [120].

Considering our exoskeleton ULEL which has 3 DOF, the standard dynamic parameters of link i (for $i = 1, \ldots, 3$) are: the elements of the inertia matrix

$$I_i = \begin{bmatrix} XX_i & XY_i & XZ_i \\ XY_i & YY_i & YZ_i \\ XZ_i & YZ_i & ZZ_i \end{bmatrix},$$

first moments $MS_i = \begin{bmatrix} MX_i, & MY_i, & MZ_i \end{bmatrix}^T$, the mass of the link m_i, and the Coulomb and viscous friction parameters F_{ci} and F_{vi} . We combine these standard parameters in the vector χ_{sd}, so the dynamic model (2.21). can be written as :

$$\tau = W_{sd}(\ q, \quad \dot{q}, \quad \ddot{q}\ )\chi_{sd} \tag{2.22}$$

where W_{sd} is the regressor matrix and $\chi_{sd} = [\chi_{sd}^{1T}, \chi_{sd}^{2T}, \chi_{sd}^{3T}]^T$, $\chi_{sd}^i = [XX_i, XY_i, XZ_i, YY_i, YZ_i, ZZ_i, MX_i, MY_i, MZ_i, m_i, F_{ci}, F_{vi}]^T$, for $i = 1, \ldots, 3$.

From theses standard parameters, calculation of the base inertial parameters was done using the method presented in [120], so the reduced dynamic model can be written as:

$$\tau = W(q, \dot{q}, \ddot{q})\chi \tag{2.23}$$

where $W(q, \dot{q}, \ddot{q})$ is the observation matrix, and χ is the vector of the base inertial parameters with:

$$\begin{aligned} \chi = \; & [l_1^2(m_2 + m_3) + ZZ_1, l_1(m_2 + m_3) + + MX_1, \\ & MY_1, ZZ_2 + YY_3 + 2\, MZ_3 r_3 + (l_2^2 + r_3^2)m_3, \\ & l_2 m_3 + MX_2, m_3 r_3 + MY_2 + MZ_3, XX_3 - YY_3, \\ & XY_3, XZ_3, YZ_3 ZZ_3, MX_3, MY_3, F_{c1}, F_{c2}, F_{c3}, F_{v1}, F_{v2}, F_{v3}]^T \end{aligned} \tag{2.24}$$

This linear dynamic model is used in order to identify the base inertial parameters. In the next section, experimental setup of parameter identification is presented.

2.6 Experimental dynamic parameter identification of ULEL

The exoskeleton ULEL used in this thesis, is a new prototype, and it has never been used before, so its dynamic parameters that we have mentioned earlier in (2.24), are unknown. It was then, essential to carry out the identification of theses parameters that will be needed to establish the models. A complete CAD model of ULEL was given under a confidentiality contract by the robot manufacturer. Despite the inaccuracy that CAD models can provide in general, we assume that the values of the parameters provided by Solidworks including the masses, geometric proprieties, and Cartesian coordinates of the centers of gravity, are satisfactory as a first approximation to be used in the initial condition of the identification algorithm.

The identification was carried out using a simple and fast method, by performing the following steps:

2.6.1 Identification of Coulomb and viscous friction parameters

Identification of the Coulomb (F_{ci}), and viscous (F_{vi}), friction parameters (see equation 2.20), is performed separately. The excitation movements that allow to identify

these parameters, are the axis-by-axis movements in speed increments. It consists of actuating each axis separately, with constant velocity ramps, which allows to eliminate the inertial terms from the dynamic model. In addition, the axis of the corresponding articulation is oriented in a vertical configuration with respect to the ground to eliminate the gravity effects as shown in Fig. 2.8.

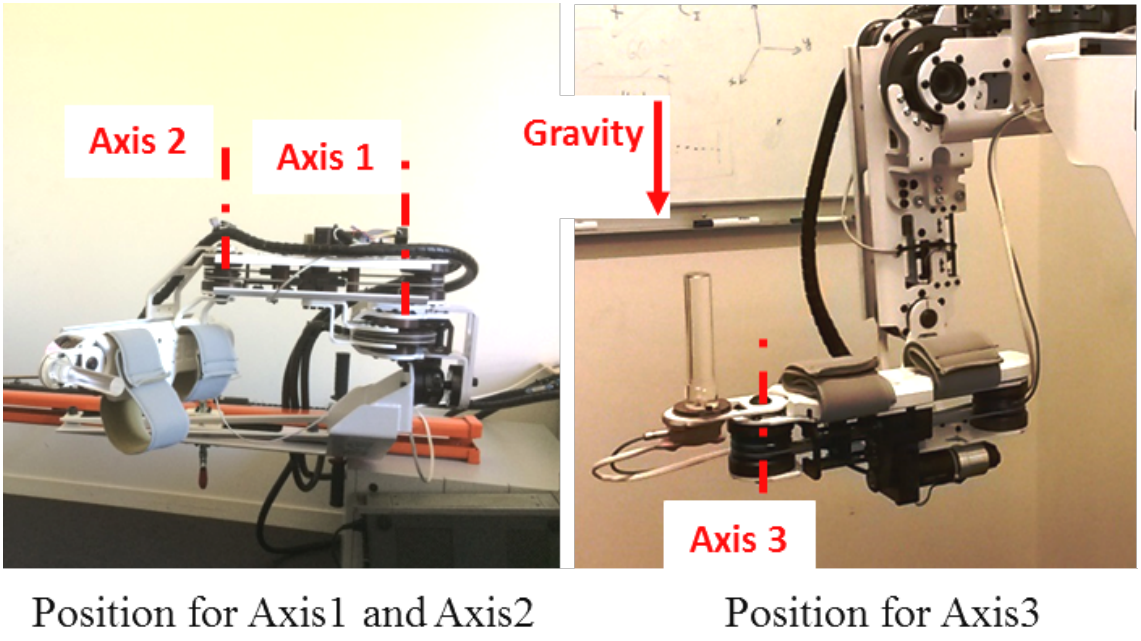

Figure 2.8: ULEL positions to eliminate the gravity effect

When only axis i is moving with a constant velocities ($\dot{q}_i = cte$, $\dot{q}_{j\neq i} = 0$ and $\ddot{q}_i = 0$), for $i = 1, \ldots, 3$, one can neglect the effects of inertia and quadratic terms of velocity ($M(q)\ddot{q} + C(q, \dot{q})\dot{q} \approx 0$). Furthermore, the rotation axis of this articulation is parallel to the gravity vector ($G(q) \approx 0$), then the dynamic model presented in (2.16) is reduced to the following equation:

$$F_{ci} sign(\dot{q}_i) + F_{vi}\dot{q}_i = \tau_i \quad \text{, for} \quad i = 1, \ldots, 3, \tag{2.25}$$

The identification is done by driving each joint separately under PD position feedback control to track constant velocity, guaranteeing low constant velocity ramps, and without any external force. During the motion of each joint, applied control currents (convertible to joint torques), as well as joint positions are recorded (see Figs. 2.9, 2.10 and 2.11)., which represents the friction torque computed via equation (2.25). To ensure consideration of only constant velocity movements, all data corresponding to the initial and final part of movement in each ramp were excluded. The average applied torque during each constant velocity ramp is considered as the joint friction torque.

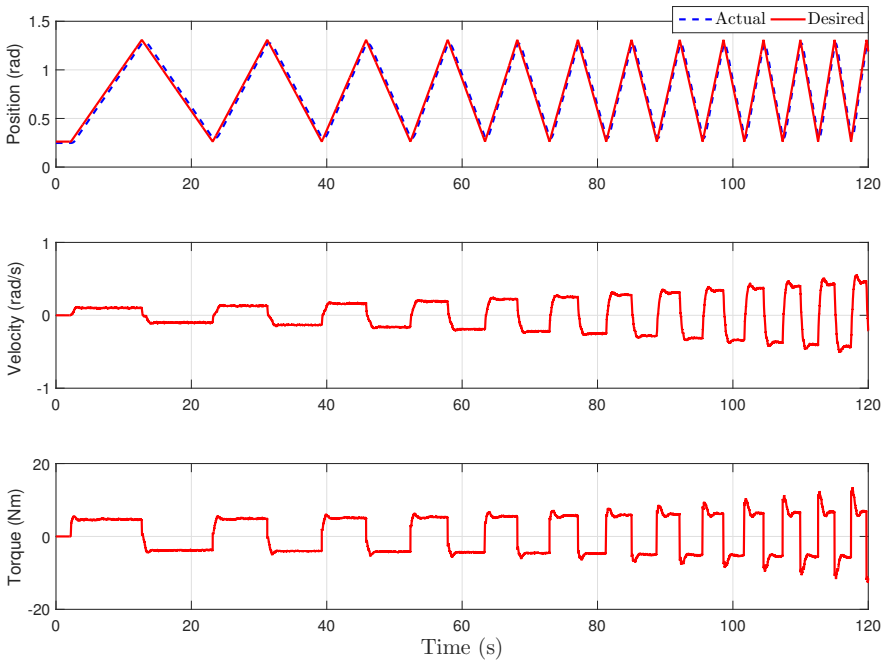

Figure 2.9: Applied position, velocity and torque for joint 1

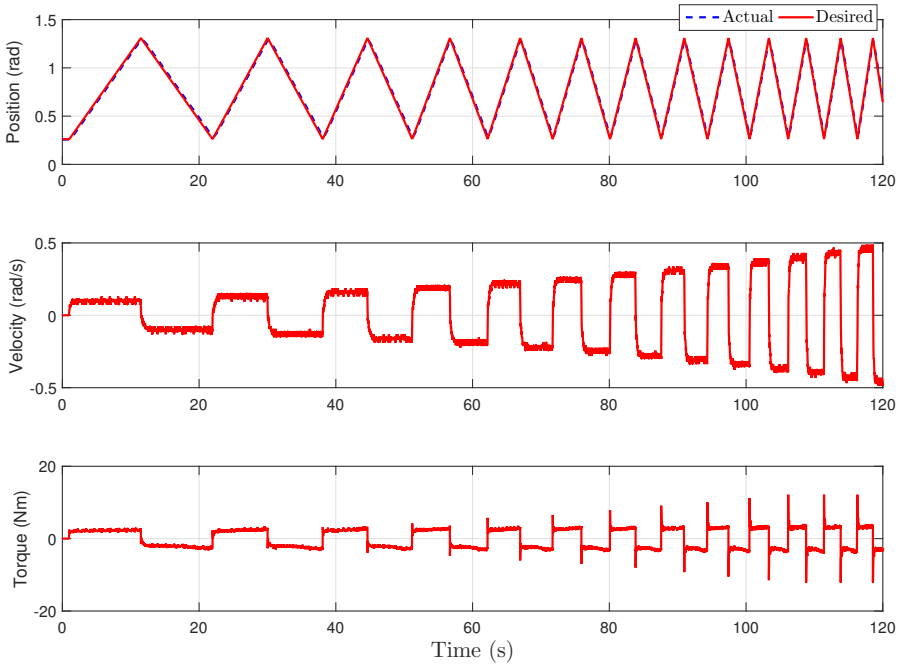

Figure 2.10: Applied position, velocity and torque for joint 2

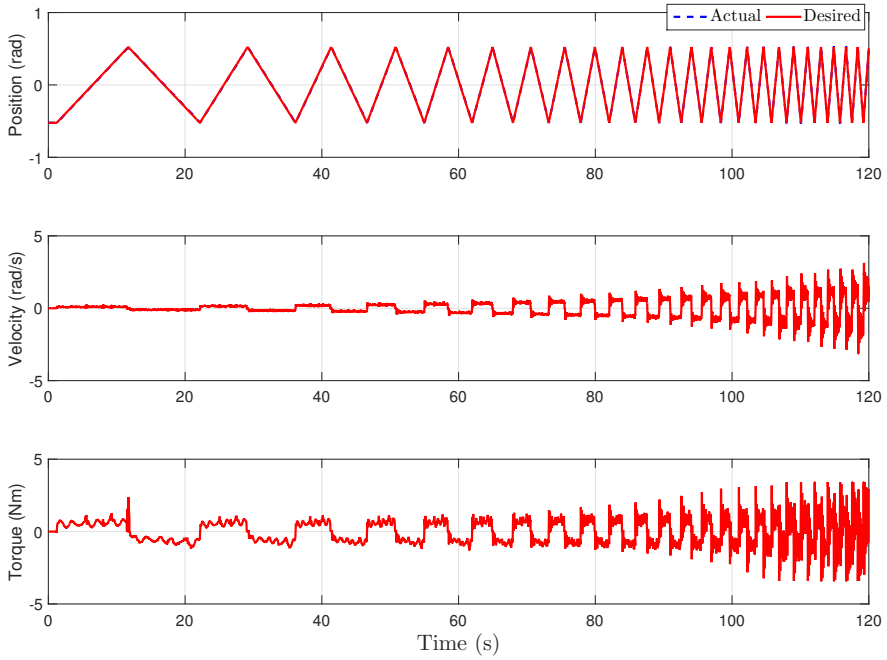

Figure 2.11: Applied position, velocity and torque for joint 3

The the position of ULEL and the choice of these exciting trajectories makes it possible to eliminate a large number of dynamic parameters and to keep only the friction parameters given in (2.25) to identify. To solve the system, we use the least squares technique of the following over-determined linear systems:

$$\begin{cases} F_{ci1}sign(\dot{q}_{i1}) + F_{vi1}\dot{q}_{i1} = \tau_{i1} \\ \vdots \qquad\qquad \text{for} \quad i = 1, \ldots, 3 \\ F_{cim}sign(\dot{q}_{im}) + F_{vim}\dot{q}_{im} = \tau_{im} \end{cases} \tag{2.26}$$

where m is the number of the performed constant velocity ramps.

The resolution of this system was performed using *lsqcurvefit* Matlab function, which allows to solve curve-fitting (data-fitting) problems in the least squares sense. The identified values of the Coulomb F_c and viscous F_v friction parameters of ULEL are presented in Table. 2.4.

Joint	F_c (Nms/rad)	F_v (Nm)
1	3.1085	7.9407
2	1.8133	4.1268
3	0.3281	0.5887

Table 2.4: Identified values of the friction parameters F_c and F_v

Figs. 2.12, 2.13 and 2.14, present the friction characteristic with respect to velocity for each joint. It can be seen that most of the friction is due to Coulomb (dry) friction and the effect of velocity on friction torques is much smaller. We can also note that the contribution of friction to the total dynamic model is significant, and this is due to the use of Screw and Cable System in the transmission mechanism at every joint.

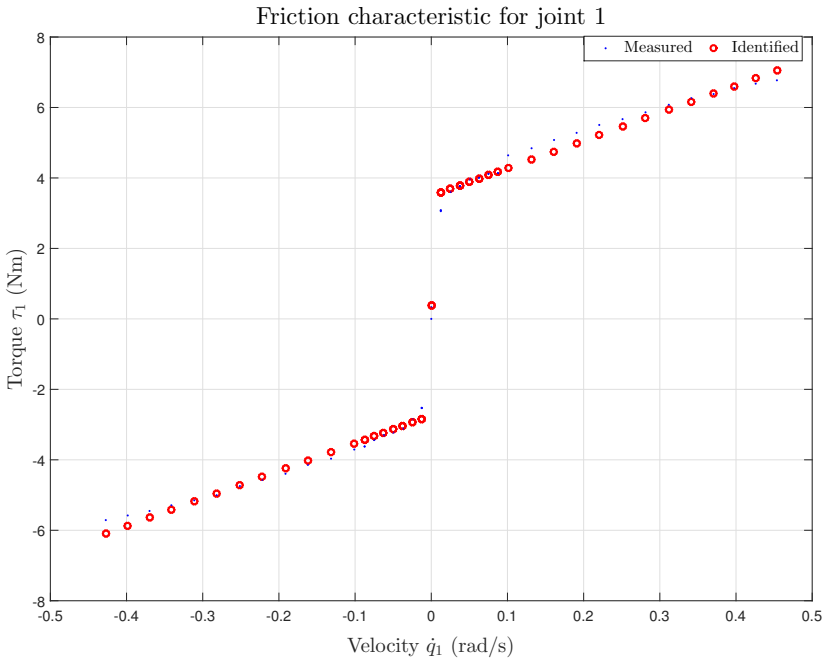

Figure 2.12: Friction characteristic for joint 1

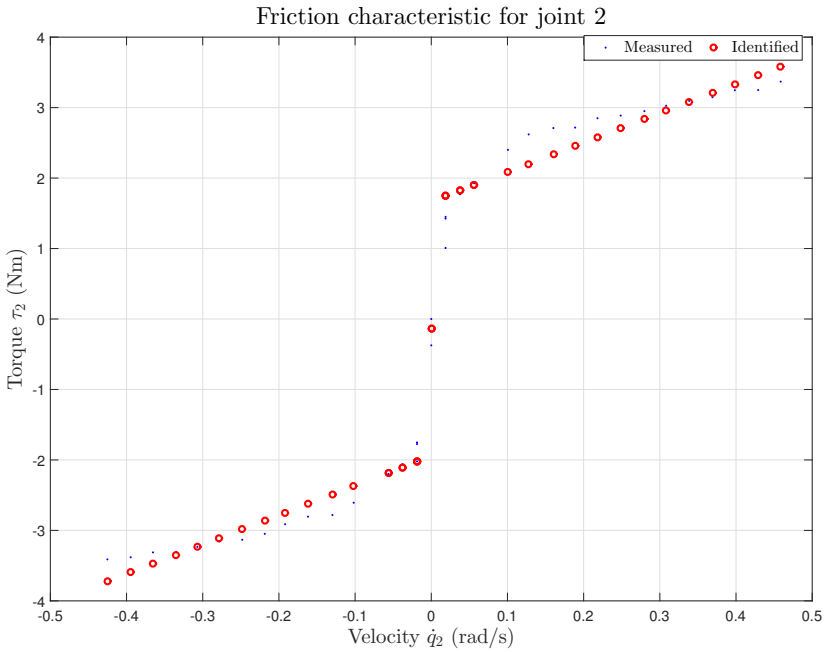

Figure 2.13: Friction characteristic for joint 2

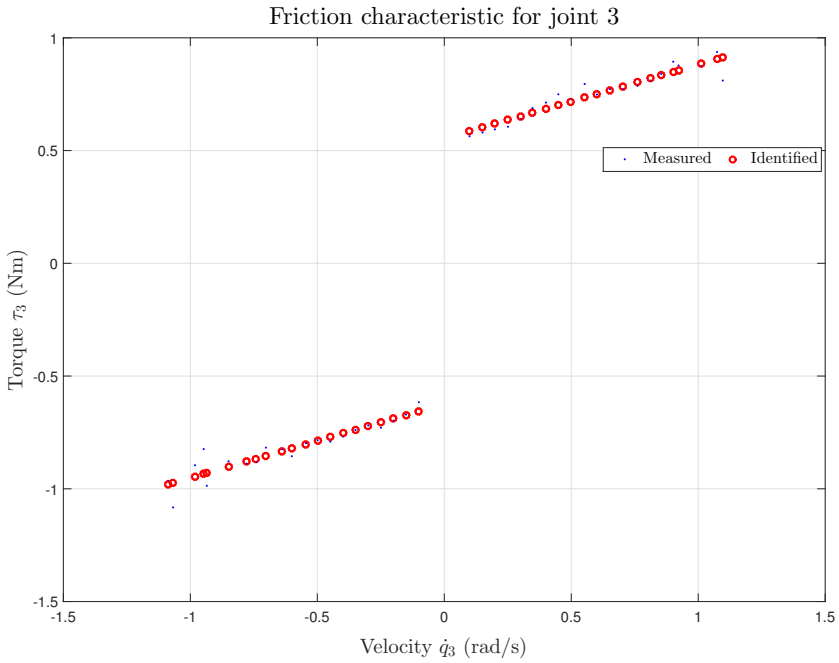

Figure 2.14: Friction characteristic for joint 3

2.6.2 Identification of inertial parameters

After having identified the friction parameters, the identification of the model inertial parameters is done by resolving the over sampled dynamic model using *lsqcurvefit* Matlab function, when tracking reference trajectories under PD control simultaneously for all joints. Experiments are considered without external forces. Estimated parameters with SolidWorks were used as initial values during identification, to obtain physically reasonable values for these parameters. Parameter ranges of variation were considered as follows:

- Mass of the links range ± 0.5 of their initial values.
- Moments of inertia parameters range from 0 to 2 of their initial values.
- Center of mass and mass products of inertia parameters to change in the range ± 2 of their initial values.

The results of this identification method applied to our exoskeleton ULEL are given in Fig. 2.15, by comparing applied torques in red, with reconstructed torques using the identified parameters in blue.

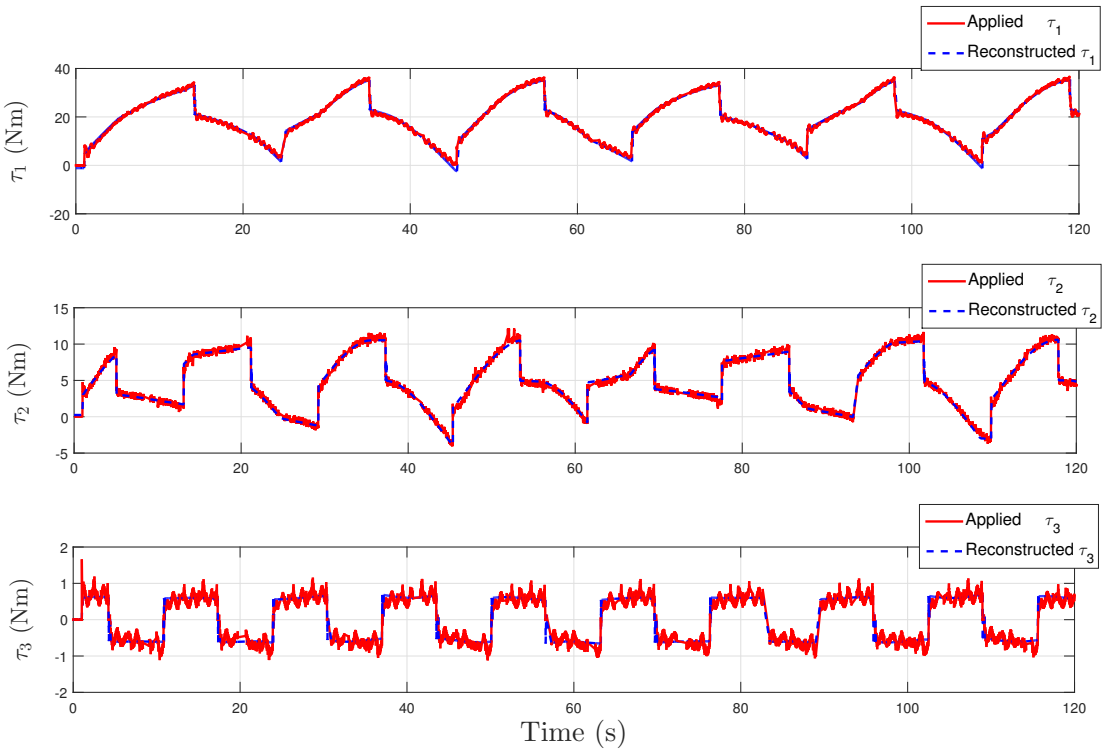

Figure 2.15: Identification results, applied torque and reconstructed torque

2.7 Conclusion

This chapter has presented the exoskeleton ULEL and its mechanical characteristics. Kinematic and dynamic models are calculated using modified DH notation. Then, identification is carried out in order to determine the model dynamic parameters, this step is very important to obtain a dynamic model close to the real model. The dynamic model will be used in simulations and during the control system design in the rest of this theses. To improve our exoskeleton design and performances, a major challenge is to develop control laws dedicated to the exoskeleton systems and making full use of their possibilities.

In Chapter 3, we present an adaptive controller, allowing to track desired trajectories in order to perform passive rehabilitation movements. The proposed approach is based on an on-line dynamic parameter estimator, allowing to compensate not only the unknown human limb dynamics, but also model uncertainties, and disturbances.

Chapter 3

Passive rehabilitation adaptive control based on on-line least square parameter estimation

Contents

3.1 Introduction

Passive rehabilitation of arm movements is the first stage of physiotherapy exercises given to patients after stroke to recover there motor abilities. Thus this passive therapy is of paramount importance [121]. Indeed, during the acute phase, rehabilitation involves postural exercises and passive mobilization of the arm while patients are unable to move voluntarily their limbs to achieve their complete range of motion [122]. Therefore, it may be interesting to address this problematic in robotic rehabilitation.

The control problem of exoskeletons in order to move the patient's limb through a desired trajectory is widely discussed in the literature. A review on upper-limb exoskeleton control strategies for rehabilitation can be found in [123]. Several control schemes have been proposed, such as the conventional PID control method [81][124], Sliding Mode Control [125][73], neuro-fuzzy control based on the EMG signals [126][127]. In general, the dynamic parameters of the human arm are unknown, and they vary significantly because of the variation in morphologies from one person to another. Therefore, conventional linear control approaches have their limitations while dealing with an upper-limb exoskeleton. Adaptive control strategies can handle the model nonlinearities and uncertainties, when guaranteeing high dynamic tracking performance [128][129]. However, in addition to hardware equipment, such as power-off applied brakes and limit switches, an adaptive controller can improve the patient's safety in presence of large parameter variance and uncertainties when getting high tracking accuracy with the rehabilitation robot.

As a contribution to exoskeletons control issue, in this chapter a nonlinear control strategy for the passive rehabilitation therapy using the upper limb exoskeleton ULEL is presented. Taking into account the above observations, the proposed adaptive control based on an on-line dynamic parameter estimation approach is able to drive the upper limb exoskeleton attached to the human arm with undetermined human arm dynamics. An efficient on-line dynamic parameter estimator is used to estimate the dynamics of the exoskeleton-human system which yielding that the tracking error converge to a small neighborhood of the origin, and also improves the input control torque signal. The the proposed control scheme can be used for users with different sizes and morphologies, with no prior adaptation. Therefore it does not require prior knowledge of the human limb dynamics.

This chapter presents an adaptive control strategy for an upper-limb exoskeleton based on an on-line dynamic parameter estimator. The objective is to improve the control performance of this system that plays a critical role in assisting patients for shoulder, elbow and wrist joint movements. In general, the dynamic parameters of the human limb are unknown and differ from a person to another, which degrade the performances of the exoskeleton-human control system. For this reason, the proposed control scheme contains a supplementary loop based on a new efficient on-line estimator of the dynamic parameters. The latter is acting upon the parameter adaptation of the controller to ensure the performances of the system in the presence of parameter uncertainties and perturbations.

The proposed control scheme can be used for users with different sizes and mor-

phologies, with no prior adaptation. Therefore it does not require prior knowledge of the human limb dynamics. In addition, it allows better trajectory tracking with improved control input. . The physical model of the exoskeleton ULEL, interacting with a 7 Degree of Freedom (DoF) upper limb model is used to illustrate the effectiveness of the proposed approach, an example of passive rehabilitation movements is performed using multi-body dynamic simulation, which aims to maneuver the exoskeleton that drive the upper limb to track desired trajectories in the case of the passive arm movements.

3.2 Dynamic model

In chapter 2, the dynamic model of ULEL was presented in (2.21), and its dynamic parameters are identified. When the exoskeleton is attached to the user's limb, the dynamic parameters of the system will change. To overcome this parameter variation, an adaptive strategy is proposed to compensate the model uncertainties. In addition, an on-line dynamic parameter estimator is introduced to improve the performances of the proposed controller.

Indeed, the dynamic model is linear with respect to the dynamic parameters, which can be written as

$$\tau = W(q, \dot{q}, \ddot{q})\chi, \tag{3.1}$$

where $W(q, \dot{q}, \ddot{q}) \in \mathbb{R}^{3\times 19}$ is the regressor matrix and $\chi \in \mathbb{R}^{19}$ is the vector of base inertial parameters given as

$$\begin{aligned} \chi = \; & [l_1^2(m_2 + m_3) + ZZ_1, l_1(m_2 + m_3) + +MX_1, \\ & MY_1, ZZ_2 + YY_3 + 2\,MZ_3 r_3 + (l_2^2 + r_3^2)m_3, \\ & l_2 m_3 + MX_2, m_3 r_3 + MY_2 + MZ_3, XX_3 - YY_3, \\ & XY_3, XZ_3, YZ_3 ZZ_3, MX_3, MY_3, F_{c1}, F_{c2}, F_{c3}, F_{v1}, F_{v2}, F_{v3}]^T \end{aligned} \tag{3.2}$$

This model will be used in the estimator and the controller syntheses. In the rest of this chapter the regressor matrix will be noted as W to simplify the notation.

3.3 Design of an on-line estimator to identify the dynamic parameters

Various dynamic identification schemes have been proposed in the literature [130][120][131][132][133]. Dynamic identification methods can be classified as on-line identification and off-line identification methods. In the off-line technique, all the data

is collected previously to be analyzed and no computation time limits are required. On the other hand, the on-line method allows parameter identification during robot exploitation which gives the possibility of real-time parameter updates. In order to identify the dynamic parameters of ULEL, we propose an efficient on-line estimator. The proposed on-line identification method is validated with simulation and experimental results and a comparison with the conventional Least-Squares (LS) off-line method is carried out.

3.3.1 The on-line estimator synthesis

The following assumptions are needed for the estimator synthesis:

- The vector τ is measurable.
- W satisfies the persistent excitation condition [134].
- χ is a constant vector.

The proposed estimator used to compute the base inertial parameters can be written as

$$\begin{cases} \dot{\hat{\Gamma}} = W\hat{\chi} + \frac{\alpha}{2}(\Gamma - \hat{\Gamma}) \\ \dot{\hat{\chi}} = KW^T(\Gamma - \hat{\Gamma}) + KW^T(\tau - W\hat{\chi}) \\ \dot{K} = -2K\,W^T W\,K + \alpha K \end{cases}, \tag{3.3}$$

with:

- $\Gamma = \int \tau dt \in \mathbb{R}^3$ is the integral of the torque vector τ.
- $\hat{\chi} \in \mathbb{R}^{19}$ and $\hat{\Gamma} \in \mathbb{R}^3$ are respectively the estimates of the vectors χ and Γ.
- $K \in \mathbb{R}^{19\times 19}$ is a bounded symmetric positive definite matrix.
- $\alpha > 0$ is a positive gain.

By defining the vector estimation error as $\tilde{\Gamma} = \Gamma - \hat{\Gamma}$ and the vector parameters error as $\tilde{\chi} = \chi - \hat{\chi}$, then their dynamics are given as

$$\begin{cases} \dot{\tilde{\Gamma}} = W\tilde{\chi} - \frac{\alpha}{2}\tilde{\Gamma} \\ \dot{\tilde{\chi}} = -KW^T\tilde{\Gamma} - KW^TW\tilde{\chi} \end{cases} \tag{3.4}$$

Let's choose the following Lyapunov-like function

$$V = \tilde{\Gamma}^T\tilde{\Gamma} + \tilde{\chi}^T K^{-1}\tilde{\chi}, \tag{3.5}$$

differentiating (3.5) with respect to time, yields

$$\dot{V} = 2\tilde{\Gamma}^T\dot{\tilde{\Gamma}} + 2\tilde{\chi}^T K^{-1}\dot{\tilde{\chi}} + \tilde{\chi}^T \tfrac{d}{dt}(K^{-1})\tilde{\chi} \ . \tag{3.6}$$

Using (3.4), the third equation of (3.3) and $\frac{d}{dt}(K^{-1}) = -K^{-1}\dot{K}K^{-1}$, equation (3.6) becomes

$$\dot{V} = -\alpha\tilde{\Gamma}^T\tilde{\Gamma} - \alpha\tilde{\chi}^T K^{-1}\tilde{\chi}, \tag{3.7}$$

then $\dot{V}$ can be written as

$$\dot{V} = -\alpha V, \tag{3.8}$$

so the solution of (3.7) is of the form

$$V(t) = V(0)\, e^{-\alpha t} \tag{3.9}$$

This result shows that V is decreasing exponentially to zero and since W satisfies the persistent excitation condition so the errors $\tilde{\Gamma}$ and $\tilde{\chi}$ tend exponentially to zero.

3.4 Adaptive controller design

Since there exits a difficulty in obtaining the reliable exoskeleton–human dynamic model, owing to the unknown parameters and uncertainties, in this section, we present an adaptive control based on the proposed on-line estimator of the exoskeleton to track desired trajectories.

Let's define the regressor matrix $W_r(q, \dot{q}, \dot{q}_r, \ddot{q}_r) \in \mathbb{R}^{3\times 19}$ as follows:

$$W_r(q, \dot{q}, \dot{q}_r, \ddot{q}_r)\chi = M(q)\ddot{q}_r + C(q, \dot{q})\dot{q}_r + G(q) + D(\dot{q}), \tag{3.10}$$

with q_r is a command vector defined such that

$$\begin{cases} \ddot{q}_r &= \ddot{q}_d - \lambda\dot{e} \\ \dot{q}_r &= \dot{q}_d - \lambda e \end{cases}$$

where $e = q - q_d$, $\dot{e} = \dot{q} - \dot{q}_d$ are the error vector and its derivative respectively, $q_d \in \mathbb{R}^3$ is used to denote the desired trajectory, $\lambda \in \mathbb{R}$ is a positive gain.

The proposed adaptive control law can be written as follows:

$$\begin{cases} \tau & = W_r \hat{\chi}_a - K_v s \\ \dot{\hat{\chi}}_a & = -K_a W_r^T s + K_a \gamma(\hat{\chi}_i - \hat{\chi}_a) \\ \dot{\hat{\chi}}_i & = K_i W^T (\tau - W \hat{\chi}_i) \\ \dot{K}_i & = -2K_i \, W^T W \, K_i + \alpha K_i \end{cases}, \tag{3.11}$$

where $K_v \in \mathbb{R}^{3\times 3}$ is a diagonal positive matrix, $\gamma \in \mathbb{R}$ is a positive gain, $\hat{\chi}_a \in \mathbb{R}^{19}$ and $\hat{\chi}_i \in \mathbb{R}^{19}$ are respectively the adaptation and identification parameter estimates of χ, $K_a \in \mathbb{R}^{19\times 19}$ is a constant symmetric positive definite matrix, $K_i \in \mathbb{R}^{19\times 19}$ is a variable symmetric positive definite matrix, and:

$$s = \dot{e} + \lambda e \tag{3.12}$$

By defining the errors as

$$\begin{cases} \tilde{\chi}_a & = \chi - \hat{\chi}_a \\ \tilde{\chi}_i & = \chi - \hat{\chi}_i \end{cases}, \tag{3.13}$$

and by using (2.21), (3.1), (3.10), (3.11) and (3.12), we can write

$$\begin{cases} M(q)\dot{s} + C(q,\dot{q})s & = -K_v s - W_r \tilde{\chi}_a \\ \dot{\tilde{\chi}}_a & = K_a W_r^T s - K_a \gamma(\tilde{\chi}_a - \tilde{\chi}_i) \\ \dot{\tilde{\chi}}_i & = -K_i W^T W \tilde{\chi}_i \end{cases}. \tag{3.14}$$

Let the Lyapunov-like function be

$$V = \frac{1}{2} s^T M s + \frac{1}{2} \tilde{\chi}_a^T K_a^{-1} \tilde{\chi}_a + \frac{1}{2} \tilde{\chi}_i^T K_i^{-1} \tilde{\chi}_i. \tag{3.15}$$

Differentiating (3.15) with respect to time yields

$$\dot{V} = -s^T K_v s - \gamma \tilde{\chi}_a^T \tilde{\chi}_a + \gamma \tilde{\chi}_a^T \tilde{\chi}_i - \frac{\alpha}{2} \tilde{\chi}_i^T K_i^{-1} \tilde{\chi}_i,$$

by choosing the vector X as follows: $X = [\tilde{\chi}_a, \tilde{\chi}_i]^T$, we get $\dot{V} = -s^T K_v s - X^T H \, X$,

with

$$H = \begin{bmatrix} \gamma I_{19} & -\frac{\gamma}{2} I_{19} \\ -\frac{\gamma}{2} I_{19} & \frac{\alpha}{2} K_i^{-1} \end{bmatrix},$$

where $I_{19} \in \mathbb{R}^{19\times 19}$ is the identity matrix. So we just need to find the condition on K_i, γ and α for that $H > 0$.

3.5 Simulation results

For the evaluation of the proposed control scheme, a multi-body system simulation of the exoskeleton ULEL interacting with the articulated arm model is used. The multi-body modeling allows simulation of both, the human limb and the dynamics of the exoskeleton, which can achieve performance very close to the real system. Therefore, it can provides a safe way to test new control schemes for exoskeletons along with evaluation of the interaction efforts. First, the proposed on-line identification method is tested and thereafter an example of passive rehabilitation movement is performed.

3.5.1 Parameter estimates

According to (3.1), the dynamic model is linear in the vector χ of the base dynamic parameters defined in (3.2). The nominal dynamic parameters χ_{nom} of ULEL, used in the simulations (all in SI Units) are extracted from a complete CAD model given by RB3D and the identified friction coefficients, where $\chi_{nom} = [\ 0.8422, 3.0454, -0.0497, 0.2437, 0.7373, -0.6872, -0.0023, -0.0035, 0, 0, 0.0026, 0.0313, 0, 3.1, 1.81, 0.33, 7.94, 4.12, 0.33]^T$. The initial value of χ used in the simulations is zero. The simulation is carried out with a random trajectory to excite the parameters in order to test the generality of this method. The estimation results are given in Fig. 3.1 with white noise of Signal to Noise Ratio (SNR) of 40dB in the joints positions. In the beginning the estimation is pointless because the observation matrix is ill-conditioned. When sampling data are enough the parameter estimation result is robust and converges to the correct parameters while estimation errors converge to zero.

The proposed identification method is efficient and gives good estimation of the model parameters even with noisy data. The actual torques (dotted blue line), the estimated torques with the identified model (solid red line) and their corresponding errors (solid black line) are shown in Fig. 3.2.

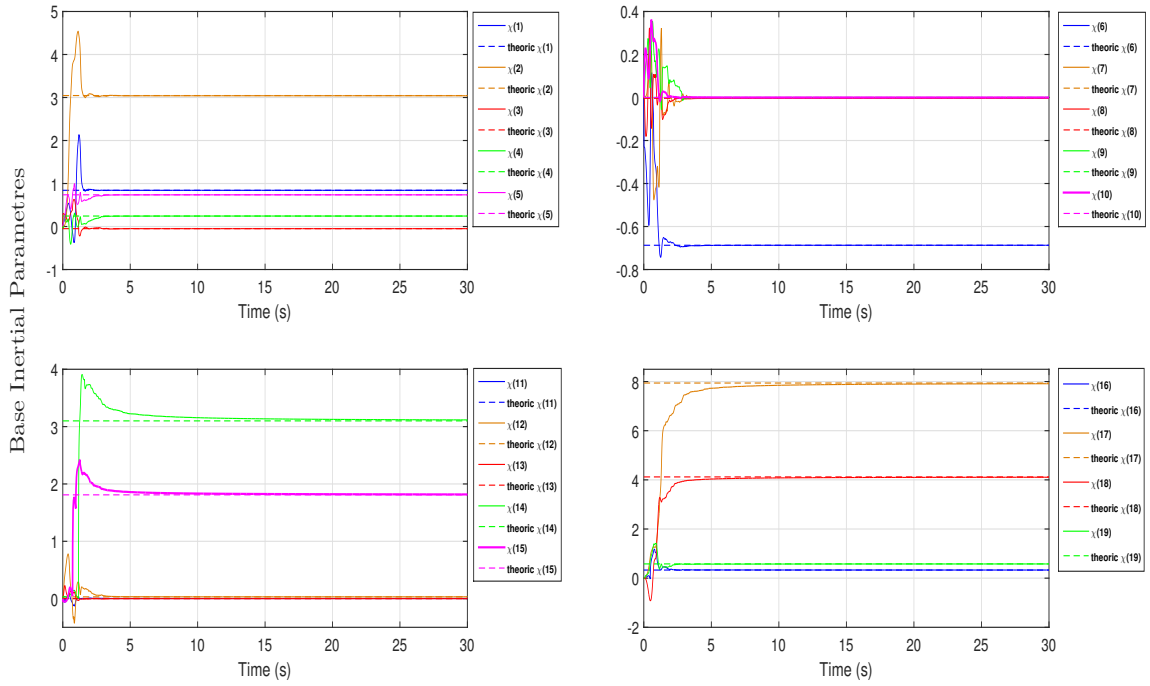

Figure 3.1: Dynamic parameter estimation with white noise of SNR=40dB in the joints positions.

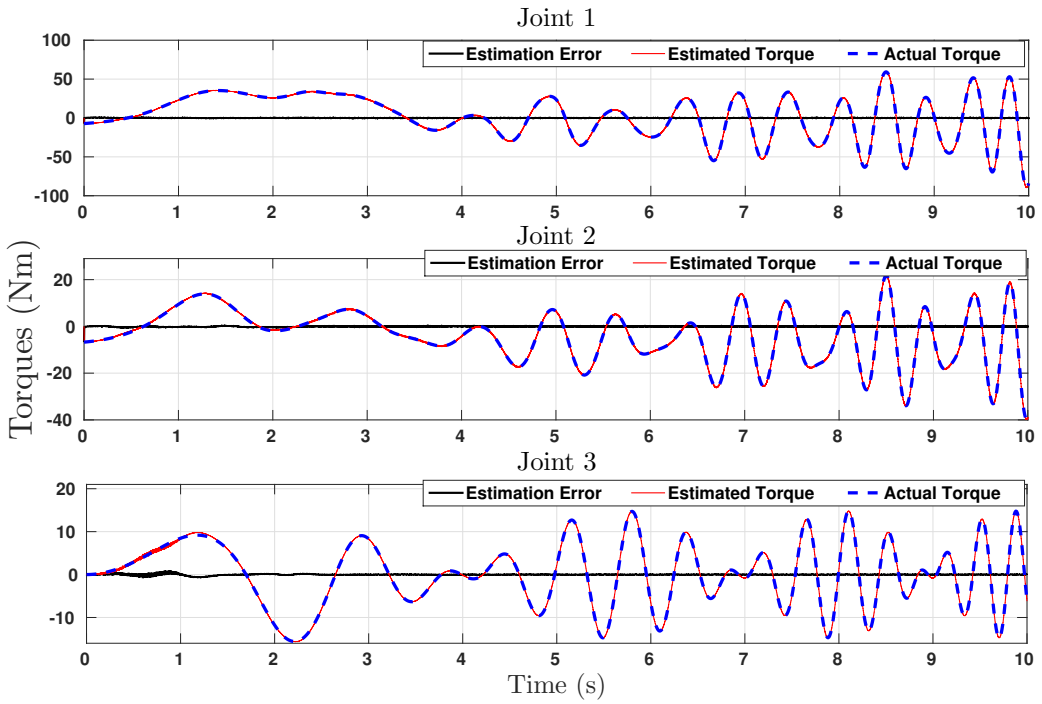

Figure 3.2: Actual torques, estimated torques and estimation errors with white noise of SNR=40dB.

This method gives a small relative norm error, $\|\tau - W\hat{\chi}\|/\|\tau\| < 0.2\%$ at convergence,

which shows a good accuracy for the identified values compared with the conventional linear off-line Least-Squares (LS) technique [109], which gives a relative norm error of $\|\tau - W\hat{\chi}_{LS}\|/\|\tau\| < 1.2\%$ using the same simulation conditions. Results show that, the proposed on-line identification method is as effective as the off-line LS method and the parameters estimation gives a better accuracy.

3.5.2 Adaptive controller

Simulations were carried out to move the exoskeleton attached to the articulated arm model presented in section 2.4, along pre-programmed trajectories to achieve passive arm movements. In this case the efforts applied by the arm on the exoskeleton are considered as an external perturbation.

The passive exercise chosen in our example consists in performing passive flexion / extension movements, first for the shoulder, then for the elbow and finally for the wrist. Simulation starts with the initial state of the system $q(0) = [\ 0 \quad 0 \quad 0\ ]^T$ and the initial gain parameters $K_a = 0.5 \cdot I_{16}$, $K_i(0) = 20 \cdot I_{16}$, $K_v = 10 \cdot I_3$,$\lambda = 10$, $\alpha = 2$, $\gamma = 20$. A white noise component of $SNR = 40dB$ is considered in the joints positions.

Results in Fig. 3.3 show that the desired trajectories (dotted blue line) nearly overlapped with the actual ones (solid red line). The tracking errors (i.e., deviation between desired and actual trajectories) have the maximal values $\pm 0.0098\,rad$, $\pm 0.0076\,rad$ and $\pm 0.0009\,rad$ for the shoulder, elbow and wrist joints respectively. For the intended application, high positioning accuracy has no practical meaning and this accuracy is sufficient. Also the input control torques are relatively smooth without any abrupt variations. From these results, even if we have no knowledge of dynamic parameters of the exoskeleton and the disturbances from the interaction with the arm model, we can still obtain a good performance by the proposed control scheme.

We also conducted a comparison simulation using conventional adaptive control without the parameters estimation ($\gamma = 0$) in the same conditions. The control results are shown in Fig. 3.4. It is seen that the performance of the adaptive control without the proposed estimator is worst, with higher and oscillating control inputs and larger tracking errors.

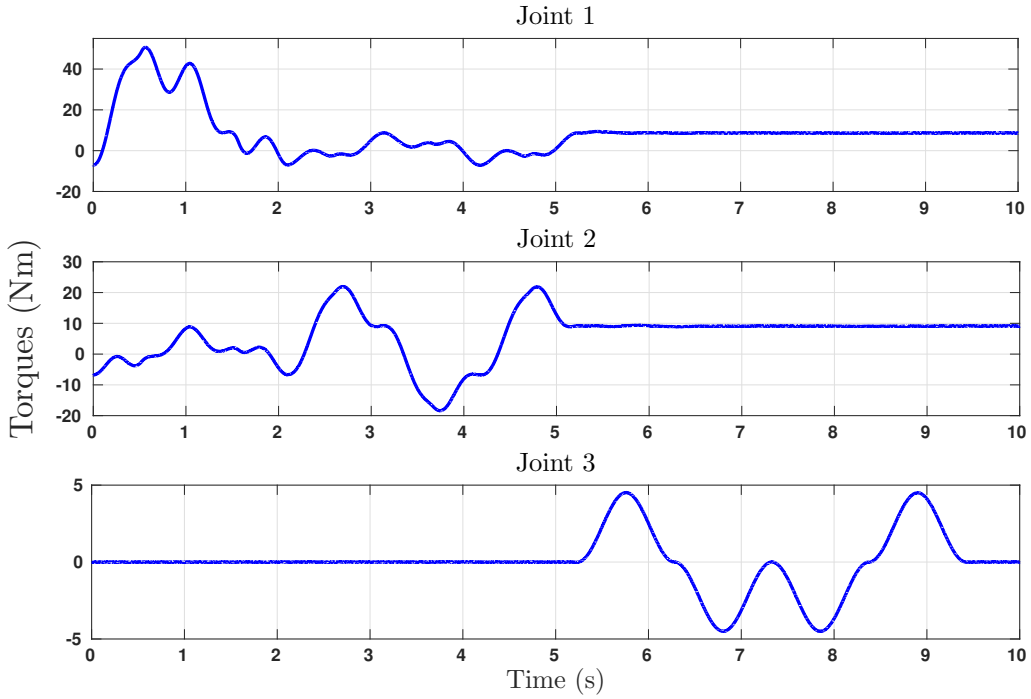

(a) The input control torque for each joint.

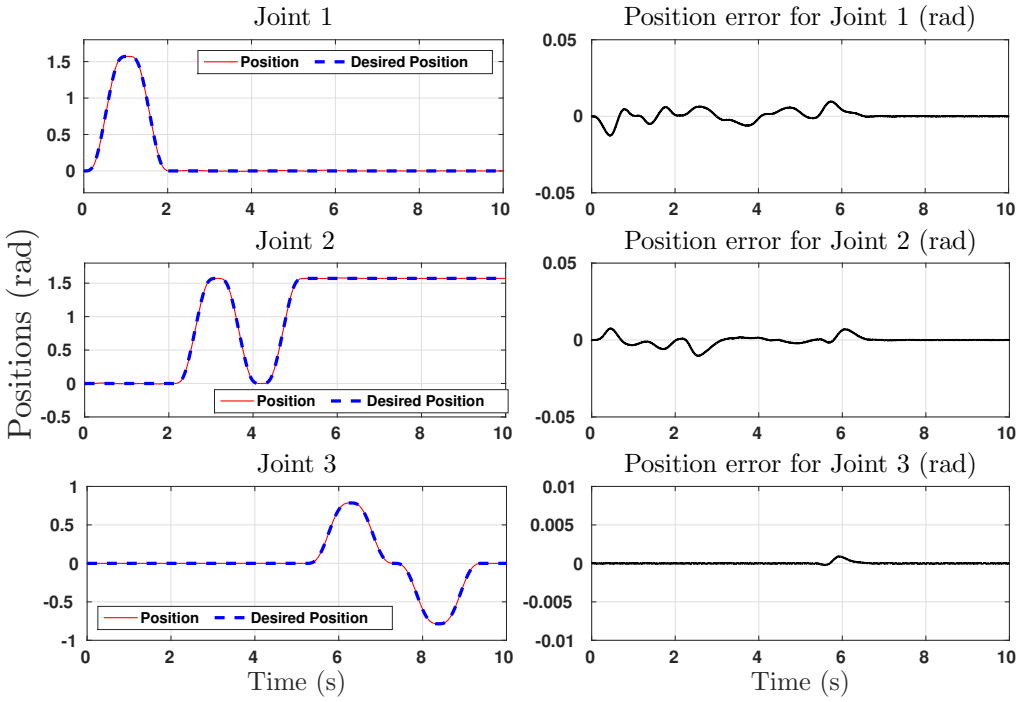

(b) Actual positions, desired positions and estimation errors.

Figure 3.3: Simulation results of the adaptive control with the proposed estimator using white noise of SNR=40dB.

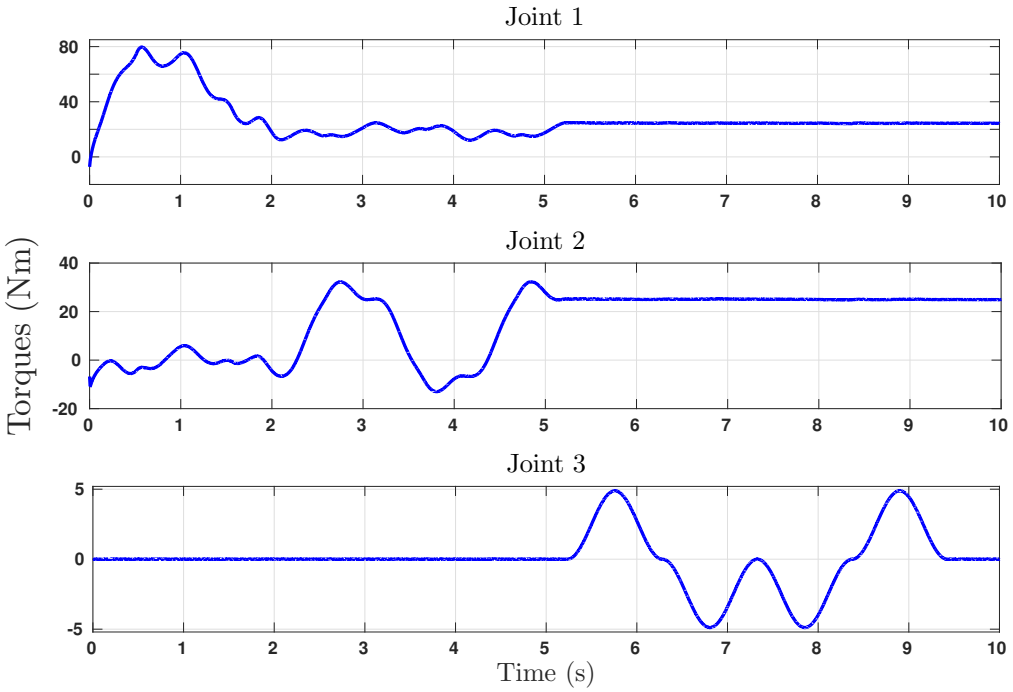

(a) The input control torque for each joint.

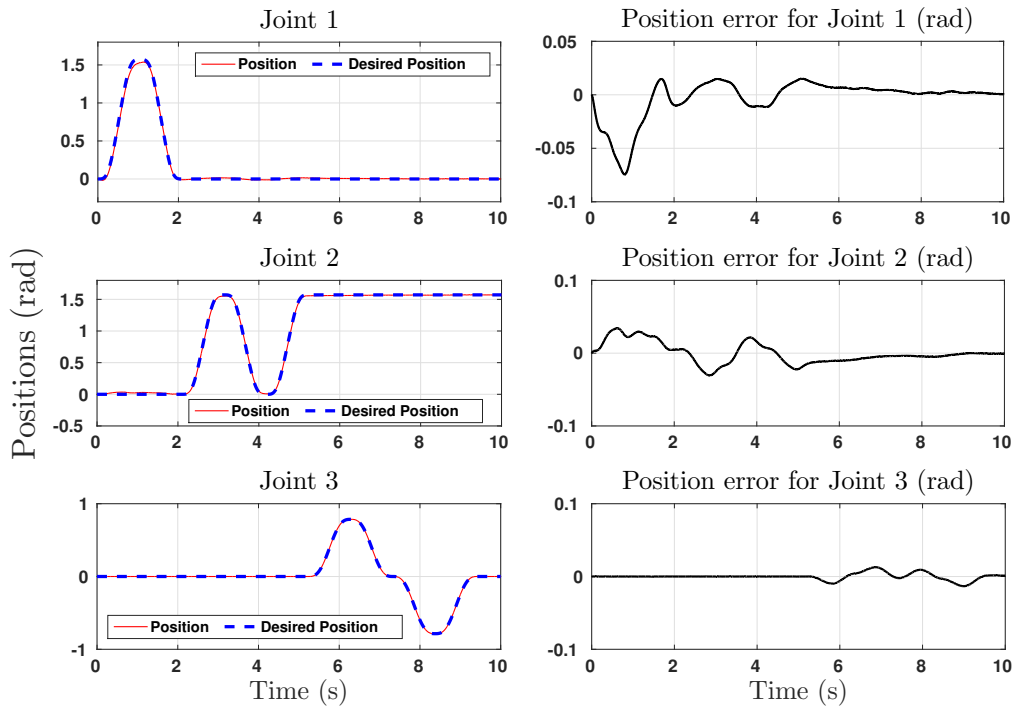

(b) Actual positions, desired positions and estimation errors.

Figure 3.4: Simulation results of the adaptive control without the proposed estimator using white noise of SNR=40dB.

The results in terms of relative tracking errors and the maximal absolute value of the control torques are listed in Table 3.1. As seen from this performance indices,

the proposed control performs better, in comparison with the conventional adaptive control without parameter estimation. The relative tracking errors and the control inputs of the proposed controller are significantly reduced by the proposed controller. It is obvious through these results, that the proposed control law can lead to better control performance.

Table 3.1: Performance indices of the adaptive control with and without parameter estimation

	Adaptive control without the proposed estimator		Adaptive control with the proposed estimator	
	$\|q - q_d\|/\|q\|$	$max\|\tau\|$	$\|q - q_d\|/\|q\|$	$max\|\tau\|$
Joint 1	4.20%	$79.67\,Nm$	0.79%	$50.69\,Nm$
Joint 2	1.20%	$32.34\,Nm$	0.24%	$21.98\,Nm$
Joint 3	1.48%	$4.89\,Nm$	0.05%	$4.52\,Nm$

3.6 Conclusion

In this chapter, an efficient on-line estimator suitable for identification of dynamic parameters is introduced. Then, an adaptive control based on the proposed on-line dynamic parameter estimator is presented for an upper limb exoskeleton to provide passive assistance, in the presence of parametric uncertainties, and disturbances. The proposed adaptive control can perform stable tracking of pre-programmed trajectories without requiring exact knowledge of the dynamic parameters. The performance of the controller is demonstrated through simulations using a multi-body dynamic model of ULEL assembled to a 7 DOF upper limb model. Also, a comparison with the conventional adaptive control has been conducted. The results show the effectiveness of the proposed control, guaranteeing the performance of an effective passive rehabilitation using the exoskeleton. This results are promising and encourage to continue the development which aims to improve our robotic prototype for the rehabilitation of the upper limb.

Chapter 4

Passive rehabilitation adaptive control using integral terminal sliding mode technique

Contents

4.1 Introduction

In the recent years, the interest in exoskeleton has increased in many application fields. Especially, medical applications paid increasing attention to exoskeletons to obtain more efficient rehabilitation therapies [51, 45, 135, 136, 137, 138], and to provide suitable health care to disabled patients and elderly people not only in hospitals but also in their own homes. The problem is that, such robotic systems are very complex

and hard to model owing to their direct interaction with the user's limb. Even if the dynamics of the exoskeleton is known, that of the human limb is typically unknown and greatly variable form a person to another. Therefore, the use of exoskeleton in interaction with a human subject, depends on the quality of the associated controller, in order to obtain satisfactory performances.

Several control strategies for exoskeletons have been proposed in the literature, for example: Adaptive control [139, 140], EMG-based control [141, 142], Admittance control [143], Fuzzy and backstepping control [144, 145], Impedance control and reinforcement learning [146] and Coordination control [147]. A recent review on control strategies for upper limb exoskeletons can be found in [123].

Among the existing robust control schemes, this work focuses on Sliding Mode Control (SMC) which is a powerful approach to control robotic systems with uncertain dynamics and bounded disturbances [148, 149, 150]. This nonlinear control strategy works by dragging the non-linear path to a predetermined hyperplane so-called sliding surface, then the system stays confined to the sliding surface while sliding along to the origin [151]. In general, conventional SMC uses linear sliding surface which can only achieve asymptotic stability of the system during the sliding mode phase [152]. Thereafter, more advanced techniques such as Terminal SMC (TSMC) were proposed [153, 154] which can guarantee finite time convergence of the tracking error to zero. The Fast Terminal Sliding Mode (FTSM) surface has been introduced to further reduce the finite-settling-time [155, 156]. However, TSMC and FTSM suffer from singularity problems due to the use of fractional power in sliding surface design. Therefore, a Nonsingular TSMC (NTSMC) have been proposed in [157, 158, 159], to overcome the singularity problem. In [160] an Integral TSMC (ITSMC) is proposed to eliminate singularities and lead to less chattering effect compared to the conventional SMC [161].

This chapter proposes an Adaptive ITSMC (AITSMC) for upper limb exoskeletons in order to perform passive rehabilitation. First, the dynamic modeling of the considered exoskeleton is introduced as well as properties and assumptions. Then, an integral terminal sliding mode surface is used to guarantee tracking errors converge to zero in finite time when the sliding surface is reached. The proposed ITSMC is thus designed to guarantee the reaching of the sliding mode, as well as the good tracking performance in finite time. With this control scheme, the singularity problem is removed without adding any constraints. Furthermore, the lack of knowledge of the system uncertainty bounds leads to set them to very high values which may result in intense control torques. To address this problem an adaptive approach is proposed to adaptively tune the uncertainty bounds while guaranteeing finite time convergence. Finally, to validate the

proposed control scheme, experiments were carried out with a healthy subject using a 3 Degrees of Freedom (DoF) upper limb exoskeleton called ULEL[1] to perform trajectories that correspond to passive arm movements.

The rest of the chapter is set as follows. Section 4.2 expresses the dynamic modeling and model properties and assumptions. In Section 4.3 controller design is presented. Section 4.4 introduces an adaptation method to tune the controller gains. Section 4.5 shows the implementation of the proposed approach for the upper limb exoskeleton ULEL and experimental results in performing passive movements with healthy subjects. Conclusion is presented in Section 5.7.

4.2 Dynamic modeling

The dynamic behavior of robotic systems can be expressed by the well known rigid body's dynamic equation

$$M(q)\ddot{q} + H(q,\dot{q}) = \tau(t), \tag{4.1}$$

with

$$H(q,\dot{q}) = C(q,\dot{q})\dot{q} + G(q) + D(\dot{q}), \tag{4.2}$$

where $q \in \mathbb{R}^n$, $\dot{q} \in \mathbb{R}^n$ and $\ddot{q} \in \mathbb{R}^n$ are respectively the joint positions, velocities and accelerations; $M(q) \in \mathbb{R}^{n\times n}$ is the inertia matrix; $C(q,\dot{q}) \in \mathbb{R}^{n\times n}$ is the Coriolis/centrifugal matrix; $G(q) \in \mathbb{R}^n$ is the gravity vector; $D(\dot{q}) \in \mathbb{R}^n$ is the dissipation term; $\tau(t) \in \mathbb{R}^n$ is the applied torque vector.

In the case of human-exoskeleton system, the dynamic model (4.1) can be used with some known parts and unknown parts. The terms $M(q)$, $H(q,\dot{q})$ and $\tau(t)$ can be written in the form

$$\begin{cases} \tau(t) &= \tau_N(t) + \tau_\Delta(t) \\ M(q) &= M_N(q) + M_\Delta(q) \\ H(q,\dot{q}) &= H_N(q,\dot{q}) + H_\Delta(q,\dot{q}) \end{cases}, \tag{4.3}$$

where $\tau_N(t)$, $M_N(q)$ and $H_N(q,\dot{q})$ are known nominal parts and $\tau_\Delta(t)$, $M_\Delta(q)$ and $H_\Delta(q,\dot{q})$ are unknown parts. The term $\tau_N(t)$ represents the actuated torque generated by the exoskeleton's motors and $\tau_\Delta(t)$ includes the all torques applied by the human arm on the exoskeleton and other external disturbances.

Using (4.3), the dynamic equation (4.1) can be written in the following form :

$$M_N(q)\ddot{q} + H_N(q,\dot{q}) = \tau_N(t) + \Delta(t), \tag{4.4}$$

[1] *Upper Limb Exoskeleton of LISSI*

where $\Delta(t)$ is the system uncertainty defined as

$$\Delta(t) = \tau_{\Delta}(t) - M_{\Delta}(q)\ddot{q} - H_{\Delta}(q, \dot{q}), \tag{4.5}$$

which is related to the position, velocity and acceleration signals.

Remark 4.1. Only the position and velocity are measurable in our application setup using an exoskeleton. Therefore, the use of acceleration term in (4.5) is the key problem for controller designing. This issue will be addressed in the following of the chapter.

4.2.1 Model properties and assumptions

In the case of robotic systems with only pivot joints (revolute joints), the following properties are obviously verified for any $q \in \mathbb{R}^n$.

Fact 4.1. *The inertia terms $M(q)$ and $M_N(q)$ are symmetric positive definite matrices. Moreover, these matrices are bounded [162]*

$$\begin{cases} \underline{m}I \leq M(q) \leq \overline{m}I \\ \underline{m}_N I \leq M_N(q) \leq \overline{m}_N I \end{cases}, \tag{4.6}$$

where $\underline{m}$, $\overline{m}$, $\underline{m}_N$ and $\overline{m}_N$ are positive constants such that $0 < \underline{m} < \overline{m}$ and $0 < \underline{m}_N < \overline{m}_N$. Therefore, it is straightforward that $M^{-1}(q)$ and $M_N^{-1}(q)$ are also positives and bounded as

$$\begin{cases} \overline{m}^{-1} I \leq M^{-1}(q) \leq \underline{m}^{-1} I \\ \overline{m}_N^{-1} I \leq M_N^{-1}(q) \leq \underline{m}_N^{-1} I \end{cases}. \tag{4.7}$$

Fact 4.2. *Using the euclidean norm, it can be written that [163]*

$$\|C(q, \dot{q})\| \leq \overline{c}\|\dot{q}\|, \tag{4.8}$$

where $\overline{c}$ is a non-negative constant.

As the exoskeleton interacts with the human arm, it is considered that the term $\Delta(t)$ is unknown. Only the following assumptions are adopted.

Assumption 1. *The gravity vector $G(q)$ is bounded such as $\|G(q)\| \leq \overline{g}_1 + \overline{g}_2\|q\|$, where $\overline{g}_1$ and $\overline{g}_2$ are non-negative constants.*

Assumption 2. *The dissipation vector $D(\dot{q})$ is bounded such as $\|D(\dot{q})\| \leq \overline{d}_1 + \overline{d}_2\|\dot{q}\|$, where $\overline{d}_1$ and $\overline{d}_2$ are non-negative constants.*

Assumption 3. *The torque vector $\tau_\Delta(t)$ is bounded such as $\|\tau_\Delta(t)\| \leq \overline{\tau}_\Delta$, where $\overline{\tau}_\Delta$ is a non-negative constant.*

Considering Property 4.2, and Assumptions 1, 2 and 3, then $H(q,\dot{q})$ in (5.2) can be upper-bounded as follows:

$$\|H(q,\dot{q})\| \leq \overline{g}_1 + \overline{d}_1 + \overline{g}_2\|q\| + \overline{d}_2\|\dot{q}\| + \overline{c}\|\dot{q}\|^2. \tag{4.9}$$

Assume that $H_N(q,\dot{q})$ and $H_\Delta(q,\dot{q})$ are upper-bounded as follows

$$\begin{cases} \|H_N(q,\dot{q})\| < \overline{h}_{N1} + \overline{h}_{N2}\|q\| + \overline{h}_{N3}\|\dot{q}\| + \overline{h}_{N4}\|\dot{q}\|^2 \\ \|H_\Delta(q,\dot{q})\| < \overline{h}_{\Delta 1} + \overline{h}_{\Delta 2}\|q\| + \overline{h}_{\Delta 3}\|\dot{q}\| + \overline{h}_{\Delta 4}\|\dot{q}\|^2 \end{cases}, \tag{4.10}$$

where $\overline{h}_{N1}, ..., \overline{h}_{N4}$ and $\overline{h}_{\Delta 1}, ..., \overline{h}_{\Delta 4}$ are non-negative constants.

Using (4.4), the acceleration $\ddot{q}$ can be written as

$$\ddot{q} = M_N^{-1}(q)\left[\tau_N(t) + \Delta(t) - H_N(q,\dot{q})\right], \tag{4.11}$$

then the dynamic model (4.1) can be written as

$$\ddot{q} = f(q,\dot{q}) + \varphi(q)u(t) + \xi(t), \tag{4.12}$$

where $u(t) = \tau_N(t)$ represents the control input torque, and the functions $f(q,\dot{q})$, $\varphi(q)$ and $\xi(t)$ are given by

$$\begin{cases} f(q,\dot{q}) &= -M_N^{-1}(q)H_N(q,\dot{q}) \\ \varphi(q) &= M_N^{-1}(q) \\ \xi(t) &= M_N^{-1}(q)\Delta(t) \end{cases}. \tag{4.13}$$

In what follows, to simplify the writing of the equations, the notational dependency will be omitted on u, f, φ, ξ, Δ, M_N, M_Δ, H_N, H_Δ, τ_N and τ_Δ.

4.2.2 The bounded property of uncertainties

Considering the model properties and assumptions presented above, the following property is demonstrated in appendix A:

$$\phi(q,\dot{q},t) - \|\xi\| \geq \eta, \tag{4.14}$$

where η is an arbitrary positive constant and $\phi(q, \dot{q}, t)$ is a scalar positive function defined as

$$\phi(q, \dot{q}, t) = \delta_1 + \delta_2\|q\| + \delta_3\|\dot{q}\| + \delta_4\|\dot{q}\|^2 + \delta_5\Omega(q, \dot{q}, t) + \eta, \tag{4.15}$$

with $\delta_1, \cdots, \delta_5$ are non-negative constants and $\Omega(q, \dot{q}, t)$ is a positive scalar function such that

$$\|u\| \leq \Omega(q, \dot{q}, t). \tag{4.16}$$

4.3 ITSMC design

For the class of nonlinear systems (4.12) with parameter uncertainties and external disturbances, this work aims to design a robust control using ITSMC in order to guarantee the reaching of the sliding mode as well as the tracking control in a finite time.

Consider the desired trajectory $q_d(t) \in \mathbb{R}^n$ which is bounded and twice differentiable with respect to time, and its first and second derivatives are also bounded. Let us define the tracking error vector and its derivative respectively as $e = q_d - q$, $\dot{e} = \dot{q}_d - \dot{q}$. Then, the error dynamics using model (4.12) can be written as

$$\ddot{e} = \ddot{q}_d - f - \varphi u - \xi. \tag{4.17}$$

Before presenting the main results of this section, the following assumption and lemma are given:

Assumption 4. *The desired position q_d, velocity $\dot{q}_d$ and acceleration $\ddot{q}_d$ trajectories are bounded.*

Lemma 4.1. *The origin of the following system is a globally finite-time-stable equilibrium*

$$\begin{cases} \dot{x}_1 = x_2 \\ \dot{x}_2 = -k_2 sgn(x_2)|x_2|^{\gamma} - k_1 sgn(x_1)|x_1|^{\frac{\gamma}{2-\gamma}} \end{cases}, \tag{4.18}$$

where k_1, k_2 and γ are positive constants, chosen such that the polynomial $r^2 + k_2 r + k_1$ is Hurwitz, and $0 < \gamma < 1$.

The proof of Lemma 4.1 can be found in Proposition 8.1 of [164].

The following theorem points out the ITSMC defined to guarantee the tracking control in finite time.

Theorem 4.1. *Consider the system (4.12) under Properties 4.1 and 4.2, and Assumptions 1, 2 and 3. By defining the ITSM surface function as*[2]

$$s = \dot{e} + \int_0^t (\alpha \dot{e}^{\frac{q}{p}} + \beta e^{\frac{q}{2p-q}}) dt, \tag{4.19}$$

where p and q are the positive odd integers such $p > q > 0$ and $\alpha = diag(\alpha_1, \cdots, \alpha_n) \in \mathbb{R}^{n\times n}$ and $\beta = diag(\beta_1, \cdots, \beta_n) \in \mathbb{R}^{n\times n}$ are positive diagonal matrices chosen such that the polynomials $r^2 + \alpha_i r + \beta_i$ for $i = 1, \cdots, n$ are Hurwitz, then the origin $(e, \dot{e})$ is globally finite-time-stable under the tracking control law

$$u = \varphi^{-1} \left[\ddot{q}_d + \alpha \dot{e}^{\frac{q}{p}} + \beta e^{\frac{q}{2p-q}} - f + \lambda s + \phi \frac{s}{\|s\|} \right], \tag{4.20}$$

where $\lambda = diag(\lambda_1, \cdots, \lambda_n) \in \mathbb{R}^{n\times n}$ is chosen as a positive diagonal matrix.

The detailed proof of Theorem 4.1 is presented in appendix B.

Remark 4.2. The function $\Omega(q, \dot{q}, t)$ introduced in (4.16) represents the upper bound of the control input u. The proposed control law given by (4.20) depends on a combination of the following terms: $\varphi^{-1} = M_N$, $f = -M_N^{-1} H_N$, $\ddot{q}_d$, $\dot{e}^{\frac{q}{p}}$, $e^{\frac{q}{2p-q}}$, s and ϕ. Recall that the acceleration $\ddot{q}_d$ is assumed to be bounded in Assumption 4, the terms M_N and M_N^{-1} are bounded according to Property 4.1, and the function H_N is bounded according to (4.10). Obviously, the variables $\dot{e}^{\frac{q}{p}}$, $e^{\frac{q}{2p-q}}$ and s can be bounded by using $\|\dot{e}^{\frac{q}{p}}\|$, $\|e^{\frac{q}{2p-q}}\|$ and $\|s\|$ respectively. Finally, ϕ represents the factor of the discontinuous term of the proposed sliding-mode-controller that has to be bounded in practice. Summing up all the latest findings, the norms $\|q\|$, $\|\dot{q}\|$, $\|\dot{q}\|^2$, $\|\dot{e}^{\frac{q}{p}}\|$, $\|e^{\frac{q}{2p-q}}\|$ and $\|s\|$ can be used to design the function $\Omega(q, \dot{q}, t)$.

Considering the approach given in Remark 4.2, the function $\Omega(q, \dot{q}, t)$ can be chosen as

$$\begin{aligned} \Omega(q, \dot{q}, t) \triangleq\ & \omega_1 + \omega_2 \|q\| + \omega_2 \|\dot{q}\| + \omega_4 \|\dot{q}\|^2 \\ & + \omega_5 \|\dot{e}^{\frac{q}{p}}\| + \omega_6 \|e^{\frac{q}{2p-q}}\| + \omega_7 \|s\| \end{aligned}, \tag{4.21}$$

where $\omega_1, \cdots, \omega_7$ are positive constants.

From (4.15) and (4.21) it yields

$$\phi = \psi^T A, \tag{4.22}$$

[2]The $\frac{q}{p}$ fractional power of vector $x \in \mathbb{R}^n$ is $x^{\frac{q}{p}} = [x_1^{\frac{q}{p}}, ..., x_n^{\frac{q}{p}}]^T$

where

$$\psi = \begin{bmatrix} 1 \\ 1+\|q\| \\ 1+\|\dot{q}\| \\ 1+\|\dot{q}\|^2 \\ 1+\|\dot{e}^{\frac{q}{p}}\| \\ 1+\|e^{\frac{q}{2p-q}}\| \\ 1+\|s\| \end{bmatrix},$$

and

$$A = \begin{bmatrix} \delta_1 - \sum_{i=2}^{4}\delta_i - \delta_5(-\omega_1 + \sum_{i=2}^{7}\omega_i) + \eta \\ \delta_2 + \delta_5\omega_2 \\ \delta_3 + \delta_5\omega_3 \\ \delta_4 + \delta_5\omega_4 \\ \delta_5\omega_5 \\ \delta_5\omega_6 \\ \delta_5\omega_7 \end{bmatrix}.$$

Remark 4.3. Since η is an arbitrary positive constant introduced by (4.14) and (4.15), then it shall satisfy the following condition:

$$\eta > -\delta_1 + \sum_{i=2}^{4}\delta_i + \delta_5(-\omega_1 + \sum_{i=2}^{7}\omega_i). \tag{4.23}$$

The controller proposed in this section ensures the reaching of the sliding mode as well as the tracking control in finite time. However, the lack of knowledge of the upper bounds (elements of vector A) leads to set them to very high values, which can result in an intensive control torques. To handle this problem, an adaptive ITSMC is proposed in the next section.

4.4 Adaptive ITSMC design

The ITSMC proposed in the previous section can guarantee the system stability and robustness. However, if the control input (4.20) is used in practice, the elements of the vector A that define the upper bounds of f_Δ, are often not easy to find. In this section, an adaptive law which aims to tune the controller gains without knowledge of the upper bounds of the system uncertainties is proposed. For this, the following modified control law based on the sliding surface function (4.19), which integrates the adjustable gain $\hat{A}(t)$ is proposed as

$$u = \varphi^{-1}\left[\ddot{q}_d + \alpha \dot{e}^{\frac{q}{p}} + \beta e^{\frac{q}{2p-q}} - f + \lambda s + \psi^T \hat{A}\frac{s}{\|s\|}\right], \tag{4.24}$$

with the adaptation law given as

$$\dot{\hat{A}} = \Gamma \psi \chi(s), \tag{4.25}$$

where $\Gamma = diag(\Gamma_1, \cdots, \Gamma_7) \in \mathbb{R}^{7\times 7}$ is chosen as positive diagonal matrix and $\chi(s)$ is a scalar function defined as

$$\chi(s) = \begin{cases} \|s\| + \mu & if \quad \|s\| \neq 0 \\ 0 & if \quad \|s\| = 0 \end{cases}, \tag{4.26}$$

with $\mu > 0$ is a positive constant.

Lemma 4.2. *Given the system (4.12) with the ITSM surface (4.19) controlled by (4.24) and the adaptation law (4.25) and (4.26), the estimation $\hat{A}(t)$ has an upper-bound, it means, there exists a positive constant vector $A^* = [A_1^*, ..., A_7^*]^T \in \mathbb{R}^7$ such that $\hat{A}_i(t) \leq A_i^*$ and $A_i \leq A_i^*$ for $i \in \{1, ..., 7\}$, $\forall t > 0$.*

The proof of Lemma 4.2 can be found in appendix C.

The following theorem point out the AITSMC defined to guarantee the tracking control in a finite time.

Theorem 4.2. *Consider (4.10) and the system (4.12) under Properties 4.1 and the sliding-surface (4.19), the origin $(\dot{e}, e) = (0, 0)$ is globally finite-time-stable equilibrium under the control (4.24) and the adaptation law defined by (4.25) and (4.26).*

The detailed proof of Theorem 4.2 is presented in appendix D.

4.5 Experimental validation

The system considered in this study is the exoskeleton ULEL which is presented in Chapter 2.

4.5.1 Experimental setup

Experiments were carried out to provide passive mode rehabilitation using the exoskeleton ULEL. The device first has been tested alone without user, then with two

healthy subjects (*Subject A:* 31 years old measuring $1.71m$, weighing $74kg$; and *Subject B:* 43 years old measuring $1.69m$, weighing $70kg$). The purpose of the test is to ensure the good performance of the proposed system in order to help therapists apply for their rehabilitation program in good conditions.

ULEL is supposed to be in direct interaction with the user, that is why safety is very important. A power-off applied brake and limit switches to constrain ranges of motion are added to each active joint. Also, an emergency stop system can be easily activated. Since ULEL is fixed on a rigid base, wearing it will not impose any load on the subject.

Maxon controller cards are used to regulate motor currents. The controller is programmed on a PC equipped with a dSpace DS1103 PPC real-time controller card, using Matlab/Simulink and dSpace Control Desk software with a sampling time of $1ms$. Incremental encoders are used to measure the angular positions. During movements, the subjects remain relaxed without applying any effort while their right upper limb is attached to ULEL using straps. The experimental setup is depicted in Fig. 4.1.

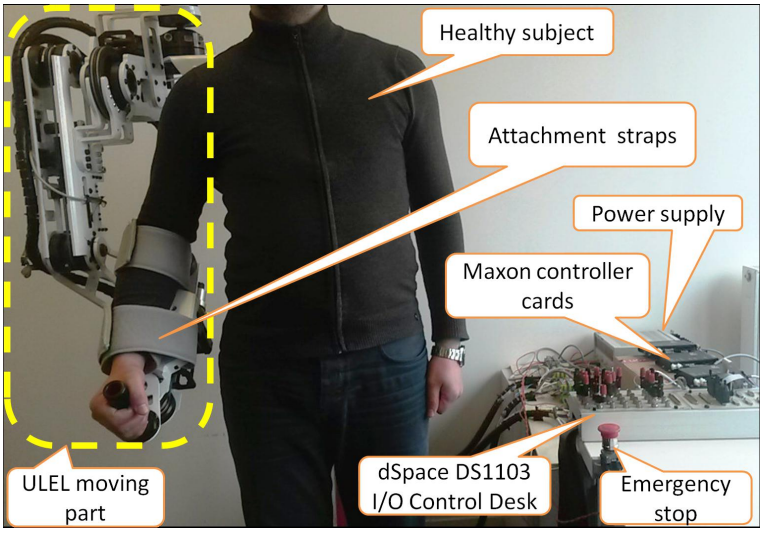

Figure 4.1: Experimental setup of ULEL.

The trajectories used in this work correspond to passive flexion/extension movements for shoulder, elbow and wrist joints used in passive rehabilitation exercises. The initial values of the system are selected as $q(0) = [0, \frac{\pi}{2}, 0]^T$, $\dot{q}(0) = [0, 0, 0]^T$. The parameters of the sliding surface function (4.19) are $p = 7$, $q = 9$, and the diagonal gain matrices are $\alpha = 3\,I$, $\beta = I$. For the control law, the gain matrix is $\lambda = 10^3\, diag([0.1, 0.3, 3])$. The initial value of the adaptation term $\hat{A}$ is equal to zero and the adaptation gain is $\Gamma = 10^2\, I$.

Indeed, actuators have delays and other imperfections, which can lead to chattering and excitation of non-modeled dynamics when sliding mode control is applied. That

is why a boundary layer technique is used to avoid chattering excitation of the control signal input. Therefore, the following functions $\sigma_\delta(s)$ and $\chi_\delta(s)$ are introduced instead of $\frac{s}{\|s\|}$ and $\chi(s)$ respectively in the control law, such as

$$\sigma_\delta(s) = \begin{cases} s/\|s\| & if \quad \|s\| > \delta \\ s/\delta & if \quad \|s\| \leq \delta \end{cases}, \tag{4.27}$$

$$\chi_\delta(s) = \begin{cases} \|s\| + \mu & if \quad \|s\| > \delta \\ 0 & if \quad \|s\| \leq \delta \end{cases}, \tag{4.28}$$

where $\delta = 0.2$ and $\mu = 0.1$.

Let the desired trajectories be defined as

$$\begin{cases} q_{d1}(t) = \frac{\pi}{10}\, sin(0.5\, t - \frac{\pi}{2}) + \frac{\pi}{6} \\ q_{d2}(t) = \frac{\pi}{10}\, sin(0.7\, t + \frac{\pi}{2}) + \frac{\pi}{6} \\ q_{d3}(t) = \frac{\pi}{10}\, sin(0.9\, t - \frac{\pi}{2}) \end{cases}. \tag{4.29}$$

The fact that ULEL is actuated by electrical DC motors, allow us to neglect the current dynamics of the motors which are very fast compared to the dynamics of the mechanical system. Then it can be assumed that:

$$u_i = \frac{1}{K_{ci} N_i}\, \tau_i, \tag{4.30}$$

where u_i is the control current of motor i , K_{ci} and N_i are the torque constant and the transmission Ratio of motor i (given in Table 2.1) respectively.

4.5.2 Experimental results

Figs. 4.2, 4.3 and 4.4 show the position tracking of each joint, as well as the tracking errors for the trials: with no subject attached to the exoskeleton, with *subject A* and with *subject B* respectively. Good tracking performance is obtained in the three cases, and errors converge to zero in less than $10s$, which shows the robustness and the advantages of the proposed finite time convergent controller. Moreover, the effects of the system uncertainties are eliminated after convergence.

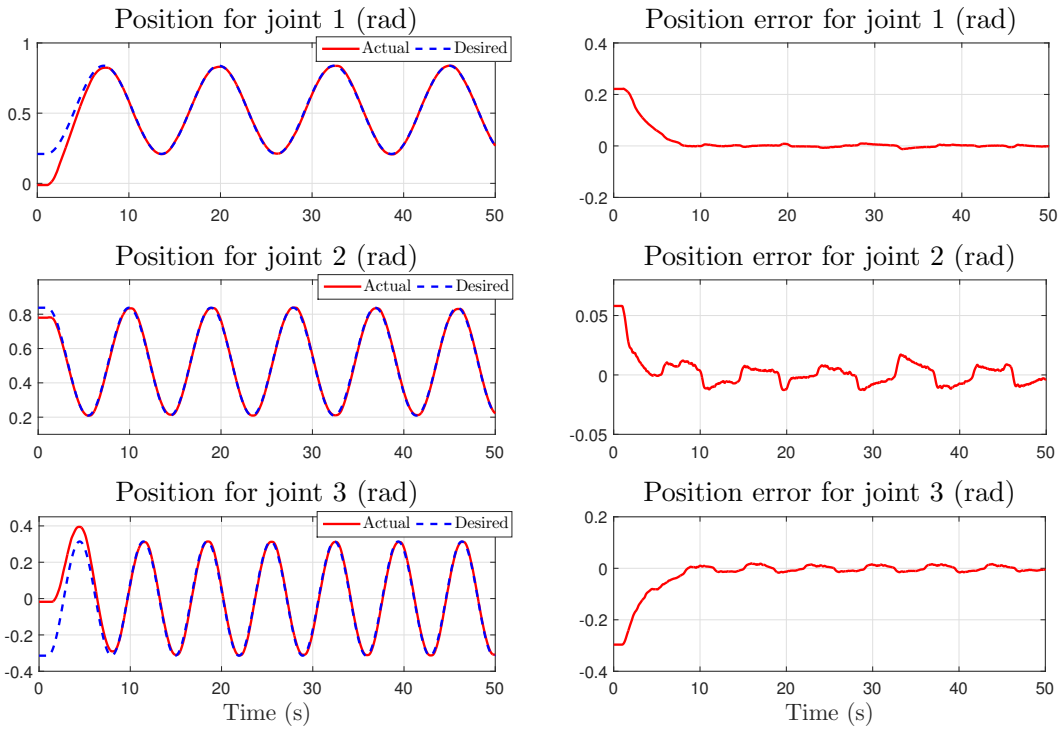

Figure 4.2: Actual positions, desired positions and position errors, trial without user

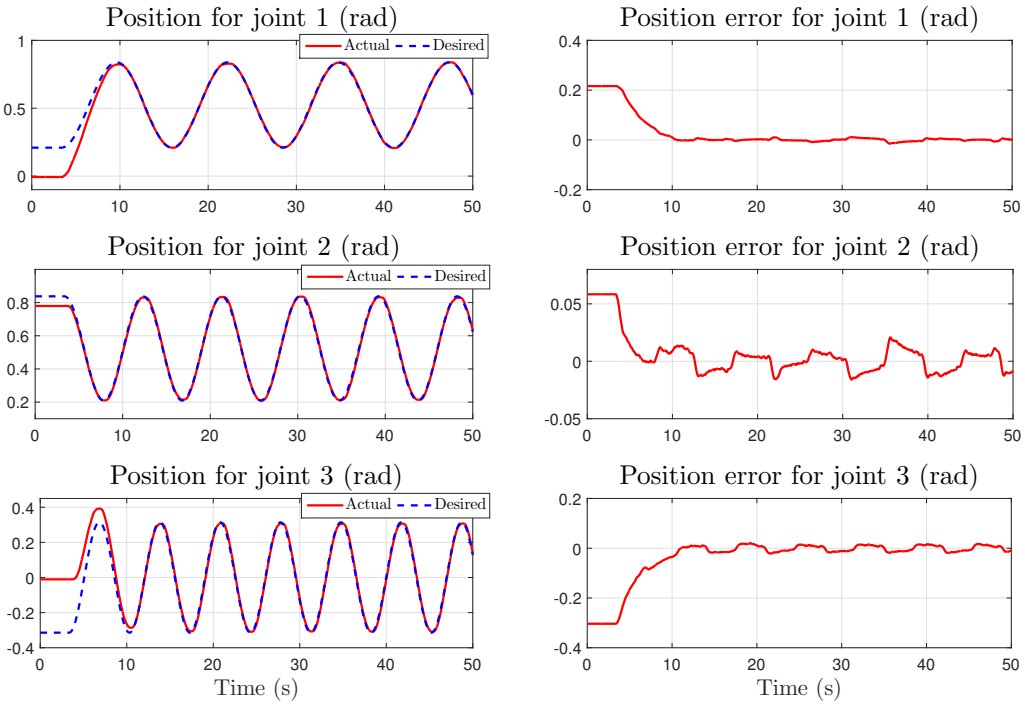

Figure 4.3: Actual positions, desired positions and position errors, trial with *Subject A*

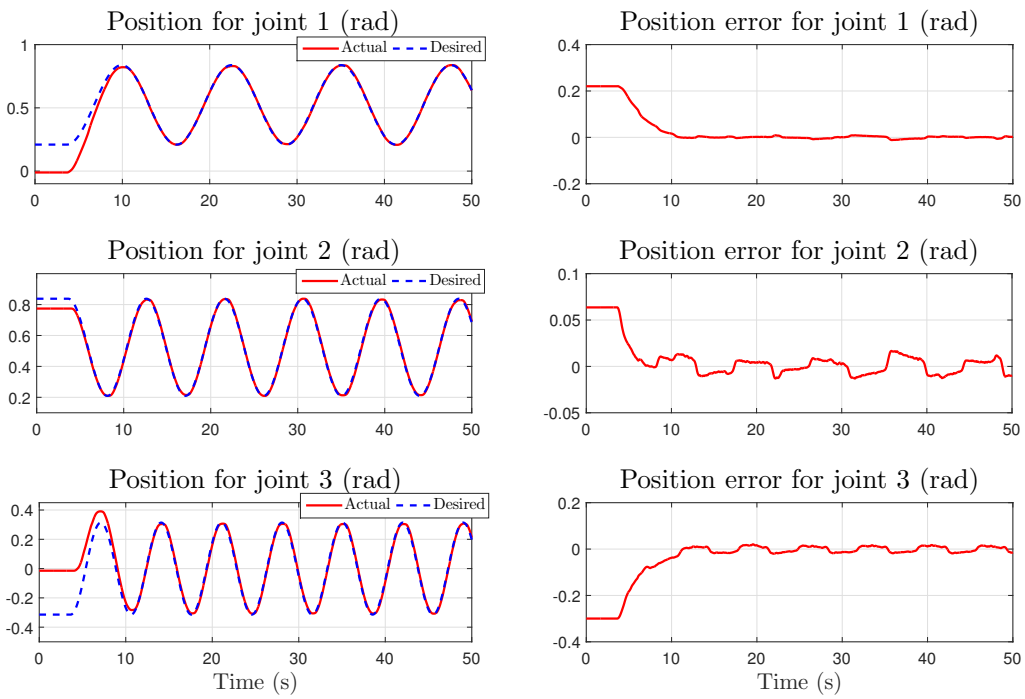

Figure 4.4: Actual positions, desired positions and position errors, trial with *Subject B*

Figs. 4.5, 4.6 and 4.7 present the control inputs for the trials: with no subject attached to the exoskeleton, with *subject A* and with *subject B* respectively. It is seen that the amplitudes of the control torques are convenient and realizable in practice. Also the boundary layer technique in (4.27) and (4.28), allows to avoid chattering.

Figs. 4.8, 4.9 and 4.10 show the estimated parameters $\hat{A}_i$, for $i = \{1, \ldots, 7\}$, for the trials: with no subject attached to the exoskeleton, with *subject A* and with *subject B* respectively. It is seen that the system uncertainty bounds are adaptively estimated even with different subjects, then prior knowledge of the upper bounds on the uncertainties is not required.

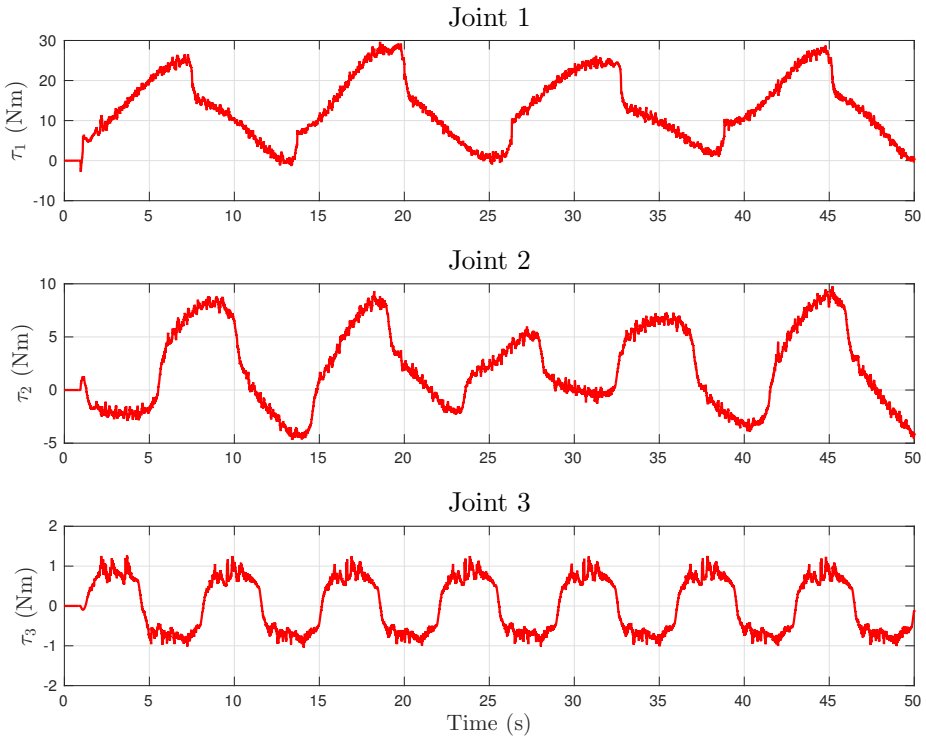

Figure 4.5: The input control torques for each joint, trial without user

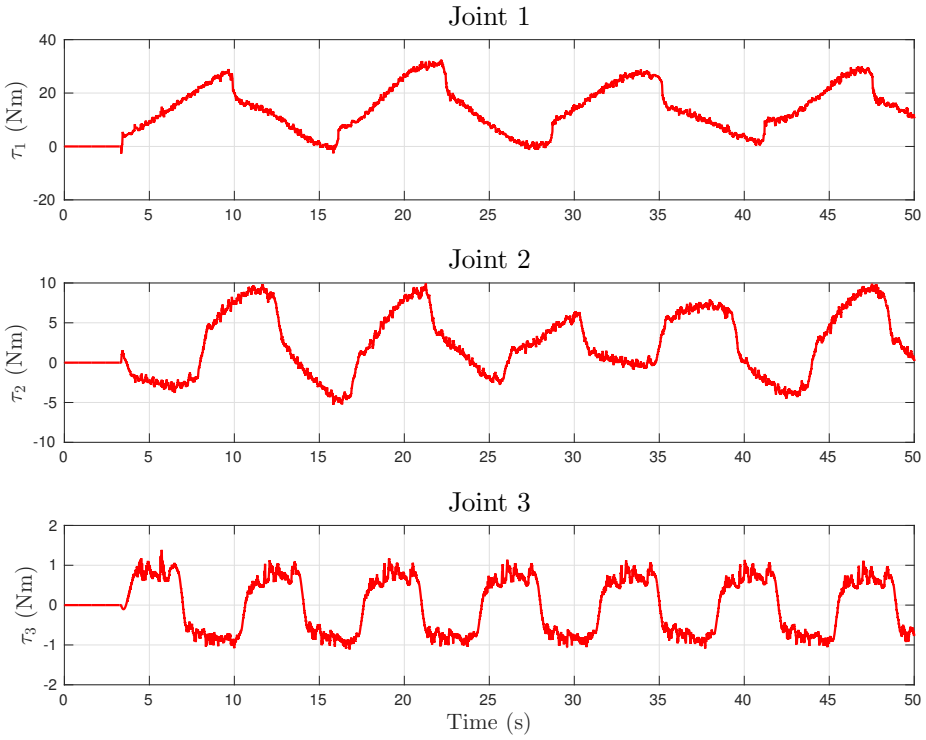

Figure 4.6: The input control torques for each joint, trial with *Subject A*

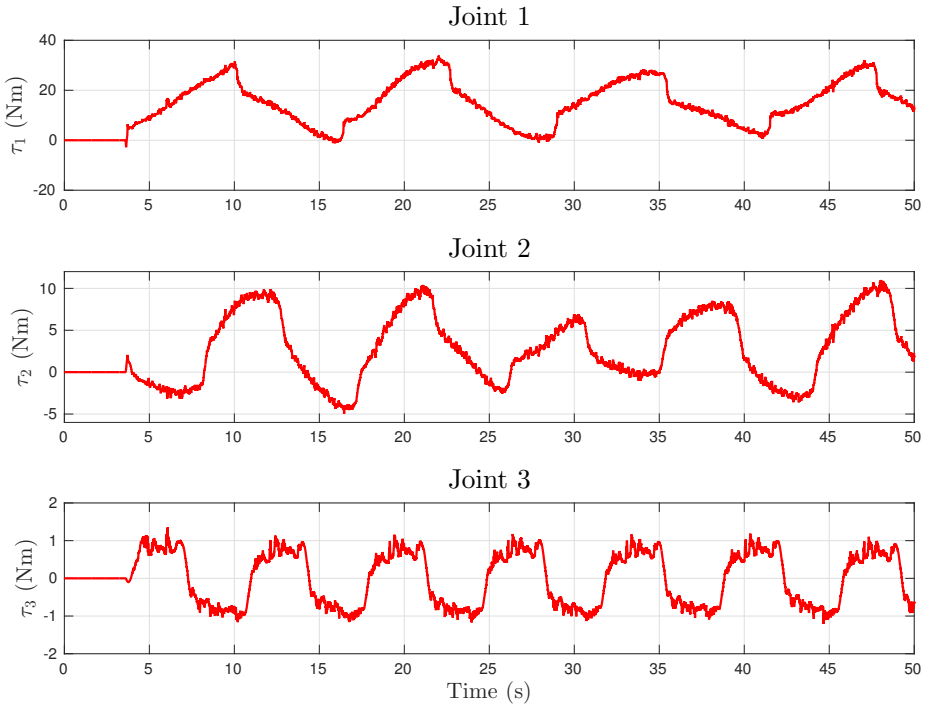

Figure 4.7: The input control torques for each joint, trial with *Subject B*

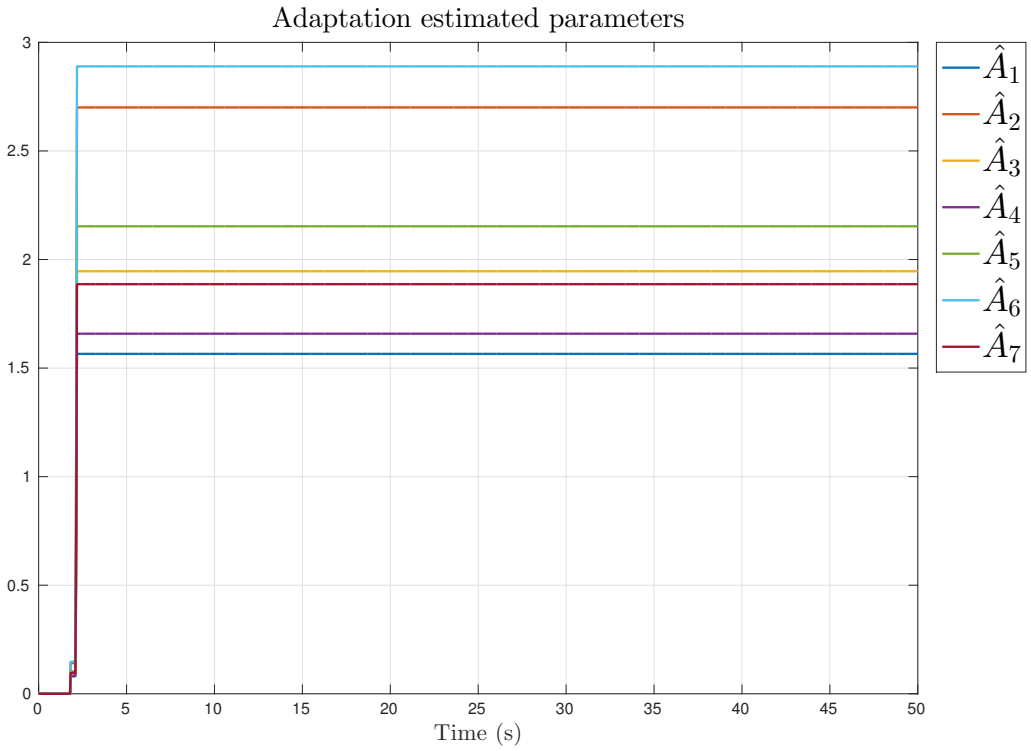

Figure 4.8: Estimated parameters $\hat{A}$, trial without user

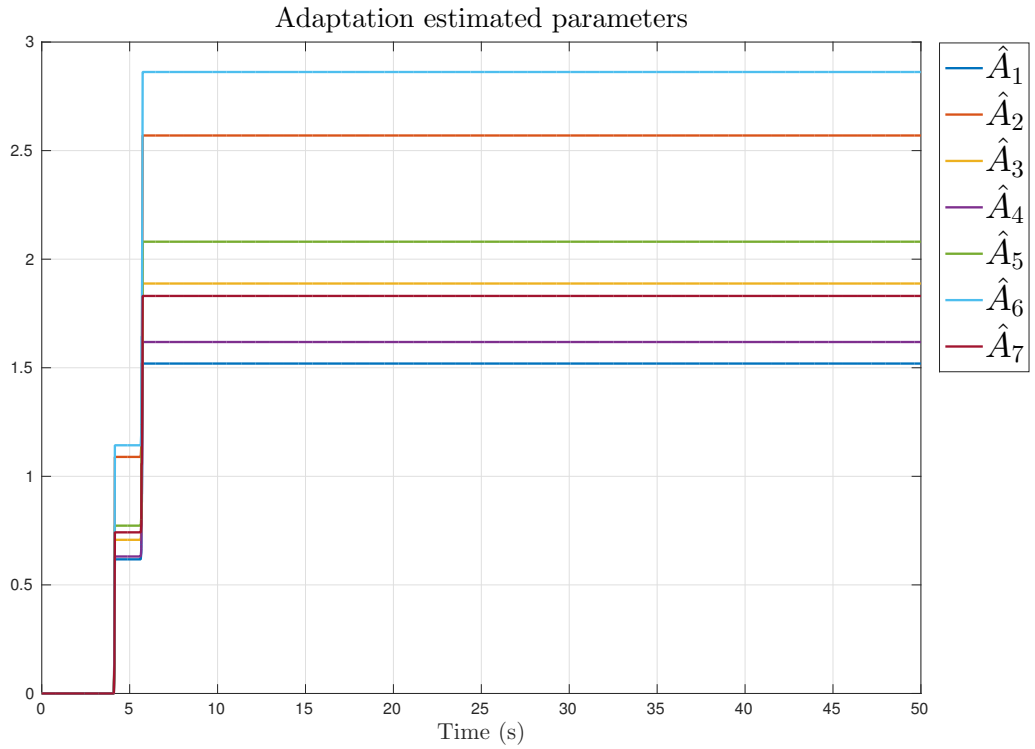

Figure 4.9: Estimated parameters $\hat{A}$, trial with *Subject A*

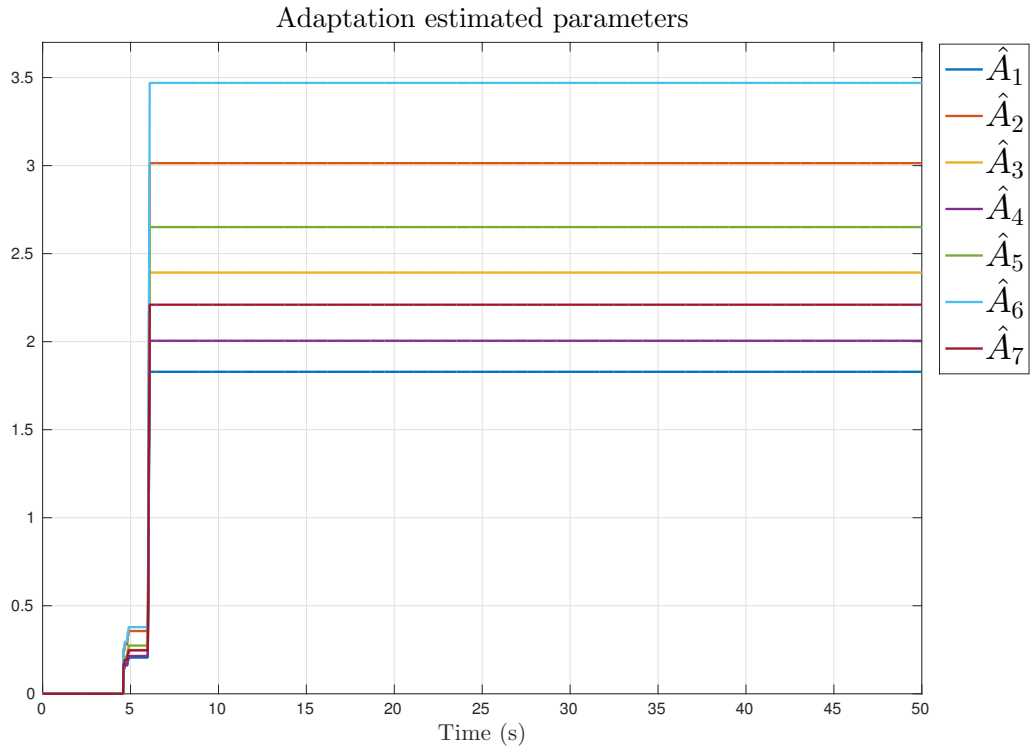

Figure 4.10: Estimated parameters $\hat{A}$, trial with *Subject B*

The results in terms of Relative-Tracking-Errors (RTE) and the Maximal-Control-Value (MCV) in the stabilization phase (between $t = 10s$ and $t = 50s$) are listed in Table 4.1. As seen from this performance indices, the proposed control is able to compensate for perturbations caused by the interaction with users of different morphologies without any prior settings. The RTE and MCV slightly increase when users are attached to the exoskeleton. Through the obtained results, it can be stated that the proposed control law can be effectively implemented for rehabilitation purposes and the control torques are convenient and realizable in practice.

Table 4.1: Performance indices of the proposed AITSMC for the carried out trials: RTE_i is the Relative-Tracking-Errors of the i^{th} joint calculated by $\sqrt{\sum_{k=1}^{N} e_i^2(t_k)}/\sqrt{\sum_{k=1}^{N} q_i^2(t_k)}$ where t_k being the k^{th} sample time and N is the total number of samples; MCV_i is the Maximum-Control-Value of the i^{th} joint calculated by the maximum of the values $|u_i(t_1)|, ..., |u_i(t_N)|$.

Experiment	Joint	RTE_i (%)	MCV_i (Nm)
without subject	$i = 1$	0.72	26.66
	$i = 2$	1.25	9.76
	$i = 3$	4.64	1.17
with *subject A*	$i = 1$	0.84	32.47
	$i = 2$	1.48	9.94
	$i = 3$	5.59	1.21
with *subject B*	$i = 1$	0.76	33.79
	$i = 2$	1.36	11
	$i = 3$	5.87	1.25

4.6 Conclusion

This chapter proposes an effective AITSMC approach which can be applied for the robust control of upper limb exoskeletons to perform passive rehabilitation movements. It is shown that the proposed method gives good tracking performance with finite time convergence and without any prior knowledge of the system uncertainty bounds. Experiments using the exoskeleton ULEL alone and with tow healthy users demonstrate the effectiveness of the proposed strategy and its satisfactory performance. It can be concluded that the proposed algorithm may be effectively used with subjects having different morphologies without any prior adaptation. Therefore, the proposed method can be effectively implemented in practice. For future work, active rehabilitation with exoskeletons will be investigated.

Chapter 5

Exact estimation of state and Human-Exoskeleton interaction torques

Contents

5.1 Introduction

Exoskeletons compared to other robotic devices are in direct interaction with the user, this is why the precise identification of human-robot interaction is essential for such applications in terms of user safety and also in control design. Besides, interaction efforts can provide quantitative data for patient's motor function recovery allowing adequate adaptation of the therapy protocols.

An obvious way to determine the interactions efforts is to use force sensors at the contact interfaces [165]. Despite the effectiveness of this method it suffers from several drawbacks namely the high cost of these devices and their complexity, also these sensors

add an additional weight to the structure and can bother the user during movements. In addition the presence of noise can degrade the quality of the measurements and precise calibration problems appear when using these sensors. The estimation of interaction efforts can solve the problems associated to the use of sensor measurements.

Several methods for interaction efforts estimation have been proposed. In [166] only the control signal (motor currents) is used to implement an impedance-based force controller for a wrist exoskeleton. Also the full dynamic model can be used to estimate the interactions [167][168][169][170]. More recently, the problem of interaction force estimation in exoskeletons was addressed in [171].

In [172], author described the higher-order sliding mode, which makes use of the inverse plant model to estimate the resultant disturbance acting on the system. Disturbance observers can improve robustness and tracking accuracy of industrial manipulators []. They are also used in haptics and power assistance control [173]. We believe that they can be used in exoskeleton systems to estimate interaction force variations if the other disturbances caused by robot dynamics and friction are accurately compensated.

In this chapter, a third-order-like sliding mode observer is proposed to estimate the human-exoskeleton interaction torques. The proposed observer is to estimate bounded torques caused by the interaction of the exoskeleton with the human limb, when only the position measurements are available with knowledge of the control input. To do so, a third-order-like sliding mode technique is used. The stability of the proposed approach is demonstrated and finite time convergence is obtained.

The rest of this chapter is structured as follows. The next Section describes the modeling of the exoskeleton. In Section 5.3 the state representation of the system is defined, and the augmented state space is presented as well as properties and assumptions needed for the observer syntheses. The proposed observer design is presented in Section 5.4. Section 5.6 shows the simulation results using our exoskeleton ULEL, to validate the efficiency of the proposed observer and finally this chapter ends with a conclusion in Section 5.7.

5.2 Dynamic model

The dynamic behavior of the human-exoskeleton system can be expressed by

$$M(q)\ddot{q} + H(q,\dot{q}) = \tau_h + \tau_e \tag{5.1}$$

with

$$H(q, \dot{q}) = C(q, \dot{q})\dot{q} + G(q) + D(\dot{q}) \tag{5.2}$$

where $q \in \mathbb{R}^n$, $\dot{q} \in \mathbb{R}^n$ and $\ddot{q} \in \mathbb{R}^n$ are respectively the joint positions, velocities and accelerations, $M(q) \in \mathbb{R}^{n\times n}$ is the inertia matrix, $C(q, \dot{q}) \in \mathbb{R}^{n\times n}$ is the Coriolis/centrifugal matrix, $G(q) \in \mathbb{R}^n$ is the gravity vector, $D(\dot{q}) \in \mathbb{R}^n$ is the dissipation term, $\tau_h \in \mathbb{R}^n$ is the torque vector applied by the human, and $\tau_e \in \mathbb{R}^n$ is the torque vector applied by the exoskeleton.

5.3 The augmented state space

Let $x_1 = q$, $x_2 = \dot{q}$ and $u = \tau_e$ then we can write

$$\begin{cases} \dot{x}_1 = x_2 \\ \dot{x}_2 = f(x_1, x_2, u) + g(x_1)\tau_h \end{cases} \tag{5.3}$$

where $f(x_1, x_2, u) = M^{-1}(q)[\tau_e - H(q, \dot{q})] \in \mathbb{R}^n$ and $g(x_1) = M^{-1}(q) \in \mathbb{R}^{n\times n}$.

- Property: The function $g(x_1)$ is invertible and differentiable.
- Assumption: The vectors x_1 and u are measurable.
- Assumption: The function $f(x_1, x_2, u)$ is known and differentiable.
- Assumption: The human torque τ_h is differentiable.

Let define the augmented state variable $x_3 \in \mathbb{R}^n$ as

$$x_3 \triangleq f(x_1, x_2, u) + g(x_1)\tau_h \tag{5.4}$$

Using (5.3) and the derivative of (5.4) gives the following augmented state space:

$$\begin{cases} \dot{x}_1 = x_2 \\ \dot{x}_2 = x_3 \\ \dot{x}_3 = \dot{f}(x_1, x_2, u) + \dot{g}(x_1)\,\tau_h + g(x_1)\,\dot{\tau}_h \end{cases} \tag{5.5}$$

5.4 Observer design

This section describes the design of an observer-based approach to estimate the interaction torque acting on a controlled rigid body from measurements of its articular

positions and knowledge of the control torques. The proposed observer has the following structure:

$$\begin{cases} \dot{\hat{x}}_1 = \hat{x}_2 + z_1 \\ \dot{\hat{x}}_2 = f(x_1, \hat{x}_2, u) + g(x_1)\,\hat{\tau}_h + z_2 \\ \dot{\hat{\tau}}_h = g^{-1}(x_1)\,z_3 \end{cases} \tag{5.6}$$

where $\hat{x}_1$, $\hat{x}_2$ and $\hat{\tau}_h$ are the estimations of x_1, x_2 and τ_h respectively and z_i, $i = 1, 2, 3$ are the correction terms given by

$$\begin{cases} z_1 = K_1\,\Phi_1(x_1 - \hat{x}_1)\,Sign(x_1 - \hat{x}_1) \\ z_2 = K_2\,\Phi_2(v_1 - \hat{x}_2)\,Sign(v_1 - \hat{x}_2) \\ z_3 = K_3\,Sign(v_2 - f(x_1, \hat{x}_2, u) - g(x_1)\,\hat{\tau}_h) \end{cases} \tag{5.7}$$

where $v_1 = \dot{\hat{x}}_1$, $v_2 = \dot{\hat{x}}_2$, the gains $K_i \in \mathbb{R}^{n\times n}$ for $i = 1, 2, 3$ are diagonal positive matrices, the function $\Phi_1(.)$, $\Phi_2(.)$ and $Sign(.)$ are defined as follows:

$$\begin{cases} \Phi_1(\chi) = diag[\,|\chi_1|^{\frac{2}{3}}\,,\,\ldots\,,\,|\chi_n|^{\frac{2}{3}}\,] \in \mathbb{R}^{n\times n} \\ \Phi_2(\chi) = diag[\,|\chi_1|^{\frac{1}{2}}\,,\,\ldots\,,\,|\chi_n|^{\frac{1}{2}}\,] \in \mathbb{R}^{n\times n} \\ Sign(\chi) = [\,sign(\chi_1)\,,\,\ldots\,,\,sing(\chi_n)\,]^T \in \mathbb{R}^n \end{cases} \tag{5.8}$$

for any $\chi = [\chi_1, \ldots, \chi_n]^T \in \mathbb{R}^n$ and $sign(.)$ is the standard signum function such that

$$sign(\chi_i) = \begin{cases} +1 & if \quad \chi_i > 0 \\ 0 & if \quad \chi_i = 0 \\ -1 & if \quad \chi_i < 0 \end{cases} \tag{5.9}$$

for $i = 1, \ldots, n$.

5.5 Proof

Let us define the estimation $\hat{x}_3$ as follows:

$$\hat{x}_3 \triangleq f(x_1, \hat{x}_2, u) + g(x_1)\,\hat{\tau}_h \tag{5.10}$$

Then, its derivative is

$$\dot{\hat{x}}_3 = \dot{f}(x_1, \hat{x}_2, u) + \dot{g}(x_1)\,\hat{\tau}_h + g(x_1)\,\dot{\hat{\tau}}_h \tag{5.11}$$

From (5.6), (5.7), (5.10) and (5.11) it yields

$$\begin{cases} \dot{\hat{x}}_1 = \hat{x}_2 + K_1\,\Phi_1(x_1 - \hat{x}_1)\,Sign(x_1 - \hat{x}_1) \\ \dot{\hat{x}}_2 = \hat{x}_3 + K_2\,\Phi_2(v_1 - \hat{x}_2)\,Sign(v_1 - \hat{x}_2) \\ \dot{\hat{x}}_3 = \dot{f}(x_1, \hat{x}_2, u) + \dot{g}(x_1)\,\hat{\tau}_h + K_3\,Sign(v_2 - \hat{x}_3) \end{cases} \tag{5.12}$$

By defining the error vectors as $\tilde{x}_i = x_i - \hat{x}_i$ for $i = 1, 2, 3$ then their dynamics are given as

$$\begin{cases} \dot{\tilde{x}}_1 = \tilde{x}_2 - K_1\,\Phi_1(x_1 - \hat{x}_1)\,Sign(x_1 - \hat{x}_1) \\ \dot{\tilde{x}}_2 = \tilde{x}_3 - K_2\,\Phi_2(v_1 - \hat{x}_2)\,Sign(v_1 - \hat{x}_2) \\ \dot{\tilde{x}}_3 = \xi(t) - K_3\,Sign(v_2 - \hat{x}_3) \end{cases} \tag{5.13}$$

where

$$\begin{aligned} \xi(t) \;=\; & \dot{f}(x_1, x_2, u) - \dot{f}(x_1, \hat{x}_2, u) \\ & + \dot{g}(x_1)\,(\tau_h - \hat{\tau}_h) + g(x_1)\,\dot{\tau}_h \end{aligned} \tag{5.14}$$

- Assumption: The vector $\xi(t)$ is bounded

$$\bar{\xi} > \|\xi(t)\| \tag{5.15}$$

  where $\bar{\xi}$ is some known positive scalar.

The finite-time convergence of the observer errors $\tilde{x}_1$, $\tilde{x}_2$ and $\tilde{x}_3$ can be demonstrated by taking

$$\begin{cases} K_1 = 3 \cdot I \cdot \bar{\xi}^{1/3} \\ K_2 = 1.5 \cdot I \cdot \bar{\xi}^{1/2} \\ K_3 = 1.1 \cdot I \cdot \bar{\xi} \end{cases} \tag{5.16}$$

and by rewriting (5.13) in the following form of differential inclusion

$$\begin{cases} \dot{\tilde{x}}_{1_i} = \tilde{x}_{2_i} - K_{1_i}|x_{1_i} - \hat{x}_{1_i}|^{\frac{2}{3}} sign(x_{1_i} - \hat{x}_{1_i}) \\ \dot{\tilde{x}}_{2_i} = \tilde{x}_{3_i} - K_{2_i}|v_{1_i} - \hat{x}_{2_i}|^{\frac{1}{2}} sign(v_{1_i} - \hat{x}_{2_i}) \\ \dot{\tilde{x}}_{3_i} \in [-\bar{\xi}, +\bar{\xi}] - K_{3_i} sign(v_{2_i} - \hat{x}_{3_i}) \end{cases} \tag{5.17}$$

for $i = 1, ..., n$ with the under index i refer the i^{th} scale element of the corresponding vector or diagonal matrix.

This inclusion is understood in Filippov sense [174]. The proof of finite-time convergence of $\tilde{x}_1$, $\tilde{x}_2$ and $\tilde{x}_3$ to zeros follows from Lemma 8 in [172]. Therefore, it comes from equations (5.4) and (5.10) that the estimation $\hat{\tau}_h$ converge also in the same finite-time to τ_h.

5.6 Simulation results

Simulations were carried out using The multi-body dynamic model of ULEL presented in chapter 2, to move the exoskeleton attached to the articulated arm along desired trajectories. External torques applied to the three exoskeleton joints are considered from the 5^{th} second. In this example, the initial values of the system are selected as $q(0) = [0, 0, 0]^T$, $\dot{q}(0) = [0, 0, 0]^T$. The fourth-order Runge-Kutta method with a sampling time of $1ms$ is used to solve the nonlinear differential equation numerically. The observer gain matrices are chosen with $\bar{\xi} = 100$. The external torques applied from the 5^{th} second are chosen as follows:

$$\begin{cases} \tau_{ext1}(t) = 3\, sin(t-5) \\ \tau_{ext2}(t) = 2\, sin(t-5) \\ \tau_{ext3}(t) = 0.1\, sin(t-5) \end{cases} \quad \text{for} \quad t \geq 5 \tag{5.18}$$

Let the applied control torques be defined as

$$\begin{cases} \tau_1(t) = 3\, sin(t) \\ \tau_2(t) = 2\, sin(t + \frac{\pi}{2}) \\ \tau_3(t) = \ sin(t) \end{cases} \tag{5.19}$$

A white noise component of Signal to Noise Ratio (SNR) equal to $40dB$ is considered in the joints positions and velocities. In addition to the proposed estimator, an Extended Kalman Filter (EKF) was implemented to estimate the state and applied external torques of the system. The use of the proposed estimator and EKF estimator, with the same simulation conditions and the chosen parameters and gains as described previously leads to the following results.

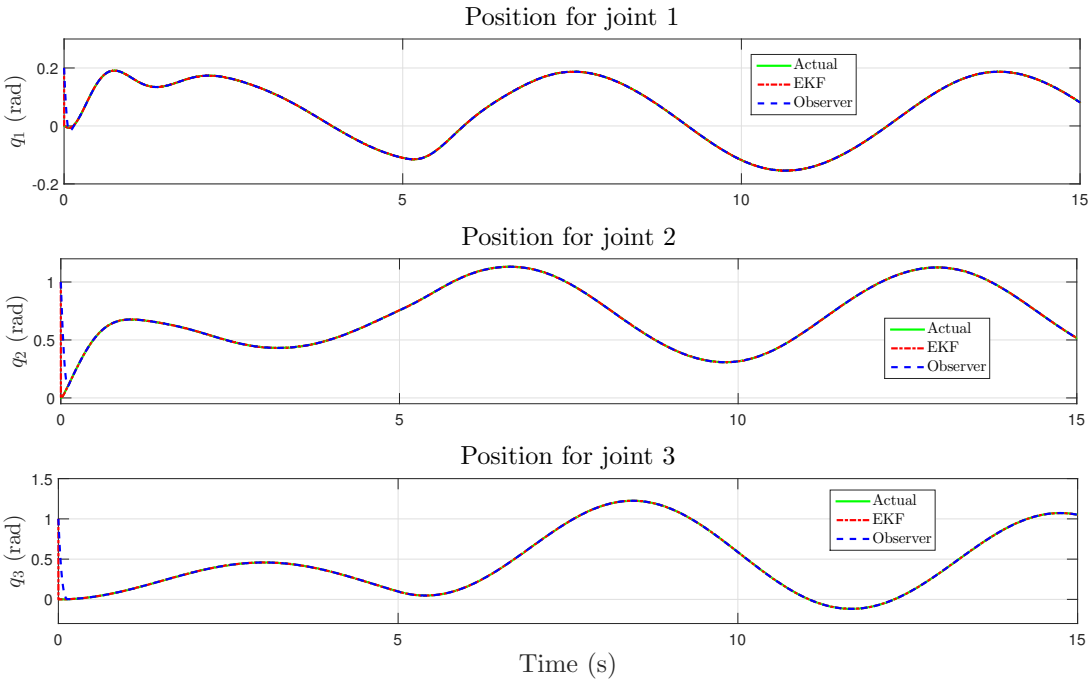

Figure 5.1: Actual and desired positions, with white noise of SNR=40dB

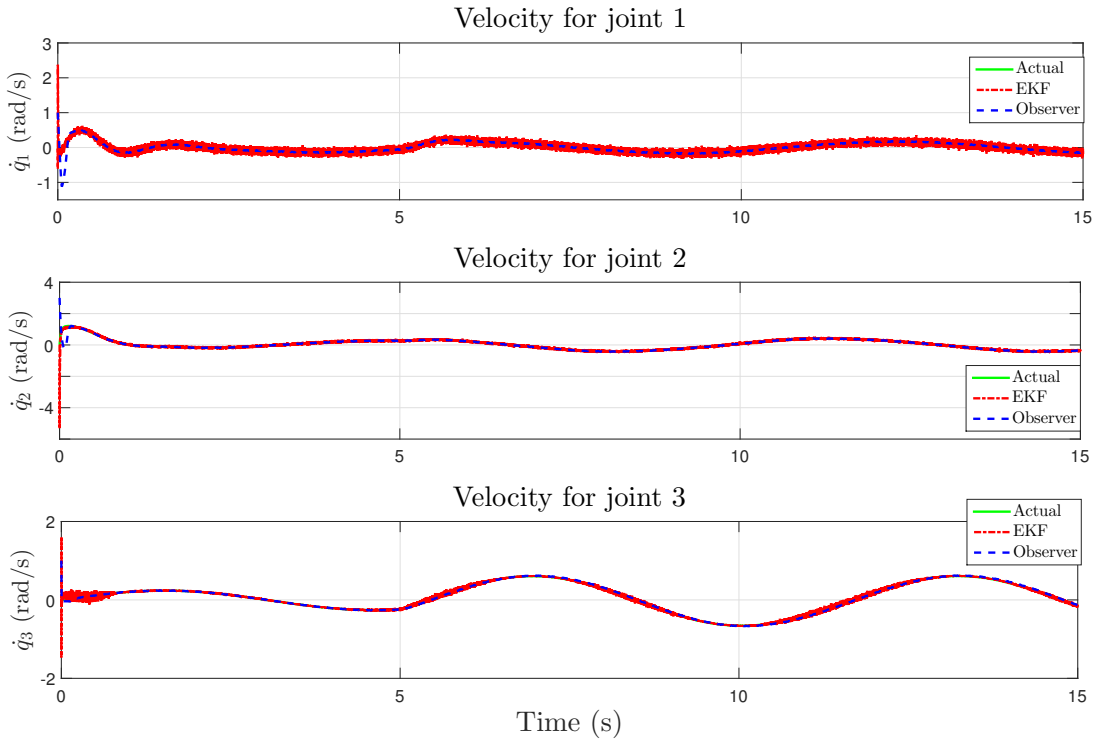

Figure 5.2: Actual and desired velocities, with white noise of SNR=40dB

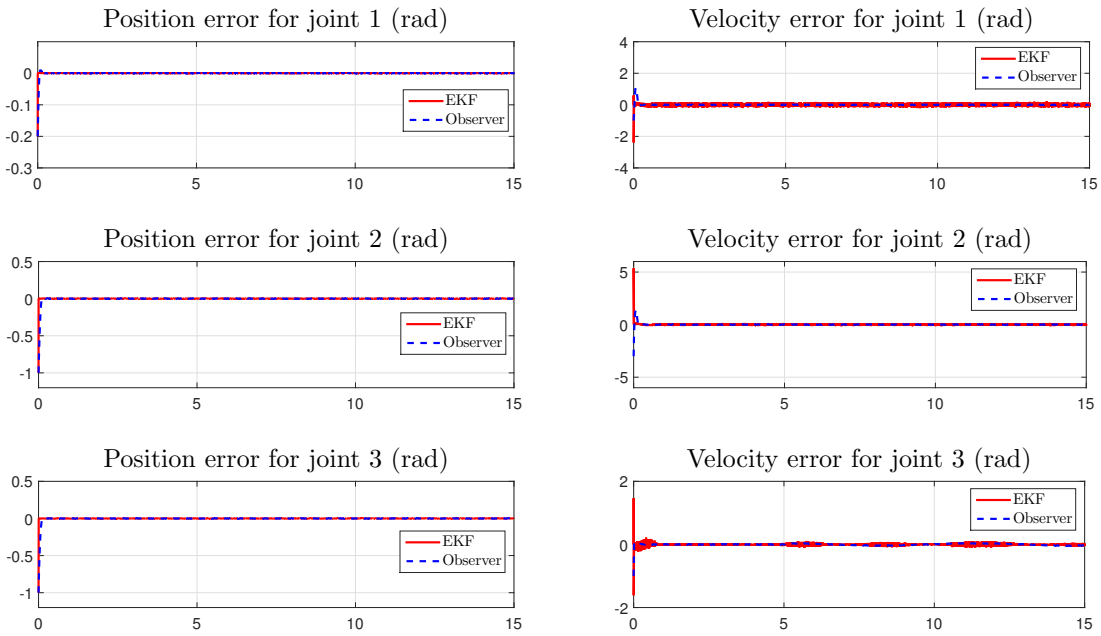

Figure 5.3: Position and velocity estimation errors using the proposed estimator and the EKF estimator, with white noise of SNR=40dB

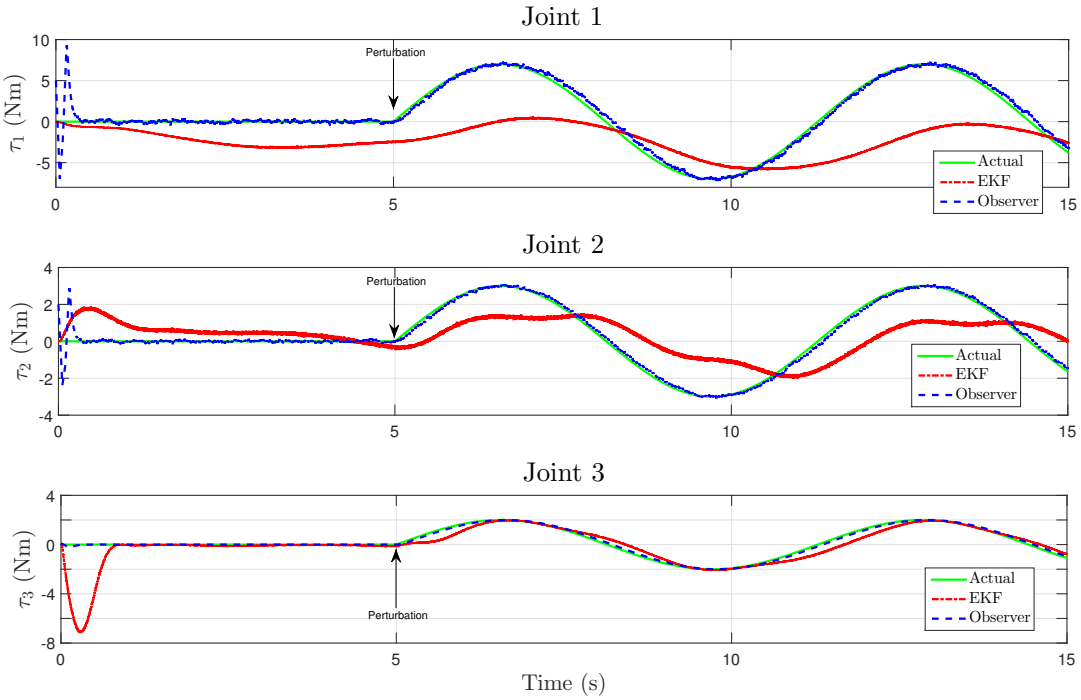

Figure 5.4: External torques applied from the 5^{th} second, with white noise of SNR=40dB

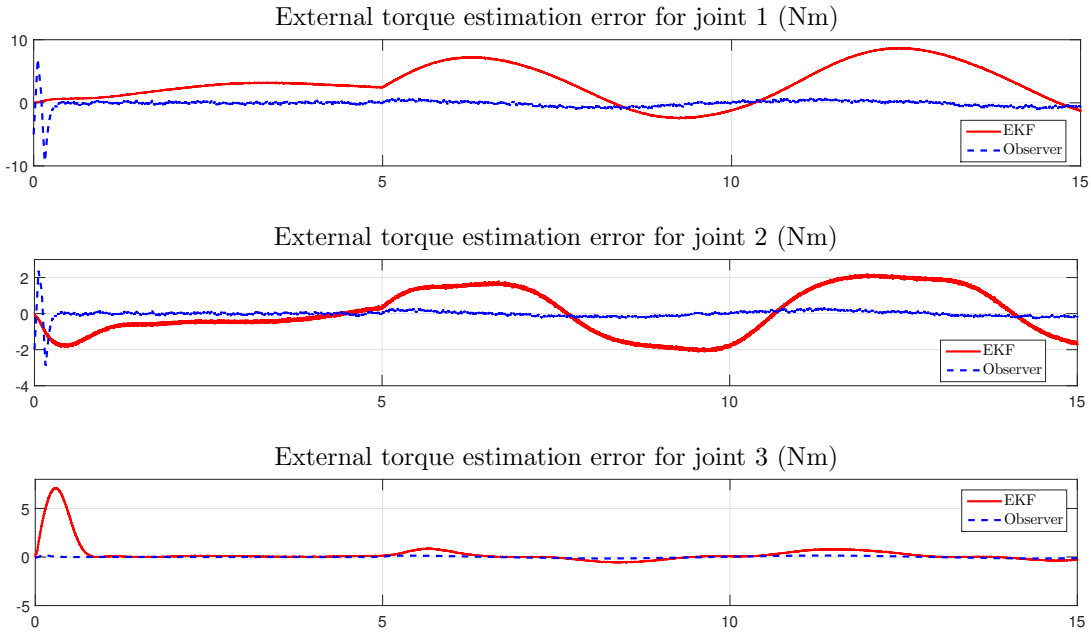

Figure 5.5: External torque estimation errors using the proposed estimator and the EKF estimator, with white noise of SNR=40dB

Figs. 5.1 and 5.2, show the estimates of joint positions and velocities respectively, using the proposed observer (in blue dotted line), and the EKF method (in red dotted line). The actual positions and velocities are presented in green solid line. We can see that the proposed observer as well as the EKF method give a good estimation of the system state, however the estimate with the proposed observer is better filtered and smoother than that with the EKF observe with the proposed observer, especially on velocity signals. State estimation errors converge to zero after a very brief transition as shown in Fig. 5.3, here also we can see that our observer is more robust against noise than the EKF method especially on velocity signals. Furthermore, the effects of the system uncertainties are eliminated. Fig. 5.4 shows the external torques estimates for each joint using the proposed observer and the EKF observer. It can be seen that the torque estimated with the proposed observer and the actual torque overlaps and the torque estimation is accurate, on the other hand the torque estimated with the EKF method is poor and doesn't match with the real torque. In order to better compare the real torque and estimated one, the interaction torque estimation errors are shown in Fig. 5.5 which shows that the estimation errors converge to zero using the proposed observer unlike the estimation using the EKF observer.

5.7 Conclusion

In this chapter a third-order-like sliding mode observer for state and human-exoskeleton interaction torque estimation is presented. The proposed observer enables the finite time convergence of the non-output states which cannot be achieved by conventional sliding mode observers. The proof and stability analysis of the observer was also introduced. Simulation using the multi-body model of the exoskeleton ULEL verifies the effectiveness of the proposed observer. Furthermore, an estimator using Extended Kalman Filter (EKF) is implemented with the same simulation conditions, and comparison is conducted in order to evaluate the performance of the proposed estimator. Simulation results show the superiority of the proposed observer over the EKF method in terms of estimation accuracy and robustness against noise, besides, the gains tuning of the proposed observer is easier compared to the tuning of the EKF parameters.

Conclusion

In this chapter we present a general conclusion by summarizing our contributions and describing some perspectives for future works, as well as publications produced during this theses.

Summary of contributions

In this thesis, we try to respond to issues related to exoskeletons use for upper limb rehabilitation and mobility assistance of people who suffer from motor deficit, characterized by a total or partial loss of motor skills. After having made a state of the art on rehabilitation robotics and the presentation of recent research in this field in the first Chapter, we have decided that our contributions in this topic should be the investigation of control strategies to perform upper limb rehabilitation using exoskeleton systems.

The robot used is a 3 DoF exoskeleton called ULEL desined by RB3D (presented in Chapter 2). Since ULEL is a new prototype and was never been used before, we stared by instrumenting our robotic system and installing all the equipment and sensors required to use the exoskeleton. Furthermore, all modeling and parameter identification is made as detailed in Chapter 2. In particular, I was interested in the design of exoskeleton control laws for functional rehabilitation of the upper limb. There are especially three majors contributions presented in this dissertation.

The first one consists of an adaptive control strategy based on an online estimator of dynamic parameters (presented in Chapter 3). This adaptation method makes it possible to improve the control performance of this system, and to compensate for parametric errors due to coupling the exoskeleton with the human limb. The proposed control allow to perform stable tracking of desired trajectories without requiring exact knowledge of the dynamic parameters. The obtained results were validated and compared to adaptive control without parameter estimation by simulations using the muti-body dynamic model of ULEL.

The second contribution is presented in Chapter 4, which consists of a robust control strategy based on integral terminal sliding mode technique. This nonlinear strategy guarantees the convergence of tracking errors to zero in finite time when the sliding mode is reached. This type of control is known by its robustness with respect to parametric variations and external disturbances. The effectiveness of the proposed method is experimentally demonstrated using the exoskeleton ULEL for the passive rehabilitation mode with healthy subjects. The obtained results show that the proposed algorithm may be effectively used with subjects having different morphologies without any prior adaptation. Therefore, the proposed method can be effectively implemented in practice.

Finally, in Chapter 5, a higher order sliding mode observer is proposed to estimate interaction torques of the human-exoskeleton system. The proposed observer is able to estimate the forces at the interaction interface between the exoskeleton and the human limb, using position measurements and control input signals. The proposed strategy is validated with simulations using the exoskeleton ULEL muti-body model, and a comparison with Extended Kalman Filter observer is performed. The obtained results show the effectiveness of the proposed solution.

Future work

In order to continue the development of this work many perspectives can be formulated to develop robotic prototype intended to upper limb rehabilitation, that we propose as follows:

- The advances so far (modeling and identification of the exoskeleton ULEL, different control strategies for passive rehabilitation mode, human-machine interaction estimation, between others) had been developed and tested with on multi-body dynamic simulations and experimentally with healthy subjects. An important next step is to consider force sensors to evaluate the human-machine interaction and validate the proposed third-order-like sliding mode observer experimentally. Solving the interaction estimation problem, will give the possibility to develop impedance and admittance controllers

- The next step is to develop control shames for active mode rehabilitation. Also, the use of electromyographic signals (EMG) and/or electroencephalogram (EEG) is a promising objective. These physiological signals can be combined with force sensor measurements or force estimations in order to provide a more detailed prediction of the subject's intention. Also, can be used alone if we can't get the interaction force information to determine the intended movement.

- Another important step in order to achieve full usability of the rehabilitation strategies is the development of scenarios and protocols for the different rehabilitation modes, then implement them in our robotic system. For this, collaboration with neuroscientists and physiotherapists is expected.
- The validation of our rehabilitation system with disabled patients in a clinical environment is an important work to validate the effectiveness of our robotic system. To proceed with this step a deep safety review is mandatory.
- The development of a virtual reality environment of the human-machine interface is also an important area, who can enhance the project by adding audio-visual feedback to rehabilitation process.

Publications

- A. Riani, T. Madani, A. El Hadri, and A. Benallegue, "Adaptive integral terminal sliding mode control of an upper limb exoskeleton," 18th International Conference on Advanced Robotics (ICAR), Hong Kong 2017 . IEEE, pp. 131–136, 2017.
- A. Riani, T. Madani, A. El Hadri, and A. Benallegue, "Adaptive control based on an on-line parameter estimation of an upper limb exoskeleton," International Conference on Rehabilitation Robotics (ICORR), London 2017. IEEE, pp. 695–701, 2017.
- A. Riani, T. Madani, A. Benallegue, and K. Djouani, "Adaptive integral terminal sliding mode control for upper-limb rehabilitation exoskeleton," Control Engineering Practice journal (CEP), vol. 75, pp. 108–117, 2018.

Appendix A

The bounded property of uncertainties

It has been noted previously in Remark 4.1 that the uncertainties $\Delta(t)$ depends on the unknown acceleration term $\ddot{q}$. In this section, a similar methodology to that proposed in [153] is used to solve this problem.

By replacing (4.11) in (4.5), it yields

$$\xi = M_N^{-1}\left[\tau_\Delta - M_\Delta M_N^{-1}\left(u + \Delta - H_N\right) - H_\Delta\right]. \tag{A.1}$$

After some simple rearrangements it comes

$$\begin{aligned}\left(I + M_N^{-1}M_\Delta\right)\xi &= M_N^{-1}[\tau_\Delta - M_\Delta M_N^{-1}u \\ &\quad + M_\Delta M_N^{-1}H_N - H_\Delta].\end{aligned} \tag{A.2}$$

Since $\left(I + M_N^{-1}M_\Delta\right) = M_N^{-1}\left(M_N + M_\Delta\right) = M_N^{-1}M$ then it can be written that

$$\begin{aligned}\xi &= M^{-1}(\tau_\Delta - M_\Delta M_N^{-1}u + M_\Delta M_N^{-1}H_N - H_\Delta) \\ &= M^{-1}(\tau_\Delta - H_\Delta) + M^{-1}M_\Delta M_N^{-1}(H_N - u).\end{aligned}$$

So the uncertainties ξ can be upper-bounded as follows:

$$\begin{aligned}\|\xi\| &\leq \|M^{-1}\|(\|\tau_\Delta\| + \|H_\Delta\|) \\ &\quad + \|M^{-1}M_\Delta M_N^{-1}\|(\|u\| + \|H_N\|).\end{aligned} \tag{A.3}$$

Considering Property 4.1, Assumption 3 it yields

$$\begin{cases} \|M^{-1}\| < a_1 \\ \|M^{-1}M_\Delta M_N^{-1}\| < a_2 \end{cases}, \tag{A.4}$$

where a_1 and a_2 are non-negative constants. Then, using (4.10), (A.4) and Assumption 3, in (A.3) it comes

$$\begin{aligned} \|\xi\| \leq \; & \left(a_1\overline{\tau}_\Delta + a_1a_2\overline{h}_{N1} + a_1\overline{h}_{\Delta 1}\right) \\ & + \left(a_1a_2\overline{h}_{N2} + a_1\overline{h}_{\Delta 2}\right)\|q\| \\ & + \left(a_1a_2\overline{h}_{N3} + a_1\overline{h}_{\Delta 3}\right)\|\dot{q}\| \\ & + \left(a_1a_2\overline{h}_{N4} + a_1\overline{h}_{\Delta 4}\right)\|\dot{q}\|^2 \\ & + a_1a_2\|u\|, \end{aligned} \tag{A.5}$$

which can be written in a simpler form as

$$\|\xi\| \leq \; \delta_1 + \delta_2\|q\| + \delta_3\|\dot{q}\| + \delta_4\|\dot{q}\|^2 + \delta_5\|u\|, \tag{A.6}$$

where $\delta_1, \cdots, \delta_5$ are non-negative constants with

$$\begin{cases} \delta_1 \geq a_1\overline{\tau}_\Delta + a_1a_2\overline{h}_{N1} + a_1\overline{h}_{\Delta 1} \\ \delta_2 \geq a_1a_2\overline{h}_{N2} + a_1\overline{h}_{\Delta 2} \\ \delta_3 \geq a_1a_2\overline{h}_{N3} + a_1\overline{h}_{\Delta 3} \\ \delta_4 \geq a_1a_2\overline{h}_{N4} + a_1\overline{h}_{\Delta 4} \\ \delta_5 \geq a_1a_2 \end{cases}.$$

It is clear from (A.6) that the upper bounds of the system uncertainties ξ depends on the control input u. Assuming that u does not contain the acceleration term $\ddot{q}$, then the upper bounds of ξ will depend only on the position and velocity measurements. Then, there exists a positive scalar function $\Omega(q, \dot{q}, t)$ such that

$$\|u\| \leq \Omega(q, \dot{q}, t). \tag{A.7}$$

By replacing (A.7) in (A.6) the following inequality is obtained:

$$\|\xi\| \leq \delta_1 + \delta_2\|q\| + \delta_3\|\dot{q}\| + \delta_4\|\dot{q}\|^2 + \delta_5\Omega(q, \dot{q}, t). \tag{A.8}$$

Then, it is obvious to write

$$\phi(q, \dot{q}, t) - \|\xi\| \geq \eta, \tag{A.9}$$

where η is an arbitrary positive constant and $\phi(q, \dot{q}, t)$ is a scalar positive function defined as

$$\phi(q, \dot{q}, t) = \delta_1 + \delta_2\|q\| + \delta_3\|\dot{q}\| + \delta_4\|\dot{q}\|^2 + \delta_5\Omega(q, \dot{q}, t) + \eta. \tag{A.10}$$

Appendix B

Proof of Theorem 4.1

Lets choose the following Lyapunov function $V = \frac{1}{2}s^T s$. Differentiating V with respect to time gives $\dot{V} = s^T \dot{s}$. Using sliding manifold function (4.19), it yields

$$\dot{s} = \ddot{e} + \alpha \dot{e}^{\frac{q}{p}} + \beta e^{\frac{q}{2p-q}}. \tag{B.1}$$

Then, the time derivative of V is $\dot{V} = s^T \left[\ddot{e} + \alpha \dot{e}^{\frac{q}{p}} + \beta e^{\frac{q}{2p-q}}\right]$ and by using (4.17) it can be obtained that $\dot{V} = s^T \left[\ddot{q}_d + \alpha \dot{e}^{\frac{q}{p}} + \beta e^{\frac{q}{2p-q}} - f - \varphi u - \xi\right]$. Finally, by considering the control law (4.20) for $\|s\| \neq 0$ it comes

$$\dot{V} \;=\; -s^T \lambda s - s^T \xi - s^T \phi \tfrac{s}{\|s\|} \;. \tag{B.2}$$

Then it can be written that

$$\dot{V} \;\leq\; \|s\|\|\xi\| - \phi\|s\|. \tag{B.3}$$

By using (A.9), the time derivative of V is upper bounded as

$$\dot{V} \leq -(\phi - \|\xi\|)\|s\| \leq -\eta\|s\|, \tag{B.4}$$

where $\eta > 0$ according to (A.9).

It can be seen that the time derivative of V is decreasing and moreover satisfies $\dot{V} \leq -\eta\sqrt{2}\, V^{\frac{1}{2}}$. Then consequently s reaches zero in finite time and the reaching time is

lower than $t = \frac{\sqrt{2}}{\eta} V(0)^{\frac{1}{2}}$. Therefore, the sliding mode $s = 0$ appears after the reaching time and consequently $\dot{s} = 0$ which allows to write the error dynamic (B.1) as follows:

$$\ddot{e} + \alpha \dot{e}^{\frac{q}{p}} + \beta e^{\frac{q}{2p-q}} = 0. \tag{B.5}$$

Then according to Lemma 4.1, (B.5) is globally finite-time-stable to the equilibrium point $(\dot{e}, e) = (0, 0)$.

Appendix C

Proof of Lemma 4.2

Considering the adaptation law (4.25) and (4.26) for $\|s\| \neq 0$, follows that $\hat{A}(t)$ is strictly increasing.

In addition

$$\dot{\hat{A}}_i(t) \geq \mu\underline{\Gamma}, \quad \text{for } i \in \{1, ..., 7\},$$

where $\underline{\Gamma} = min(\Gamma_1, ..., \Gamma_7)$.

Therefore, there exists a time

$$t_1 \leq \frac{1}{\mu\underline{\Gamma}}\|A\|_\infty,$$

such that $\hat{A}_i(t) \geq A_i$ for $i \in \{1, ..., 7\}$, $\forall t > t_1$.

From $t = t_1$, the vector $\hat{A}(t)$ is large enough to ensure the finite time convergence of $s(t)$ according to Theorem 4.1. It yields that the convergence of $s(t)$ to zero is achieved in the finite time

$$t_2 \leq t_1 + \frac{\sqrt{2}}{\eta}V(t_1)^{\frac{1}{2}}.$$

Using (4.25) and (4.26) gives

$$\dot{\hat{A}}(t) = 0 \quad , \ \forall t > t_2.$$

It means that $\hat{A}(t)$ admits a bounded constant vector A^* such that

$$\hat{A}(t) = A^* \quad , \ \forall t > t_2.$$

Finally, it can be agreed that $\hat{A}_i(t) \leq A_i^*$ and $A_i \leq A_i^*$ for $i \in \{1, ..., 7\}$, $\forall t > 0$.

Appendix D

Proof of Theorem 4.2

Let define the adaptation error $\tilde{A} = A^* - \hat{A}$ and the Lyapunov function

$$W = \tfrac{1}{2} s^T s + \tfrac{1}{2} \tilde{A}^T \Gamma^{-1} \tilde{A}. \tag{D.1}$$

By using (4.19), the time derivative of W yields

$$\dot{W} = s^T \left[\ddot{e} + \alpha \dot{e}^{\frac{q}{p}} + \beta e^{\frac{q}{2p-q}} \right] - \tilde{A}^T \Gamma^{-1} \dot{\hat{A}}, \tag{D.2}$$

then using error dynamics (4.17) and adaptation law (4.25) and (4.26) for $\|s\| \neq 0$, the time derivative of W is computed as

$$\begin{aligned} \dot{W} &= s^T \left(\ddot{q}_d + \alpha \dot{e}^{\frac{q}{p}} + \beta e^{\frac{q}{2p-q}} - f - \varphi u - \xi \right) \\ &\quad -\tilde{A}^T \psi (\|s\| + \mu) \\ &= -s^T \lambda s - s^T \xi - \psi^T \hat{A} \|s\| - \tilde{A}^T \psi \|s\| - \tilde{A}^T \psi \mu \\ &= -s^T \lambda s - s^T \xi - \psi^T A \|s\| + \psi^T A \|s\| - \psi^T \hat{A} \|s\| \\ &\quad -A^{*T} \psi \|s\| + \hat{A}^T \psi \|s\| - \tilde{A}^T \psi \mu. \end{aligned} \tag{D.3}$$

It has been shown in Lemma 4.2 there always exists a positive vector A^* in such a way that $\forall t > 0$, $\tilde{A}_i \geq 0$ and $A_i^* \geq A_i$ for $i \in \{1, ..., 7\}$. It yields, $\psi^T (A^* - A)$ and $\psi^T \tilde{A}$ are always positives and then the time derivative of W can be upper bounded

$$\dot{W} \leq -s^T \lambda s + \|\xi\| \|s\| - \psi^T A \|s\| - \tilde{A}^T \psi \mu. \tag{D.4}$$

Since $-\tilde{A}^T\psi \leq -\|\tilde{A}\|_1 \leq -\|\tilde{A}\|$ and by using (B.4), then

$$\begin{aligned} \dot{W} &\leq -(\psi^T A - \|\xi\|)\|s\| - \mu\|\tilde{A}\| \\ &\leq -\eta\|s\| - \mu\|\tilde{A}\|. \end{aligned} \tag{D.5}$$

It can be seen that the time derivative of W satisfies $\dot{W} \leq -\kappa W^{\frac{1}{2}}$ where $\kappa = min(\eta\sqrt{2}, \mu\sqrt{2\underline{\Gamma}})$ with $\underline{\Gamma} = min(\Gamma_1, ..., \Gamma_7)$ as mentioned previously. Then consequently, W reaches zero in finite time and the reaching time is lower than $t = \frac{2}{\kappa}W(0)^{\frac{1}{2}}$. Therefore, both s and $\tilde{A}$ reach zero in finite time. Finally, the error dynamic (B.5) is globally finite-time-stable to the equilibrium point $(\dot{e}, e) = (0, 0)$ according to Lemma 4.1.

Bibliography

[1] N. Norouzi Gheidari, P. S. Archambault, and J. Fung, "Effects of robot-assisted therapy on stroke rehabilitation in upper limbs: systematic review and meta-analysis of the literature," *Journal of rehabilitation research and development*, vol. 49, no. 4, p. 479, 2012.

[2] S. Mendis, "Stroke disability and rehabilitation of stroke: World health organization perspective," *Int J Stroke*, vol. 8, no. 1, pp. 3–4, 2013.

[3] H. S. Lo and S. Q. Xie, "Exoskeleton robots for upper-limb rehabilitation: state of the art and future prospects," *Medical engineering & physics*, vol. 34, no. 3, pp. 261–268, 2012.

[4] A. Frisoli, C. Procopio, C. Chisari, Creatini *et al.*, "Positive effects of robotic exoskeleton training of upper limb reaching movements after stroke," *JNER*, vol. 9, no. 1, p. 36, 2012.

[5] T. Nef, M. Guidali, and R. Riener, "Armin iii–arm therapy exoskeleton with an ergonomic shoulder actuation," *Applied Bionics and Biomechanics*, vol. 6, no. 2, pp. 127–142, 2009.

[6] N. Jarrassé and G. Morel, "A formal method for avoiding hyperstaticity when connecting an exoskeleton to a human member," in *IEEE International Conference on Robotics and Automation, 2010. ICRA 2010.* IEEE, 2012, pp. 1188–1195.

[7] J. Perry, J. Rosen, and S. Burns, "Upper-limb powered exoskeleton design," *Mechatronics, IEEE/ASME Transactions on*, vol. 12, no. 4, pp. 408–417, Aug 2007.

[8] S. Balasubramanian *et al.*, "Rupert: An exoskeleton robot for assisting rehabilitation of arm functions," in *Virtual Rehabilitation, 2008.* IEEE, 2008, pp. 163–167.

[9] M. H. Rahman, M. Rahman, O. L. Cristobal, M. Saad, J.-P. Kenné, and P. S. Archambault, "Development of a whole arm wearable robotic exoskeleton for rehabilitation and to assist upper limb movements," *Robotica*, vol. 33, no. 01, pp. 19–39, 2015.

[10] E. F. Lemonnier, "La prevention et la prise en charge des accidents vasculaires cerebraux en france," *Haute Autorite de Sante*, juin 2009.

[11] Y. Béjot, H. Bailly, J. Durier, and M. Giroud, "Epidemiology of stroke in europe and trends for the 21st century," *La Presse Médicale*, vol. 45, no. 12, pp. e391–e398, 2016.

[12] K. Chevreul, I. Durand-Zaleski, A. Gouepo, E. Fery-Lemonnier, M. Hommel, and F. Woimant, "Cost of stroke in france," *European journal of neurology*, vol. 20, no. 7, pp. 1094–1100, 2013.

[13] R. C. Loureiro, W. S. Harwin, K. Nagai, and M. Johnson, "Advances in upper limb stroke rehabilitation: a technology push," *Medical & biological engineering & computing*, vol. 49, no. 10, pp. 1103–1118, 2011.

[14] M. Dijkers, "Patient and staff acceptance of robotic technology in occupational therapy a pilot study," *Journal of rehabilitation research and development*, vol. 28, no. 2, 1991.

[15] I. Kapandji, *The Physiology of the Joints*, C. LIVINGSTONE, Ed. Edinburgh London Melbourne And New York, 1982.

[16] B. Tondu, "A kinematic model of the upper limb with a clavicle-like link for humanoid robots," *International Journal of Humanoid Robotics*, vol. 5, no. 01, pp. 87–118, 2008.

[17] P. M. Ludewig, V. Phadke, J. P. Braman, D. R. Hassett, C. J. Cieminski, and R. F. LaPrade, "Motion of the shoulder complex during multiplanar humeral elevation," *The Journal of Bone & Joint Surgery*, vol. 91, no. 2, pp. 378–389, 2009.

[18] C. Neu, J. Crisco, and S. Wolfe, "In vivo kinematic behavior of the radio-capitate joint during wrist flexion–extension and radio-ulnar deviation," *Journal of Biomechanics*, vol. 34, no. 11, pp. 1429–1438, 2001.

[19] R. Gopura, D. Bandara, K. Kiguchi, and G. Mann, "Developments in hardware systems of active upper-limb exoskeleton robots: A review," *Robotics and Autonomous Systems*, vol. 75, pp. 203–220, 2016.

[20] HAS, "Accident vasculaire cerebral : methodes de reeducation de la fonction motrice chez l'adulte," *Haute Autorite de Sante*, 2012.

[21] J. Carr and R. Shepard, "Upper limb function," *A motor relearning programme for stroke. Oxford: Butterworth-Heineman*, pp. 43–72, 1987.

[22] B. Bobath, *Adult hemiplegia: evaluation and treatment*. Elsevier Health Sciences, 1990.

[23] s. Boudrahem, "Reeducation a la marche chez le patient hemiplegique selon le concept perfetti," *Centre medical Mangini*, 2008.

[24] E. Cotton and R. Kinsman, *Conductive education for adult hemiplegia*. Churchill Livingstone Edinburgh, 1983.

[25] M. S. Rood, "Neurophysiological reactions as a basis for physical therapy." *The Physical therapy review*, vol. 34, no. 9, pp. 444–449, 1954.

[26] S. A. Stockmeyer, "An interpretation of the approach of rood to the treatment of neuromuscular dysfunction." *American journal of physical medicine & rehabilitation*, vol. 46, no. 1, pp. 900–956, 1967.

[27] H. Kabat, "Studies of neuromuscular dysfunction; treatment of chronic multiple sclerosis with neostigmine and intensive muscle re-education." *Permanente Foundation medical bulletin*, vol. 5, no. 1, pp. 1–14, 1947.

[28] ——, "Proprioceptive facilitation technics for treatment of paralysis," *Phys Ther Rev*, vol. 33, pp. 53–64, 1953.

[29] M. J. Sharman, A. G. Cresswell, and S. Riek, "Proprioceptive neuromuscular facilitation stretching," *Sports Medicine*, vol. 36, no. 11, pp. 929–939, 2006.

[30] M. Garry, A. Loftus, and J. Summers, "Mirror, mirror on the wall: viewing a mirror reflection of unilateral hand movements facilitates ipsilateral m1 excitability," *Experimental brain research*, vol. 163, no. 1, pp. 118–122, 2005.

[31] L. H. Ramsey, C. W. Karlson, and A. B. Collier, "Mirror therapy for phantom limb pain in a 7-year-old male with osteosarcoma," *Journal of pain and symptom management*, vol. 53, no. 6, pp. e5–e7, 2017.

[32] T. A. Thrasher and M. R. Popovic, "Functional electrical stimulation of walking: function, exercise and rehabilitation," in *Annales de réadaptation et de médecine physique*, vol. 51, no. 6. Elsevier, 2008, pp. 452–460.

[33] Z. Huang, Z. Wang, X. Lv, Y. Zhou, H. Wang, and S. Zong, "A novel functional electrical stimulation-control system for restoring motor function of post-stroke hemiplegic patients," *Neural regeneration research*, vol. 9, no. 23, p. 2102, 2014.

[34] E. Ernst, "A review of stroke rehabilitation and physiotherapy." *Stroke*, vol. 21, no. 7, pp. 1081–1085, 1990.

[35] C. M. Sackley and N. B. Lincoln, "Physiotherapy treatment for stroke patients: a survey of current practice," *Physiotherapy Theory and Practice*, vol. 12, no. 2, pp. 87–96, 1996.

[36] S. Coote and E. K. Stokes, "Physiotherapy for upper extremity dysfunction following stroke," *Physical Therapy Reviews*, vol. 6, no. 1, pp. 63–69, 2001.

[37] g. R. J. Luaute, "Reeducation de la commande motrice (commande motrice, imagerie motrice)," *Spiral Connect Lyon 1*, 2013.

[38] A. Sunderland, D. Fletcher, L. Bradley, D. Tinson, R. L. Hewer, and D. T. Wade, "Enhanced physical therapy for arm function after stroke: a one year follow up study." *Journal of Neurology, Neurosurgery & Psychiatry*, vol. 57, no. 7, pp. 856–858, 1994.

[39] G. Kwakkel, R. C. Wagenaar, T. W. Koelman, G. J. Lankhorst, and J. C. Koetsier, "Effects of intensity of rehabilitation after stroke," *Stroke*, vol. 28, no. 8, pp. 1550–1556, 1997.

[40] N. B. Lincoln, R. H. Parry, and C. D. Vass, "Randomized, controlled trial to evaluate increased intensity of physiotherapy treatment of arm function after stroke," *Stroke*, vol. 30, no. 3, pp. 573–579, 1999.

[41] C. D. Takahashi, L. Der-Yeghiaian, V. Le, R. R. Motiwala, and S. C. Cramer, "Robot-based hand motor therapy after stroke," *Brain*, vol. 131, no. 2, pp. 425–437, 2008.

[42] N. Hogan, H. I. Krebs, J. Charnnarong, P. Srikrishna, and A. Sharon, "Mitmanus: a workstation for manual therapy and training. i," in *Proceedings IEEE International Workshop on Robot and Human Communication, 1992.* IEEE, 1992, pp. 161–165.

[43] V. Crocher, "Commande d un exosquelette du membre superieur a des fins de reeducation neuromotrice," Ph.D. dissertation, Universite Pierre et Marie Curie - Paris VI, septembre 2012.

[44] H. Krebs, N. Hogan, B. Volpe, M. Aisen, L. Edelstein, and C. Diels, "Overview of clinical trials with mit-manus: a robot-aided neuro-rehabilitation facility," *Technology and Health Care*, vol. 7, no. 6, pp. 419–423, 1999.

[45] H. Krebs, B. Volpe, M. Aisen, and N. Hogan, "Increasing productivity and quality of care: robot-aided neuro-rehabilitation," *Journal of rehabilitation research and development*, vol. 37, no. 6, pp. 639–652, 2000.

[46] H. I. Krebs, M. Ferraro, S. P. Buerger, M. J. Newbery, A. Makiyama, M. Sandmann, D. Lynch, B. T. Volpe, and N. Hogan, "Rehabilitation robotics: pilot trial of a spatial extension for mit-manus," *Journal of NeuroEngineering and Rehabilitation*, vol. 1, no. 1, p. 5, 2004.

[47] D. J. Reinkensmeyer, L. E. Kahn, M. Averbuch, A. McKenna-Cole *et al.*, "Understanding and treating arm movement impairment after chronic brain injury: progress with the arm guide," *Journal of rehabilitation research and development*, vol. 37, no. 6, p. 653, 2000.

[48] L. Kahn, M. Zygman, W. Rymer, and D. Reinkensmeyer, "Effect of robot-assisted and unassisted exercise on functional reaching in chronic hemiparesis," in *Proceedings of the 23rd Annual International Conference of the IEEE Engineering in Medicine and Biology Society, 2001.*, vol. 2. IEEE, 2001, pp. 1344–1347.

[49] P. S. Lum, C. G. Burgar, P. C. Shor, M. Majmundar, and M. Van der Loos, "Robot-assisted movement training compared with conventional therapy techniques for the rehabilitation of upper-limb motor function after stroke," *Archives of physical medicine and rehabilitation*, vol. 83, no. 7, pp. 952–959, 2002.

[50] P. S. Lum, C. G. Burgar, and P. C. Shor, "Evidence for improved muscle activation patterns after retraining of reaching movements with the mime robotic system in subjects with post-stroke hemiparesis," *IEEE Transactions on Neural Systems and Rehabilitation Engineering*, vol. 12, no. 2, pp. 186–194, 2004.

[51] C. G. Burgar, P. S. Lum, P. C. Shor, and H. M. Van der Loos, "Development of robots for rehabilitation therapy: The palo alto va/stanford experience," *Journal of rehabilitation research and development*, vol. 37, no. 6, pp. 663–674, 2000.

[52] W. Harwin, R. Loureiro, F. Amirabdollahian, M. Taylor, G. Johnson, E. Stokes, S. Coote, M. Topping, C. Collin, S. Tamparis *et al.*, "The gentle/s project: A new method of delivering neuro-rehabilitation," *Rehabilitation, Allied Medicine*, 2001.

[53] R. Loureiro, F. Amirabdollahian, M. Topping, B. Driessen, and W. Harwin, "Upper limb robot mediated stroke therapy-gentle/s approach," *Autonomous Robots*, vol. 15, no. 1, pp. 35–51, 2003.

[54] F. Amirabdollahian, E. Gradwell, R. Loureiro, C. Collin, and W. Harwin, "Effects of the gentle/s robot mediated therapy on the outcome of upper limb rehabilitation post-stroke: Analysis of the battle hospital data," in *Proceedings of the 8th International Conference on Rehabilitation Robotics, ICORR 2003, Daejeon, Korea.*, 2003, pp. 55–58.

[55] F. Amirabdollahian, R. Loureiro, E. Gradwell, C. Collin, W. Harwin, and G. Johnson, "Multivariate analysis of the fugl-meyer outcome measures assessing the effectiveness of gentle/s robot-mediated stroke therapy," *Journal of NeuroEngineering and Rehabilitation*, vol. 4, no. 1, p. 4, 2007.

[56] R. S. Mosher, "Handyman to hardiman," SAE Technical Paper, Tech. Rep., 1967.

[57] (Accessed on September 2017) "les robots au service des hommes". [Online]. Available: http://www.astrosurf.com/luxorion/robot3.htm

[58] R. Riener, T. Nef, and G. Colombo, "Robot-aided neurorehabilitation of the upper extremities," *Medical and Biological Engineering and Computing*, vol. 43, no. 1, pp. 2–10, 2005.

[59] M. Mihelj, T. Nef, and R. Riener, "Armin ii - 7 dof rehabilitation robot: mechanics and kinematics," in *IEEE International Conference on Robotics and Automation, ICRA 2007.*, April 2007, pp. 4120–4125.

[60] E. Flores, G. Tobon, E. Cavallaro, F. I. Cavallaro, J. C. Perry, and T. Keller, "Improving patient motivation in game development for motor deficit rehabilitation," in *Proceedings of the International Conference on Advances in Computer Entertainment Technology, 2008.* ACM, 2008, pp. 381–384.

[61] M. Guidali, A. Duschau-Wicke, S. Broggi, V. Klamroth-Marganska, T. Nef, and R. Riener, "A robotic system to train activities of daily living in a virtual environment," *Medical & Biological Engineering & Computing*, vol. 49, no. 10, p. 1213, Jul 2011. [Online]. Available: https://doi.org/10.1007/s11517-011-0809-0

[62] J. Perry and J. Rosen, "Design of a 7 degree-of-freedom upper-limb powered exoskeleton," in *The First IEEE/RAS-EMBS International Conference on Biomedical Robotics and Biomechatronics, 2006. BioRob 2006.*, Feb 2006, pp. 805–810.

[63] C. Carignan, M. Liszka, and S. Roderick, "Design of an arm exoskeleton with scapula motion for shoulder rehabilitation," in *12th International Conference on Advanced Robotics, 2005. ICAR'05. Proceedings.* IEEE, 2005, pp. 524–531.

[64] C. R. Carignan and H. I. Krebs, "Telerehabilitation robotics: bright lights, big future?" *Journal of rehabilitation research and development*, vol. 43, no. 5, p. 695, 2006.

[65] C. Carignan, J. Tang, and S. Roderick, "Development of an exoskeleton haptic interface for virtual task training," in *IEEE/RSJ International Conference on Intelligent Robots and Systems, 2009. IROS 2009.* IEEE, 2009, pp. 3697–3702.

[66] A. Frisoli, F. Rocchi *et al.*, "A new force-feedback arm exoskeleton for haptic interaction in virtual environments," in *Proceedings of the First Joint Eurohaptics Conference and Symposium on Haptic Interfaces for Virtual Environment and Teleoperator Systems, HAPTICS 2005.* IEEE, 2005, pp. 195–201.

[67] N. G. Tsagarakis and D. G. Caldwell, "Development and control of a soft-actuated exoskeleton for use in physiotherapy and training," *Autonomous Robots*, vol. 15, no. 1, pp. 21–33, 2003.

[68] J. C. Perry, H. Zabaleta, A. Belloso, and T. Keller, "Armassist: A low-cost device for telerehabiltation of post-stroke arm deficits," in *World Congress on Medical Physics and Biomedical Engineering, September 7-12, 2009, Munich, Germany.* Springer, 2009, pp. 64–67.

[69] N. R. Butler, S. A. Goodwin, and J. C. Perry, "Design parameters and torque profile modification of a spring-assisted hand-opening exoskeleton module," in *International Conference on Rehabilitation Robotics, ICORR 2017.*, July 2017, pp. 591–596.

[70] S. Dunaway, D. B. Dezsi, J. Perkins, D. Tran, and J. Naft, "Case report on the use of a custom myoelectric elbow–wrist–hand orthosis for the remediation of upper extremity paresis and loss of function in chronic stroke," *Military Medicine*, vol. 182, no. 7, pp. e1963–e1968, 2017.

[71] M. V. Radomski and C. A. T. Latham, *Occupational therapy for physical dysfunction.* Lippincott Williams & Wilkins, 2008.

[72] J. Klein, S. Spencer, J. Allington, K. Minakata, E. Wolbrecht, R. Smith, J. Bobrow, and D. Reinkensmeyer, "Biomimetic orthosis for the neurorehabilitation of

the elbow and shoulder (bones)," in *2nd IEEE RAS & EMBS International Conference on Biomedical Robotics and Biomechatronics, 2008. BioRob 2008.* IEEE, 2008, pp. 535–541.

[73] M. H. Rahman, M. Saad, J.-P. Kenné, and P. S. Archambault, "Control of an exoskeleton robot arm with sliding mode exponential reaching law," *IJCAS*, vol. 11, no. 1, pp. 92–104, 2013.

[74] S. J. Housman, V. Le, T. Rahman, R. J. Sanchez, and D. J. Reinkensmeyer, "Arm-training with t-wrex after chronic stroke: preliminary results of a randomized controlled trial," in *IEEE 10th International Conference on Rehabilitation Robotics, 2007. ICORR 2007.* IEEE, 2007, pp. 562–568.

[75] L. Marchal-Crespo and D. J. Reinkensmeyer, "Review of control strategies for robotic movement training after neurologic injury," *Journal of NeuroEngineering and Rehabilitation*, vol. 6, no. 1, pp. 1–15, 6 2009. [Online]. Available: http:https://doi.org/10.1186/1743-0003-6-20

[76] J. C. Perry, "Design and development of a 7 degree-of-freedom powered exoskeleton for the upper limb," dissertation, University of Washington, 2006.

[77] T. Nef, M. Mihelj, and R. Riener, "Armin: a robot for patient-cooperative arm therapy," *Medical & biological engineering & computing*, vol. 45, no. 9, pp. 887–900, 2007.

[78] S. Kousidou, N. Tsagarakis, C. Smith, and D. Caldwell, "Task-orientated biofeedback system for the rehabilitation of the upper limb," in *IEEE 10th International Conference on Rehabilitation Robotics, 2007. ICORR 2007.* IEEE, 2007, pp. 376–384.

[79] R. A. R. C. Gopura, K. Kiguchi, and Y. Li, "Sueful-7: A 7dof upper-limb exoskeleton robot with muscle-model-oriented emg-based control," in *IEEE/RSJ International Conference on Intelligent Robots and Systems, 2009. IROS 2009. IEEE/RSJ International Conference on.* IEEE, 2009, pp. 1126–1131.

[80] H. Vallery, J. Veneman, E. Van Asseldonk, R. Ekkelenkamp, M. Buss, and H. Van Der Kooij, "Compliant actuation of rehabilitation robots," *IEEE Robotics & Automation Magazine*, vol. 15, no. 3, 2008.

[81] W. Yu and J. Rosen, "A novel linear pid controller for an upper limb exoskeleton," in *49th IEEE CDC.* IEEE, 2010, pp. 3548–3553.

[82] R. Vertechy, A. Frisoli, A. Dettori, M. Solazzi, and M. Bergamasco, "Development of a new exoskeleton for upper limb rehabilitation," in *IEEE International Conference on Rehabilitation Robotics, 2009. ICORR 2009.* IEEE, 2009, pp. 188–193.

[83] A. H. Stienen, E. E. Hekman, F. C. Van der Helm, G. B. Prange, M. J. Jannink, A. M. Aalsma, and H. Van der Kooij, "Dampace: dynamic force-coordination trainer for the upper extremities," in *IEEE 10th International Conference on Rehabilitation Robotics, 2007. ICORR 2007.* IEEE, 2007, pp. 820–826.

[84] M. H. Rahman, M. Saad, J. P. Kenné, and P. S. Archambault, "Modeling and control of a 7dof exoskeleton robot for arm movements," in *IEEE International Conference on Robotics and Biomimetics, ROBIO 2009.* IEEE, 2009, pp. 245–250.

[85] N. Hogan, H. I. Krebs, B. Rohrer, J. J. Palazzolo *et al.*, "Motions or muscles? some behavioral factors underlying robotic assistance of motor recovery," *Journal of rehabilitation research and development*, vol. 43, no. 5, p. 605, 2006.

[86] J. L. Emken, R. Benitez, A. Sideris, J. E. Bobrow, and D. J. Reinkensmeyer, "Motor adaptation as a greedy optimization of error and effort," *Journal of neurophysiology*, vol. 97, no. 6, pp. 3997–4006, 2007.

[87] V. Squeri, A. Basteris, and V. Sanguineti, "Adaptive regulation of assistance 'as needed' in robot-assisted motor skill learning and neuro-rehabilitation," in *IEEE International Conference on Rehabilitation Robotics, ICORR 2011.* IEEE, 2011, pp. 1–6.

[88] C. Trombly, "Theoretical foundations for practice," *Occupational therapy for physical dysfunction*, pp. 15–27, 1995.

[89] L. L. Cai, A. J. Fong, C. K. Otoshi, Y. Liang, J. W. Burdick, R. R. Roy, and V. R. Edgerton, "Implications of assist-as-needed robotic step training after a complete spinal cord injury on intrinsic strategies of motor learning," *Journal of Neuroscience*, vol. 26, no. 41, pp. 10 564–10 568, 2006.

[90] E. T. Wolbrecht, V. Chan, D. J. Reinkensmeyer, and J. E. Bobrow, "Optimizing compliant, model-based robotic assistance to promote neurorehabilitation," *IEEE Transactions on Neural Systems and Rehabilitation Engineering*, vol. 16, no. 3, pp. 286–297, 2008.

[91] M. Casadio, P. Morasso, V. Sanguineti, and P. Giannoni, "Minimally assistive robot training for proprioception enhancement," *Experimental brain research*, vol. 194, no. 2, pp. 219–231, 2009.

[92] E. Vergaro, M. Casadio, V. Squeri, P. Giannoni, P. Morasso, and V. Sanguineti, "Self-adaptive robot training of stroke survivors for continuous tracking movements," *Journal of neuroengineering and rehabilitation*, vol. 7, no. 1, p. 13, 2010.

[93] S. Hesse, G. Schulte-Tigges, M. Konrad, A. Bardeleben, and C. Werner, "Robot-assisted arm trainer for the passive and active practice of bilateral forearm and wrist movements in hemiparetic subjects," *Archives of physical medicine and rehabilitation*, vol. 84, no. 6, pp. 915–920, 2003.

[94] H. Vallery, M. Guidali, A. Duschau-Wicke, and R. Riener, "Patient-cooperative control: providing safe support without restricting movement," in *World Congress on Medical Physics and Biomedical Engineering, September 7-12, 2009, Munich, Germany*. Springer, 2009, pp. 166–169.

[95] J. P. Dewald, P. S. Pope, J. D. Given, T. S. Buchanan, and W. Z. Rymer, "Abnormal muscle coactivation patterns during isometric torque generation at the elbow and shoulder in hemiparetic subjects," *Brain*, vol. 118, no. 2, pp. 495–510, 1995.

[96] M. Cirstea, A. Mitnitski, A. Feldman, and M. Levin, "Interjoint coordination dynamics during reaching in stroke," *Experimental Brain Research*, vol. 151, no. 3, pp. 289–300, 2003.

[97] V. Crocher, A. Sahbani, J. Robertson, A. Roby-Brami, and G. Morel, "Constraining upper limb synergies of hemiparetic patients using a robotic exoskeleton in the perspective of neuro-rehabilitation," *IEEE Transactions on Neural Systems and Rehabilitation Engineering*, vol. 20, no. 3, pp. 247–257, 2012.

[98] T. M. Sukal, M. D. Ellis, and J. P. Dewald, "Dynamic characterization of upper limb discoordination following hemiparetic stroke," in *9th International Conference on Rehabilitation Robotics, 2005. ICORR 2005.* IEEE, 2005, pp. 519–521.

[99] A. M. Acosta, H. A. Dewald, and J. P. Dewald, "Pilot study to test effectiveness of video game on reaching performance in stroke," *Journal of rehabilitation research and development*, vol. 48, no. 4, p. 431, 2011.

[100] R. Shadmehr and F. A. Mussa-Ivaldi, "Adaptive representation of dynamics during learning of a motor task," *Journal of Neuroscience*, vol. 14, no. 5, pp. 3208–3224, 1994.

[101] J. L. Patton, M. E. Stoykov, M. Kovic, and F. A. Mussa-Ivaldi, "Evaluation of robotic training forces that either enhance or reduce error in chronic hemiparetic stroke survivors," *Experimental brain research*, vol. 168, no. 3, pp. 368–383, 2006.

[102] Y. Wei, P. Bajaj, R. Scheidt, and J. Patton, "Visual error augmentation for enhancing motor learning and rehabilitative relearning," in *9th International Conference on Rehabilitation Robotics, 2005. ICORR 2005.* IEEE, 2005, pp. 505–510.

[103] B. Volpe, H. Krebs, N. Hogan, L. Edelstein, C. Diels, and M. Aisen, "A novel approach to stroke rehabilitation robot-aided sensorimotor stimulation," *Neurology*, vol. 54, no. 10, pp. 1938–1944, 2000.

[104] S. E. Fasoli, H. I. Krebs, J. Stein, W. R. Frontera, and N. Hogan, "Effects of robotic therapy on motor impairment and recovery in chronic stroke," *Archives of physical medicine and rehabilitation*, vol. 84, no. 4, pp. 477–482, 2003.

[105] M. Ferraro, J. Palazzolo, J. Krol, H. Krebs, N. Hogan, and B. Volpe, "Robot-aided sensorimotor arm training improves outcome in patients with chronic stroke," *Neurology*, vol. 61, no. 11, pp. 1604–1607, 2003.

[106] S. Hesse, C. Werner, M. Pohl, S. Rueckriem, J. Mehrholz, and M. Lingnau, "Computerized arm training improves the motor control of the severely affected arm after stroke," *Stroke*, vol. 36, no. 9, pp. 1960–1966, 2005.

[107] G. Philippe, "Screw and nut transmission and cable attached to the screw," Jul. 11 2006, uS Patent 7.073.406.

[108] P. Garrec, *Screw and Cable Acutators (SCS) and Their Applications to Force Feedback Teleoperation, Exoskeleton and Anthropomorphic Robotics.* INTECH Open Access Publisher, 2010.

[109] W. Khalil and E. Dombre, *Modeling, identification and control of robots*, W. Khalil and E. Dombre, Eds. Oxford: Butterworth-Heinemann, 2004.

[110] H. Wang, H. Qi, M. Xu *et al.*, "Research on the relationship between classic denavit-hartenberg and modified denavit-hartenberg," in *ISCID, 2014*, vol. 2. IEEE, 2014, pp. 26–29.

[111] M. Renaud, "Contribution a l'étude de la modélisation et de la commande des systèmes mécaniques articulés," Ph.D. dissertation, UPS, Toulouse, France, 1975.

[112] P. Coiffet, *Modelling and control.* Springer Science & Business Media, 2012, vol. 1.

[113] B. S. Armstrong, "Dynamics for robot control: friction modeling and ensuring excitation during parameter identification," Ph.D. dissertation, STANFORD UNIV CA DEPT OF COMPUTER SCIENCE, 1988.

[114] B. Armstrong-Hélouvry, P. Dupont, and C. C. De Wit, "A survey of models, analysis tools and compensation methods for the control of machines with friction," *Automatica*, vol. 30, no. 7, pp. 1083–1138, 1994.

[115] L. Gaul and R. Nitsche, "The role of friction in mechanical joints," *Applied Mechanics Reviews*, vol. 54, no. 2, pp. 93–106, 2001.

[116] P. de Leva, "Adjustments to zatsiorsky-seluyanov's segment inertia parameters," *Journal of Biomechanics*, vol. 29, no. 9, pp. 1223 – 1230, 1996. [Online]. Available: //www.sciencedirect.com/science/article/pii/0021929095001786

[117] V. Zatsiorsky and V. Seluyanov, "The mass and inertia characteristics of the main segments of the human body," *Biomechanics viii-b*, vol. 56, no. 2, pp. 1152–1159, 1983.

[118] D. Galinski, J. Sapin, and B. Dehez, "Optimal design of an alignment-free two-dof rehabilitation robot for the shoulder complex," in *17th International Conference on Rehabiltitation Robotics, ICORR, 2013*, June 2013, pp. 1–7.

[119] J. Hollerbach, W. Khalil, and M. Gautier, "Model identification," in *Springer Handbook of Robotics*. Springer, 2008, pp. 321–344.

[120] M. Gautier and W. Khalil, "Direct calculation of minimum set of inertial parameters of serial robots," *Robotics and Automation, IEEE Transactions on*, vol. 6, no. 3, pp. 368–373, 1990.

[121] C. Carel, I. Loubinoux, K. Boulanouar, C. Manelfe, O. Rascol, P. Celsis, and F. Chollet, "Neural substrate for the effects of passive training on sensorimotor cortical representation: a study with functional magnetic resonance imaging in healthy subjects," *Journal of Cerebral Blood Flow & Metabolism*, vol. 20, no. 3, pp. 478–484, 2000.

[122] P. Marque, D. Gasq, E. Castel-Lacanal, X. De Boissezon, and I. Loubinoux, "Post-stroke hemiplegia rehabilitation: evolution of the concepts," *Annals of physical and rehabilitation medicine*, vol. 57, no. 8, pp. 520–529, 2014.

[123] T. Proietti, V. Crocher, A. Roby-Brami, and N. Jarrassé, "Upper-limb robotic exoskeletons for neurorehabilitation: a review on control strategies," *IEEE reviews in biomedical engineering*, vol. 9, pp. 4–14, 2016.

[124] A. Wege and G. Hommel, "Development and control of a hand exoskeleton for rehabilitation of hand injuries," in *2005 IEEE/RSJ IROS*. IEEE, 2005, pp. 3046–3051.

[125] P. Beyl, M. Van Damme, R. Van Ham, R. Versluys, B. Vanderborght, and D. Lefeber, "An exoskeleton for gait rehabilitation: prototype design and control principle," in *IEEE International Conference on Robotics and Automation, 2008. ICRA 2008.* IEEE, 2008, pp. 2037–2042.

[126] K. Kiguchi, T. Tanaka, and T. Fukuda, "Neuro-fuzzy control of a robotic exoskeleton with emg signals," *IEEE Transactions on fuzzy systems*, vol. 12, no. 4, pp. 481–490, 2004.

[127] K. Kiguchi, Y. Imada, and M. Liyanage, "Emg-based neuro-fuzzy control of a 4dof upper-limb power-assist exoskeleton," in *29th Annual International Conference of the IEEE Engineering in Medicine and Biology Society, 2007. EMBS 2007.* IEEE, 2007, pp. 3040–3043.

[128] Y. Li, S. Tong, and T. Li, "Adaptive fuzzy output feedback control of uncertain nonlinear systems with unknown backlash-like hysteresis," *Information Sciences*, vol. 198, pp. 130–146, 2012.

[129] H.-B. Kang and J.-H. Wang, "Adaptive control of 5 dof upper-limb exoskeleton robot with improved safety," *ISA transactions*, vol. 52, no. 6, pp. 844–852, 2013.

[130] M. Gautier and W. Khalil, "On the identification of the inertial parameters of robots," in *Proceedings of the 27th IEEE Conference on Decision and Control, 1988.* IEEE, 1988, pp. 2264–2269.

[131] M. Gautier and P. Poignet, "Extended kalman filtering and weighted least squares dynamic identification of robot," *Control Engineering Practice*, vol. 9, no. 12, pp. 1361–1372, 2001.

[132] M. Gautier, A. Janot, and P.-O. Vandanjon, "Didim: A new method for the dynamic identification of robots from only torque data," in *IEEE International Conference on Robotics and Automation, 2008. ICRA 2008.* IEEE, 2008, pp. 2122–2127.

[133] M. Gautier and S. Briot, "Dynamic parameter identification of a 6 dof industrial robot using power model," in *IEEE International Conference on Robotics and Automation (ICRA), 2013.* IEEE, 2013, pp. 2914–2920.

[134] N. Shimkin and A. Feuer, "Persistency of excitation in continuous-time systems," *Systems & control letters*, vol. 9, no. 3, pp. 225–233, 1987.

[135] S. Masiero and M. Armani, "Upper-limb robot-assisted therapy in rehabilitation of acute stroke patients: focused review and results of new randomized controlled trial," *Journal of rehabilitation research and development*, vol. 48, no. 4, pp. 355–366, 2011.

[136] W. Xu, B. Chu, and E. Rogers, "Iterative learning control for robotic-assisted upper limb stroke rehabilitation in the presence of muscle fatigue," *Control Engineering Practice*, vol. 31, no. Supplement C, pp. 63 – 72, 2014.

[137] J. M. Veerbeek, A. C. Langbroek-Amersfoort, E. E. van Wegen, C. G. Meskers, and G. Kwakkel, "Effects of robot-assisted therapy for the upper limb after stroke: a systematic review and meta-analysis," *Neurorehabilitation and Neural Repair*, p. 1545968316666957, 2017.

[138] F. Marini, C. M. Hughes, V. Squeri, L. Doglio, P. Moretti, P. Morasso, and L. Masia, "Robotic wrist training after stroke: Adaptive modulation of assistance in pediatric rehabilitation," *Robotics and Autonomous Systems*, vol. 91, pp. 169–178, 2017.

[139] R. Wei, S. Balasubramanian, L. Xu, and J. He, "Adaptive iterative learning control design for rupert iv," in *2nd IEEE RAS & EMBS International Conference on Biomedical Robotics and Biomechatronics, BioRob 2008.* Scottsdale, AZ, USA: IEEE, 2008, pp. 647–652.

[140] A. U. Pehlivan, D. P. Losey, and M. K. O'Malley, "Minimal assist-as-needed controller for upper limb robotic rehabilitation," *IEEE Transactions on Robotics*, vol. 32, no. 1, pp. 113–124, 2016.

[141] K. Kiguchi, M. H. Rahman, M. Sasaki, and K. Teramoto, "Development of a 3dof mobile exoskeleton robot for human upper-limb motion assist," *Robotics and Autonomous systems*, vol. 56, no. 8, pp. 678–691, 2008.

[142] C. Loconsole, S. Dettori, A. Frisoli, C. A. Avizzano, and M. Bergamasco, "An emg-based approach for on-line predicted torque control in robotic-assisted rehabilitation," in *IEEE Haptics Symposium (HAPTICS), 2014.* Houston, Texas, USA: IEEE, 2014, pp. 181–186.

[143] P. R. Culmer, A. E. Jackson, S. Makower, R. Richardson, J. A. Cozens, M. C. Levesley, and B. B. Bhakta, "A control strategy for upper limb robotic rehabilitation with a dual robot system," *IEEE/ASME Transactions on Mechatronics*, vol. 15, no. 4, pp. 575–585, 2010.

[144] Z. Li, C.-Y. Su, G. Li, and H. Su, "Fuzzy approximation-based adaptive backstepping control of an exoskeleton for human upper limbs," *IEEE Transactions on Fuzzy Systems*, vol. 23, no. 3, pp. 555–566, 2015.

[145] Z. Chen, Z. Li, and C. P. Chen, "Disturbance observer-based fuzzy control of uncertain mimo mechanical systems with input nonlinearities and its application to robotic exoskeleton," *IEEE transactions on cybernetics*, vol. 47, no. 4, pp. 984–994, 2017.

[146] Z. Li, J. Liu, Z. Huang, Y. Peng, H. Pu, and L. Ding, "Adaptive impedance control of human-robot cooperation using reinforcement learning," *IEEE Transactions on Industrial Electronics*, 2017.

[147] Z. Li, Y. Kang, Z. Xiao, and W. Song, "Human–robot coordination control of robotic exoskeletons by skill transfers," *IEEE Transactions on Industrial Electronics*, vol. 64, no. 6, pp. 5171–5181, 2017.

[148] M. Zhihong, A. P. Paplinski, and H. R. Wu, "A robust mimo terminal sliding mode control scheme for rigid robotic manipulators," *IEEE Transactions on Automatic Control*, vol. 39, no. 12, pp. 2464–2469, 1994.

[149] P. Park, D. J. Choi, and S. G. Kong, "Output feedback variable structure control for linear systems with uncertainties and disturbances," *Automatica*, vol. 43, no. 1, pp. 72–79, 2007.

[150] S. Yuri, E. Christopher, F. Leonid, and L. Arie, *Sliding mode control and observation*. Springer, 2014, vol. 10.

[151] J.-J. E. Slotine, W. Li *et al.*, *Applied nonlinear control*. prentice-Hall Englewood Cliffs, NJ, 1991, vol. 199, no. 1.

[152] W. Perruquetti and J.-P. Barbot, *Sliding mode control in engineering*. CRC Press, 2002.

[153] M. Zhihong and X. Yu, "Adaptive terminal sliding mode tracking control for rigid robotic manipulators with uncertain dynamics." *JSME International Journal Series C*, vol. 40, no. 3, pp. 493–502, 1997.

[154] Y. Feng, M. Zhou, X. Zheng, and F. Han, "Continuous adaptive terminal sliding-mode control," in *IEEE 11th Conference on Industrial Electronics and Applications (ICIEA), 2016*. Hefei, China: IEEE, 2016, pp. 184–188.

[155] X. Yu and M. Zhihong, "Fast terminal sliding-mode control design for nonlinear dynamical systems," *IEEE Transactions on Circuits and Systems I: Fundamental Theory and Applications*, vol. 49, no. 2, pp. 261–264, Feb 2002.

[156] T. Madani, B. Daachi, and K. Djouani, "Modular-controller-design-based fast terminal sliding mode for articulated exoskeleton systems," *IEEE Transactions on Control Systems Technology*, vol. 25, no. 3, pp. 1133–1140, May 2017.

[157] Y. Feng, X. Yu, and Z. Man, "Non-singular terminal sliding mode control of rigid manipulators," *Automatica*, vol. 38, no. 12, pp. 2159–2167, 2002.

[158] H. Komurcugil, "Non-singular terminal sliding-mode control of dc-dc buck converters," *Control Engineering Practice*, vol. 21, no. 3, pp. 321 – 332, 2013.

[159] T. Madani, B. Daachi, and K. Djouani, "Non-singular terminal sliding mode controller: Application to an actuated exoskeleton," *Mechatronics*, vol. 33, pp. 136–145, 2016.

[160] L. Peng, M. Jianjun, G. Lina, and Z. Zhiqiang, "Integral terminal sliding mode control for uncertain nonlinear systems," in *Control Conference (CCC), 2015 34th Chinese*. Hangzhou, China: IEEE, 2015, pp. 824–828.

[161] M. J. Morshed and A. Fekih, "A comparison study between two sliding mode based controls for voltage sag mitigation in grid connected wind turbines," in *IEEE Conference on Control Applications (CCA), 2015*. Sydney, Australia: IEEE, 2015, pp. 1913–1918.

[162] F. Ghorbel, B. Srinivasan, and M. W. Spong, "On the uniform boundedness of the inertia matrix of serial robot manipulators," *Journal of Robotic Systems*, vol. 15, no. 1, pp. 17–28, 1998.

[163] J. I. Mulero Martínez, "Uniform bounds of the coriolis/centripetal matrix of serial robot manipulators," *IEEE Transactions on Robotics*, vol. 23, no. 5, pp. 1083–1089, 2007.

[164] S. P. Bhat and D. S. Bernstein, "Geometric homogeneity with applications to finite-time stability," *Mathematics of Control, Signals and Systems*, vol. 17, no. 2, pp. 101–127, 2005.

[165] Y. S. Kim, J. Lee, S. Lee, and M. Kim, "A force reflected exoskeleton-type masterarm for human-robot interaction," *IEEE Transactions on Systems, Man, and Cybernetics-Part A: Systems and Humans*, vol. 35, no. 2, pp. 198–212, 2005.

[166] A. Gupta, M. K. O'Malley, V. Patoglu, and C. Burgar, "Design, control and performance of ricewrist: a force feedback wrist exoskeleton for rehabilitation and training," *The International Journal of Robotics Research*, vol. 27, no. 2, pp. 233–251, 2008.

[167] K. S. Eom, I. H. Suh, W. K. Chung, and S.-R. Oh, "Disturbance observer based force control of robot manipulator without force sensor," in *IEEE International Conference on Robotics and Automation, 1998. Proceedings. 1998*, vol. 4. IEEE, 1998, pp. 3012–3017.

[168] A. Alcocer, A. Robertsson, A. Valera, and R. Johansson, "Force estimation and control in robot manipulators," in *Proc. 7th IFAC Symp. Robot Control (SYROCO). Wrocław, Poland, September 2003*, 2003.

[169] A. Colomé, D. Pardo, G. Alenya, and C. Torras, "External force estimation during compliant robot manipulation," in *IEEE International Conference on Robotics and Automation, ICRA 2013.* IEEE, 2013, pp. 3535–3540.

[170] S. Gholami, A. Arjmandi, and H. D. Taghirad, "An observer-based adaptive impedance-control for robotic arms: Case study in smos robot," in *4th International Conference on Robotics and Mechatronics (ICROM), 2016 4th International Conference on.* IEEE, 2016, pp. 49–54.

[171] B. Ugurlu, M. Nishimura, K. Hyodo, M. Kawanishi, and T. Narikiyo, "Proof of concept for robot-aided upper limb rehabilitation using disturbance observers," *IEEE Transactions on Human-Machine Systems*, vol. 45, no. 1, pp. 110–118, 2015.

[172] A. Levant, "Higher-order sliding modes, differentiation and output-feedback control," *International journal of Control*, vol. 76, no. 9-10, pp. 924–941, 2003.

[173] A. Gupta and M. K. O'Malley, "Disturbance-observer-based force estimation for haptic feedback," *Journal of Dynamic Systems, Measurement, and Control*, vol. 133, no. 1, p. 014505, 2011.

[174] A. Filippov, "Equations with the right-hand side continuous in x and discontinuous in t," in *Differential equations with discontinuous righthand sides.* Springer, 1988, pp. 3–47.